

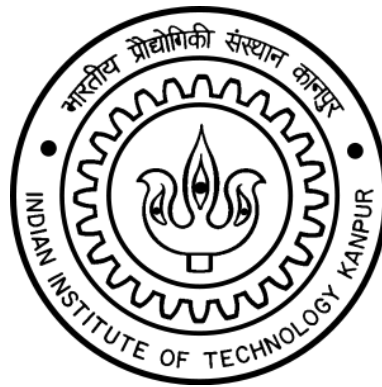
In-Process Monitoring of Abrasive Water Jet Milling

A thesis submitted
in partial fulfillment of the requirements
for the Degree of

DOCTOR OF PHILOSOPHY

By

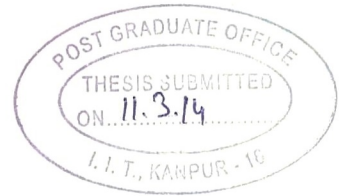
T V K Gupta



to the

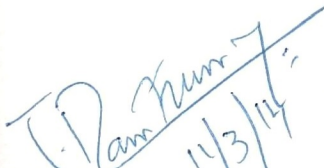
**DEPARTMENT OF MECHANICAL ENGINEERING
INDIAN INSTITUTE OF TECHNOLOGY KANPUR
KANPUR, INDIA**

March 2014



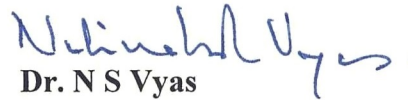
CERTIFICATE

It is certified that the work contained in the thesis entitled "*In-Process Monitoring of Abrasive Water Jet Milling*," by T. V. K. Gupta, has been carried out under our supervision and that this work has not been submitted elsewhere for a degree.


14/3/14

Dr. J Ramkumar

Associate Professor
Department of Mechanical Engineering
Indian Institute of Technology Kanpur
Kanpur-208 016
India



Dr. N S Vyas

Professor
Department of Mechanical Engineering
Indian Institute of Technology Kanpur
Kanpur-208 016
India



Dr. Puneet Tandon

Professor
Mechanical Engineering Discipline & Design Discipline
PDPM Indian Institute of Information Technology Design & Manufacturing Jabalpur
Jabalpur-482 005
India

February, 2014

Dedicated

to

Srilu, Sanju, Sruju

ACKNOWLEDGEMENT

It gives me an immense pleasure in expressing my deep sense of gratitude to my thesis supervisors, Prof. J Ramkumar, Prof. N S Vyas and Prof. Puneet Tandon under whose guidance and supervision, I could complete my research work. Their expertise in guiding me, encouragement and inspiring advices apart from constructive criticism made me to think differently and analyze the research topic. The technical and personnel support that I gained from them will form a strong foundation for the rest of my professional career.

I am highly indebted to and express my heartiest thanks to Prof. Aparajita Ojha, Director, PDPM IIITDM Jabalpur for extending me all the support for my research in terms of funding, facilities and resources at IIITDMJ. It would have been extremely difficult for me had I not developed the setup at IIITDMJ.

I would have not accomplished this task, if I am not there in IITK, for which my sincere regards to Prof. S G Dhande by virtue of whom I came to IITK.

On behalf of my family and on my own behalf I would like to owe my sincere thanks and regards to Prof. Vyas and Dr. Mamta Vyas madam for their commendable support towards me and my family during the last ten years of my stay at IITK.

I would extend my sincere regards to Prof. V K Jain, Prof. S K Choudhury, Prof. Shantanu Bhattacharya, Prof. Brahma Deo and Prof. Sandeep Sangal for guiding me during my course work.

My heartiest thanks and acknowledgments to my faculty colleagues at IIITDMJ, Dada Saheb Ramteke, Dr. Pritee Khanna, Dr. Rajesh Pandey, Dr. Prabir, Dr. Pavan Kankar and Dr. Jawar Singh for continuous encouragement and support during my work at IIITDMJ.

I would express my sincere thanks for the support of past and present members of 4i-lab, Mr. Virendra Singh, Mr. Mohd. Mohsin, Mr. Vijay Pandey, Mr. Manoj Rawat, Mr. Anupam Shukla, Mr. Vijay Pal, Mr. Rajesh, and Mr. Santosh Pramanik. I also wish to express my thanks to the staff of Workshop Annexe, IIITDMJ for their support in conducting the experiments. I would also pay my sincere regards to the staff of manufacturing science lab, IITK.

I am very much thankful for the financial support accorded by DORA, IITK in spite of me being an external candidate for attending a conference abroad. The technical support team of OMAX, USA helped me as and when required while conducting trials. My sincere regards to Dr. Ohlsen, Dr. Patrick Turpin and Dr. Lars Fischer.

The technical discussions I had with my friends of manufacturing science lab, Dr. Karhikeyan, Dr. Subbu, Nadeem, Dr. Ajay, Dr. Ravi Shankar and Anirbhan are highly acknowledged. The time I spent with my friends of AP particularly Sastry, Yugandar, Bhanu Kishore, Dr. Suresh Behara, Dr. Madan, Dr. Surender, Dr. Venu Chandra who made my stay at IITK very enjoyable and memorable.

Lastly, I am very much grateful to my wife and parents who understood my interest and motivation for a research career even after a long gap of 7 years. Without their continuous moral support, this work wouldn't have been possible. The enormous support of my wife Srilu in lending her hand towards my work and managing kids alone in my absence many times during my research, motivated me to complete the task smoothly. Special thanks to my children Sanjana and Srujan, who made my life always happier and cheerful all the times beyond academics and research.

There are many friends, colleagues and others whose direct and indirect involvement has helped me to complete this research work. I once again thank one and all of them.

T V K GUPTA

SYNOPSIS

| | |
|---|---|
| Name of the Student: T V K Gupta | Roll No: Y8105090 |
| Degree for which submitted: Ph.D. | Department: Mechanical Engineering |
| Thesis Title: In-Process monitoring of Abrasive Water Jet Milling | |
| Name(s) of the thesis supervisors: | |
| <i>Internal</i> | <i>External</i> |
| Prof. J. Ramkumar, Prof. N. S. Vyas, Department of Mechanical Engg. I.I.T.Kanpur | Prof. Puneet Tandon, Mechanical Engineering Discipline PDPM I.I.I.T.D.M Jabalpur |
| Month and year of thesis submission: March 2014 | |

Development of exotic materials and machining of complex features is a major challenge in the current manufacturing scenario, which led to the development of new hybrid and allied unconventional manufacturing processes like Electric Discharge Machining (EDM), Electrochemical Machining (ECM), Water Jet Machining (WJM), Abrasive Water Jet machining (AWJM), Electric Discharge Deposition(EDD), Magnetic Abrasive Finishing(MAF) to name a few. Amongst the unconventional processes, AWJM technique is used for processing all kinds of materials e.g. hard/soft/fragile, etc. Some of the major advantages of AWJM include minimum HAZ, higher cutting ability, etc. which lead to an increased demand of components/products made of hard to cut materials in a variety of engineering sectors. While, AWJM is an established method for through cutting, the recent focus is on blind pocket milling to generate features in a cost effective manner.

The need to remove redundant material, from components made of hard materials without losing strength, is increasing rapidly, especially in aerospace and defense industries. Chemical milling has been extensively used for this purpose. However, the disadvantage with chemical process is the high cost and the reduced fatigue life of the post processed components, due to induction of residual stresses.

AWJM can be considered as a machining process for milling applications with the added advantage of low cutting forces and minimum distortion in the workpiece after machining. The present research work investigates AWJM process for milling of blind pocket generation. Stainless Steel (SS304) material is chosen as the milling

material due to its increased demand in aerospace and automobile manufacturing sectors.

A major disadvantage of AWJ-milling is poor finish and therefore maintaining precise dimensional and machining tolerances became an important requirement. The aerospace industry considers surface finish as a prime characteristic of the component apart from the dimensional tolerances. The factors that affect tolerance and surface finish are process parameters like jet pressure, abrasive flow rate, feed rate, standoff distance, traverse speed, etc. Besides the impact force, the high energy collimated jet generates deflection and vibration which influence the geometry of the feature. Based on the previous published reports, attempts were made to address the role of process parameters on material removal rate (mrr), surface roughness and depth, separately. Not much literature is available on dimensional accuracies, surface morphology, and process monitoring methods on AWJ milling applications. The objectives of the present work are:

- To develop a setup for conducting statistically designed experiments to study the role of individual process parameters on mrr rate, depth and surface roughness for pocket milling; further, to develop an empirical model for volumetric material removal rate and comparison with a generic mathematical model.
- To conduct experiments for fabrication of micro-channels on the developed setup and to investigate the effect of process parameters on the geometrical parameters of the micro-channel and to develop regression models to characterize the fabricated channel.
- To develop a theoretical model for the jet impact force acting on the surface and understand the influence of process parameters on the force which affect the geometry.
- Multi-response optimization of the channel geometry and to assess the advantage of using artificial neural networks (ANN) for AWJ milling process monitoring using force and jet vibration signals.

Attempt is made in the present work to gain an insight into the physics of AWJ milling and to evaluate the performance in terms of the dimensional accuracies, tolerances, etc. The four parameters considered in the present work are traverse speed, abrasive flow rate, abrasive size and standoff distance (SOD). Taking each parameter at

3-levels, full factorial experimental set is generated using DOE approach which lead to a total of 81 (3^4) runs. Experiments are conducted to generate blind pockets of size 20 mm X 20 mm using raster tool path with 0.4 mm step over. The milled pockets are measured for mrr, surface roughness and pocket depth.

Buckingham π -theorem dimensional analysis technique is used to develop an empirical model for the mrr in pocket milling. This method offers the advantage of being simpler than the method of solving simultaneous equations for obtaining the influence of parameters on the output. The developed predicted model has a variation of 0.1-0.5 mm³/sec in mrr with the experimental results. The percentage deviations range from 0.5-8.5% for various SODs, 0.2-12.0% at different abrasive flow rates and 0.1-7.0% for varying abrasive sizes. The experimental results on pocket milling show that at SOD 4 mm and at abrasive flow rate 0.38 kg/min the mrr are higher with improved surface roughness. Here the material removal mechanism shifts from cutting wear mode to deformation mode. A fine abrasive mesh (# 160) size gives a better surface. The experimental and the predicted mrr are then compared with the generic material removal model.

In abrasive water jet milling digging has been observed frequently at the corners of the features. This is due to deceleration of the jet at the corners, where the jet changes its direction of motion. Owing to this phenomenon, the force data captured in pocket milling could not provide much conclusive information to understand the mechanism of material removal. Following this, linear micro-channels were milled to enable interpretation of the measured forces.

Experiments were conducted to fabricate linear micro-channels with force and vibration as monitoring parameters. Experimental investigations are carried to study the role of process parameters on the channel (width, depth, taper and surface roughness) characteristics. The significant parameters from ANOVA results were used to develop generalized regression models. Abrasive size and traverse speeds and their interaction were found to be the influencing parameters on the channel topology. A theoretical force model developed based on theory of particle momentum is validated. The error between the theoretical and experimental force at abrasive flow rate of 0.49 kg/min shows that collisions and fragmentation phenomenon is dominated at high abrasive flow rates which reduces the cutting efficiency.

Multi-response optimization has been carried out using grey relational analysis. The maximum grey relational grade gives an optimum set of input parameters.

Another objective of this research work was to develop online monitoring to increase the efficiency and quality of the process. Artificial Neural Networks (ANN) back propagation algorithm has been used to estimate the dimensional parameters of the channels. Force and jet vibration signal, and the input process parameters are taken as the elements of the input vector; the output vector consists of micro-channel characteristics. Training and validation results from various architectures are presented and a comparison is made with the experimental results within an error of 5-6%.

The thesis consists of the following seven chapters.

Chapter 1 gives a general introduction of unconventional machining processes while describing in detail the abrasive water jet machining process. This is followed by the motivation behind the present research and identified research gaps in milling process with AWJM. Chapter 1 finally outlines the scope of the research carried out. **Chapter 2** presents the literature covering the developments of AWJM process, classification of water jets, water preparation systems, pressure generation, abrasive feeding systems, etc. A brief theory of jet formation, material removal mechanism, structure of the cut surfaces, parametric optimization, mathematical and regression models, process monitoring techniques is also presented. The chapter concludes with on date state of the art research on AWJ milling. **Chapter 3** deals with design and development of experimental setup fixtures, experimentation and data acquisition. Two experimental setups are developed, one for pocket milling and another for fabrication of micro-channels. The investigations on the role of individual process parameters on mrr, depth and surface roughness for pocket milling are reported. **Chapter 4** details the empirical model development for volumetric mrr for pocket milling using dimensional analysis technique. This is followed by a comparison of the predicted and experimental values with the theoretical model. The chapter also discusses the development of jet impact force model and its validation. In **Chapter 5** the dimensional accuracies and surface characteristics of the micro channels are discussed. This includes study of the parametric effect on the channels dimensions (both linear and angular), followed by regression and ANOVA analysis. Further, investigations on the surface characteristics using scanning electron microscopy are reported. Control, monitoring and optimization techniques in AWJM are discussed in **Chapter 6**. Grey relational analysis for multi-objective optimization of the channel geometry has been carried and an attempt to use

ANN to access the process performance is reported. Various network architectures tested to supervise the process are explained. **Chapter 7** outlines the major conclusions based on the outcome of the research carried out and concludes with a comprehensive scope for future work on AWJM milling.

TABLE OF CONTENTS

| | |
|------------------------|------------|
| LIST OF FIGURES | XV |
| LIST OF TABLES | XIX |
| NOMENCLATURES | XX |

CHAPTER 1: INTRODUCTION

| | | |
|-----|---|---|
| 1.1 | Background | 1 |
| 1.2 | Abrasive Water Jet Machining | 2 |
| | 1.2.1. Introduction to Abrasive Water Jet Machining | 2 |
| | 1.2.2. Process characteristics | 3 |
| | 1.2.3. Monitoring and Control | 3 |
| 1.3 | Motivation | 4 |
| 1.4 | Research Gaps | 5 |
| 1.5 | Aim | 5 |
| 1.6 | Objectives and scope of the work | 6 |
| 1.7 | Organization of the thesis | 6 |

CHAPTER 2: LITERATURE REVIEW

| | | |
|-----|---|----|
| 2.1 | Introduction | 9 |
| 2.2 | Classification of high speed water jets | 10 |
| 2.3 | Abrasive water jet injection systems | 12 |
| | 2.3.1. High pressure generation system | 12 |
| | 2.3.2. Water jet cutting head | 14 |
| | 2.3.3. Abrasive feeding system | 15 |
| | 2.3.4. Catcher unit | 16 |
| | 2.3.5. CNC motion controller | 16 |
| 2.4 | Theory of abrasive water jet generation | 17 |

| | | |
|------|--|----|
| 2.5 | Material removal mechanism in AWJM | 20 |
| 2.6 | Abrasive water jet cut surface | 22 |
| 2.7 | Role of process parameters | 25 |
| | 2.7.1 Hydraulic parameters | 26 |
| | 2.7.2 Abrasive parameters | 27 |
| | 2.7.3 Mixing parameters | 28 |
| | 2.7.4 Cutting parameters | 28 |
| 2.8 | Control and supervision of AWJM process | 30 |
| 2.9 | Signal Processing techniques and methods | 33 |
| | 2.9.1 Statistical analysis | 33 |
| | 2.9.2 Time series analysis | 33 |
| | 2.9.3 Fast Fourier Transform (FFT) | 34 |
| | 2.9.4 Wavelet Transform | 34 |
| 2.10 | Process modeling in AWJM | 35 |
| 2.11 | Concept of AWJ Milling: Current status | 37 |
| 2.12 | Motivation for AWJ Milling | 39 |
| 2.13 | Summary of literature | 39 |

CHAPTER 3: EXPERIMENTAL INVESTIGATIONS ON ABRASIVE WATER JET MILLING

| | | |
|-----|---|----|
| 3.1 | Introduction | 41 |
| 3.2 | Design of experiments | 42 |
| | 3.2.1 Analysis of data | 43 |
| | 3.2.2 Analysis of variance (ANOVA) | 43 |
| 3.3 | Methodology | 44 |
| 3.4 | Experimental setup | 44 |
| | 3.4.1 Fixture and tool path strategy | 48 |
| | 3.4.2 Materials | 51 |
| 3.5 | Full factorial experimental design | 53 |
| 3.6 | Measurement and examination of the process and pocket milling characteristics | |
| | 3.6.1 Material removal rate | 54 |
| | 3.6.2 Surface roughness | 54 |
| | 3.6.3 Pocket depth | 54 |

| | | |
|-------|---|----|
| 3.7 | Experimental investigations on pocket milling | 56 |
| 3.7.1 | Role of traverse speed | 57 |
| 3.7.2 | Effect of pressure | 57 |
| 3.7.3 | Effect of standoff distance | 59 |
| 3.7.4 | Influence of abrasive flow rate | 60 |
| 3.7.5 | Role of abrasive size | 61 |
| 3.7.6 | Effect of process parameters on pocket depth | 63 |
| 3.8 | Summary and conclusions | 65 |

CHAPTER 4: EMPIRICAL AND THEORETICAL MODELLING

| | | |
|-------|---|----|
| 4.1 | Introduction | 67 |
| 4.2 | Material removal by an individual abrasive particle | 68 |
| 4.3 | Dimensional analysis for material removal rate | 69 |
| 4.3.1 | Predictive model for material removal rate | 72 |
| 4.3.2 | Nomenclature | 72 |
| 4.3.3 | Predictive model for material removal rate | 73 |
| 4.4 | Theoretical modeling of forces | 75 |
| 4.4.1 | Calculation of abrasive water jet velocity | 78 |
| 4.4.2 | Experimental validation and conclusions | 80 |
| 4.5 | Theoretical calculations for MRR | 85 |
| 4.6 | Summary | 89 |

CHAPTER 5: GEOMETRY AND CHARACTERISTICS OF THE MICRO CHANNELS FABRICATED WITH AWJM

| | | |
|-------|--|-----|
| 5.1 | Introduction | 91 |
| 5.2 | Cut geometry measurements | 92 |
| 5.3 | Role of process parameters on channel geometry | 95 |
| 5.3.1 | Influence of process parameters on channel width/depth ratio | 96 |
| 5.3.2 | Effect of process parameters on channel depth | 99 |
| 5.3.3 | Influence of process parameters on taper | 103 |
| 5.3.4 | Role of process parameters on the channel surface roughness | 105 |

| | | |
|-----|-------------------------------|-----|
| 5.4 | Regression Analysis | 109 |
| 5.5 | Surface morphological studies | 110 |
| 5.6 | Summary | 112 |

CHAPTER 6: OPTIMIZATION, CONTROL AND ARTIFICIAL NEURAL NETWORKS

| | | |
|-----|---|-----|
| 6.1 | Introduction to supervision and monitoring | 115 |
| 6.2 | Optimization using Grey Relational Analysis | 117 |
| | 6.2.1. Grey relational analysis for AWJM micro-channel geometry | 119 |
| | 6.2.2. Results and discussion | 121 |
| 6.3 | ANN for AWJM | 123 |
| | 6.3.1 Preparation of training and target vector set | 125 |
| | 6.3.2 Network Architecture and Training | 126 |
| | 6.3.3 Results and discussion | 130 |
| 6.4 | Summary | 132 |

CHAPTER 7: CONCLUSIONS AND SCOPE FOR FUTURE WORK

| | | |
|------|---|-----|
| 7.1. | Conclusions | 135 |
| | 7.1.1. Pocket Milling | 135 |
| | 7.1.2. Micro-channels | 136 |
| | 7.1.3. Analysis of theoretical and empirical models | 137 |
| | 7.1.4. Multi-response optimization | 137 |
| | 7.1.5. Artificial neural networks | 138 |
| 7.2. | Scope for future work | 138 |

| | |
|-------------------|-----|
| REFERENCES | 140 |
|-------------------|-----|

| | |
|---------------------|-----|
| PUBLICATIONS | 150 |
|---------------------|-----|

LIST OF FIGURES

| | | |
|-----------|---|----|
| Fig. 2.1 | Classification of water jets | 11 |
| Fig. 2.2 | Schematic of the Abrasive Water Injection Jet System (AWIJS) | 12 |
| Fig. 2.3 | Schematic of an ultra-high pressure water preparation system | 13 |
| Fig. 2.4 | Cutting head assembly | 14 |
| Fig. 2.5 | Abrasive particle acceleration process inside the nozzle | 14 |
| Fig. 2.6 | Schematic of (a) focusing nozzle and (b) orifice | 16 |
| Fig. 2.7 | Structure of high speed water jet | 18 |
| Fig. 2.8 | Material-removal mechanisms by solid particle erosion | 21 |
| Fig. 2.9 | Different stages in AWJ cutting | 23 |
| Fig. 2.10 | Schematic of the kerf geometry obtained with AWJ cutting | 24 |
| Fig. 2.11 | Relative strength zones in a water jet | 25 |
| Fig. 2.12 | Process parameters in AWJ cutting | 26 |
| Fig. 3.1 | OMAX 2626 Unit-Experimental setup photograph | 45 |
| Fig. 3.2 | High pressure generation pumping system | 46 |
| Fig. 3.3 | Schematic of the experimental setup for pocket milling | 47 |
| Fig. 3.4 | Experimental setup photograph for pocket milling | 47 |
| Fig. 3.5 | Cutting head assembly | 47 |
| Fig. 3.6 | Work holding fixture | 48 |
| Fig. 3.7 | (a) Tool path strategy and (b) sample pocket image | 48 |
| Fig. 3.8 | Typical force signal for a raster tool path pocket milling | 49 |
| Fig. 3.9 | Schematic of the experimental setup for micro-channel fabrication | 49 |
| Fig. 3.10 | Experimental Setup for the micro-channel fabrication | 50 |

| | | |
|--------------|---|----|
| Fig. 3.11 | Micro channels fabricated on SS304 plate | 50 |
| Fig. 3.12 | Typical force signal for a micro-channel | 50 |
| Fig. 3.13 | Jet vibration signal during the channel fabrication | 51 |
| Fig. 3.14(a) | Abrasive particle photograph for # 80 abrasive | 52 |
| Fig. 3.14(b) | Abrasive Particle photograph for # 120 abrasive | 52 |
| Fig. 3.14(c) | Abrasive Particle photograph for # 160 abrasive | 53 |
| Fig. 3.15 | Effect of Pressure and Traverse speed on MRR | 58 |
| Fig. 3.16 | Effect of Pressure and Traverse speed on Ra | 58 |
| Fig. 3.17 | Effect of SOD and Traverse speed on MRR and Ra | 59 |
| Fig. 3.18 | Effect of AFR and Traverse speed on MRR and Ra | 61 |
| Fig. 3.19 | Effect of Abrasive size and Traverse speed on MRR and Ra | 62 |
| Fig. 3.20 | Effect of SOD and Traverse speed on pocket depth | 63 |
| Fig. 3.21 | Effect of AFR and Traverse speed on pocket depth | 64 |
| Fig. 3.22 | Effect of Abrasive size and Traverse speed on pocket depth | 64 |
| Fig. 4.1 | Comparision between predicated vs experimental values for MRR at SOD (a) 3 mm (b) 4 mm (c) 5mm (d) % deviation | 74 |
| Fig. 4.2 | Comparision between predicated vs experimental values for MRR at AFR (a) 0.27 kg/min (b) 0.38 kg/min (c) 0.49 kg/min (d) % deviation | 74 |
| Fig. 4.3 | Comparision between predicated vs experimental values for MRR at (a) # 80 abrasive (b) # 120 abrasive (c) #160 abrasive (d) % deviation | 75 |
| Fig. 4.4 | Schematic of the abrasives impacting the surface | 76 |
| Fig. 4.5 | Traverse tool paths of the focusing tube. | 76 |
| Fig. 4.6 | Particle distributions on the exit focus diameter. | 77 |
| Fig. 4.7 | Theoretical and experimental forces for different abrasive sizes | 82 |
| Fig. 4.8 | % Error in experimental and theoretical forces for various abrasive sizes and AFRs | 82 |
| Fig. 4.9 | Theoretical and experimental forces for different SOD | 83 |

| | | |
|-----------|--|-----|
| Fig. 4.10 | % Error in experimental and theoretical forces at various SODs and AFRs | 83 |
| Fig. 4.11 | Theoretical and experimental forces for different traverse speeds | 84 |
| Fig. 4.12 | % Error in experimental and theoretical forces at various traverse speeds and AFRs | 84 |
| Fig. 4.13 | Comparison of experimental, predicted and theoretical MRR | 88 |
| Fig. 5.1 | Cross-section of the profile | 92 |
| Fig. 5.2 | Schematic of the cut geometry | 93 |
| Fig. 5.3 | Sample surface roughness profile of the micro-channel | 93 |
| Fig. 5.4 | Cut geometry photographs for different abrasive sizes | 94 |
| Fig. 5.5 | Effect of traverse speed and SOD on kerf width to depth ratio | 96 |
| Fig. 5.6 | Effect of traverse speed and AFR on kerf width to depth ratio | 97 |
| Fig. 5.7 | Effect of traverse speed and abrasive size on kerf width/depth ratio | 98 |
| Fig. 5.8 | Effect of traverse speed and SOD on channel depth | 100 |
| Fig. 5.9 | Effect of traverse speed and AFR on channel depth | 101 |
| Fig. 5.10 | Effect of traverse speed and abrasive size on channel depth | 101 |
| Fig. 5.11 | Effect of traverse speed and SOD on taper | 103 |
| Fig. 5.12 | Effect of traverse speed and AFR on taper | 104 |
| Fig. 5.13 | Effect of traverse speed and abrasive size on taper | 104 |
| Fig. 5.14 | Effect of traverse speed and SOD on surface roughness | 106 |
| Fig. 5.15 | Effect of traverse speed and AFR on surface roughness | 107 |
| Fig. 5.16 | Effect of traverse speed and abrasive size on surface roughness | 107 |
| Fig. 5.17 | SEM image of the experimental machined sample # 80 abrasive | 111 |
| Fig. 5.18 | SEM image of the experimental machined sample # 120 abrasive | 111 |
| Fig. 5.19 | SEM image of the experimental machined sample #160 abrasive | 112 |
| Fig. 6.1 | Response graph for the mean grey relational grades | 122 |

| | | |
|----------|---|-----|
| Fig. 6.2 | Grey Relational Grade Graph | 123 |
| Fig. 6.3 | A typical 3-layer back propagation network | 124 |
| Fig. 6.4 | Convergence pattern for various Back Propagation Neural Networks | 128 |
| Fig. 6.5 | Regression Plot for Architecture 9 (6-12-10-4) | 130 |
| Fig. 6.6 | Comparison of the experimental and ANN predicted values on (a) Width (b) Depth (c) Taper (d) Surface roughness | 131 |

LIST OF TABLES

| | |
|--|-----|
| Table 2.1 Significance of AWJ parameters on the operational and design factors | 29 |
| Table 2.2 Significance of AWJ parameters on machining results | 30 |
| Table 3.1 Technical Specifications of Abrasive Water Jet Machining System | 46 |
| Table 3.2 Mechanical Properties of the SS 304 | 51 |
| Table 3.3 Physical and chemical properties of garnet | 51 |
| Table 3.4 Range of input process parameters | 53 |
| Table 3.5 Experimental data for pocket milling | 54 |
| Table 4.1 Typical experimental data of the impact forces | 80 |
| Table 5.1 Experimental data of width, depth, taper and surface roughness of the micro channels | 94 |
| Table 5.2 ANOVA analysis-channel width | 99 |
| Table 5.3 ANOVA analysis-channel depth | 102 |
| Table 5.4 ANOVA analysis-channel taper | 105 |
| Table 5.5 ANOVA analysis-surface roughness | 108 |
| Table 6.1 Grey relational coefficients, Grey Relational Grade and Rank for the micro channels | 119 |
| Table 6.2 Average Grey Relational Grade for Factor and Levels | 122 |
| Table 6.3 Typical input and output data for the neural network | 125 |
| Table 6.4 List of neural network architectures | 127 |
| Table 6.5 Results of various ANN architectures | 127 |
| Table 6.6 Experimental and ANN predicted values of test set target parameters | 129 |

NOMENCLATURES

| | |
|-------------------|--|
| \dot{m}_L | Air mass flow rate |
| \dot{m}_a | Abrasive mass flow rate |
| \dot{m}_w | Water mass flow rate |
| A_o | Orifice cross-sectional area |
| A | Focusing tube cross-sectional area |
| E_w | Energy of water jet |
| F_X | Horizontal force |
| F_Y | Vertical force |
| F | Impact Force |
| H_w | Vicker's Hardness |
| K_1 | Constant |
| K | Constant, ratio of vertical to horizontal force |
| M_1 | Momentum |
| N | No. of abrasive particles |
| P_{atm} | Atmospheric pressure |
| P_{awj} | Power of abrasive water jet |
| P | Water Jet Pressure |
| Q | Water flow rate |
| R | Ratio of abrasive mass flow rate to water mass flow rate |
| \dot{V} | Volumetric material removal rate |
| $V_{Cutting}$ | Cutting volume |
| $V_{Deformation}$ | Deformation volume |
| c_d | Co-efficient of discharge |
| d_F | Focusing tube diameter |
| d_o | Orifice diameter |

| | |
|--------------|---------------------------------------|
| m_p | Mass of abrasive particle |
| v_L | Velocity of air |
| v_{awj} | Velocity of abrasive water jet |
| v_{el} | Elastic velocity |
| v_o | Velocity of water at orifice exit |
| v_{oth} | Theoretical velocity |
| v_p | Velocity of particle |
| v_{pipe} | Water velocity at the orifice entry |
| v_{po} | Initial velocity of abrasive particle |
| Δt_F | Focusing tube interaction time |
| Δt_o | Layer interaction time |
| Δt | Time available per particle |
| h | Standoff distance |
| d | Diameter of abrasive |
| g | Acceleration due to gravity |
| l | Length of traverse path |
| t | Interaction time |

GREEK SYMBOLS

| | |
|----------------------|-------------------------------------|
| α | Constant |
| ε | Specific energy |
| ε_{Mcut} | Specific energy in cutting mode |
| ε_{Mdef} | Specific energy in deformation mode |
| μ | Efficiency coefficient |
| ρ | Density of abrasive |
| ρ_w | Density of water |
| σ_f | Flow stress |
| Γ | Grey relational grade |

| | |
|--------|--|
| π | Pi |
| χ | % of abrasives in the abrasive water jet mixture |
| η | Momentum transfer efficiency |
| ψ | Constant |

ACRONYMS

| | |
|-------|------------------------------|
| AWJM | Abrasive Water Jet Machining |
| AFR | Abrasive Flow Rate |
| ANOVA | Analysis of Variance |
| MRR | Material Removal Rate |
| SEM | Scanning Electron Microscope |

Chapter 1

INTRODUCTION

| | |
|---|---|
| 1.1 Background | 1 |
| 1.2 Abrasive Water Jet Machining | 2 |
| 2.2.1. Introduction to Abrasive Water Jet Machining | 2 |
| 2.2.2. Process characteristics | 3 |
| 2.2.3. Monitoring and Control | 3 |
| 1.3 Motivation | 4 |
| 1.4 Research Gaps | 5 |
| 1.5 Aim | 5 |
| 1.6 Objectives and scope of the work | 6 |
| 1.7 Organization of the thesis | 6 |

1.1 Background

Development of new materials leads to evolution and development of new manufacturing processes. The present day industries are known for their innovations in new methods/technologies to process the new materials. The current era in manufacturing is concentrating towards the modern manufacturing methods which are either conventional or unconventional in nature. Due to the requirements in processing of hard and brittle materials, modern manufacturing has led to the development of latest unconventional manufacturing methods. For the past few decades, there has been considerable interest in the development of special materials that are difficult to machine. The extraordinary properties of these materials are high specific stiffness, high strength and heat resistant, high hardness and resistant to corrosion. To name a few materials in this category used for aerospace, automobile and space applications include tough alloys, composites, hard materials (Tonshoff et al. 1988). Processing of such materials using conventional machining processes incorporate lot of technical and economic difficulties. The demand to make intricate and complex shapes with these materials has led to the development of several unconventional machining processes.

These processes can be classified into several categories such as mechanical, electrical, thermal and chemical methods based on the energy utilized and the material removal mechanisms. Most commonly used unconventional machining processes

INTRODUCTION

include Ultrasonic Machining (USM), Abrasive Jet Machining (AJM), Abrasive Water Jet Machining (AWJM), Electric Discharge machining (EDM), Electrochemical Machining (ECM), Chemical Machining (ChM), Electron Beam Machining (EBM), Laser Beam Machining (LBM) and Plasma Arc Machining (PAM). The recent developments are towards in hybrid processes, where combination of two or more processes put together to make use the advantages of each process for achieving better performance.

1.2 Abrasive Water Jet Machining

1.2.1 Introduction to Abrasive Water Jet Machining

AWJM is one of the commonly used unconventional machining techniques making use of high pressure water, which is converted to a high velocity jet and mixed with abrasives. The process of material removal is by means of erosion, and deformation caused due to high velocity impact of the abrasive particles. This process enhances the ability to cut a variety of materials, ranging from soft to hard like rubber, polymers, plastics to Titanium, Inconel, etc. as noted by Momber and Kovacevic (1998). AWJM is a complex and stochastic process influenced by a large set of process parameters which determine efficiency, economy and quality of the process. Hashish (1997) classifies the process parameters into three groups such as dynamic variables, quasi-static variables and static variables based on characteristics of the parameters. The dynamic variables include water jet pressure, abrasive flow rate, traverse rate and jet impingement angle. The quasi-static variables include the orifice size and the internal diameter of the focusing tube and the static variables include abrasive material and size, and mixing tube length. Of these parameters, dynamic variables are controllable whereas quasi- static variables are uncontrollable. Earlier investigations found that the dynamic variables have significant role in the cutting performance which is expressed in terms of depth of cut, material removal rate, kerf geometry and surface topography of the cut. The quasi-static variables undergo variation in the geometry due to wear with the continuous operation of AWJM process. This variation affects the energy of jet, mixing of abrasive particles and coherency of jet, which in turn affect the cutting results significantly (Hashish 1986a; 1991). Hence, controlling of AWJ cutting process to achieve the best quality is a challenging task.

Efforts were put by researchers to understand and improve the cutting process performance. The mechanism of material removal in AWJM process includes material erosion phenomenon by micro cutting (Finnie 1960) which involves the plastic response character of a material determined by its flow stress. As per Bitter (1963a, 1963b), material removal takes process into two modes known as ‘cutting wear’ and ‘deformation wear’. Cutting wear occurs at low impact angles and deformation wear occurs at high impact angles. Eltobgy et al. (2005) employed the concept of multiple particles erosion for surface regeneration capabilities and considered a new surface after erosion of every single particle. The work on thick materials machining reported by Kovacevic et al. (1991a) characterized the cutting process with two types of textures i.e., top smooth texture and bottom rough texture to develop a mathematical model consisting of surface roughness and process variables.

1.2.2 Process Characteristics

Striation formation is a characteristic of the AWJM technique which is a major limitation of the process. The striations formation is due to the diverging nature of the jet as the jet ejects from the mixing tube/focusing tube. The jet deviation increases with increase in the traverse speed. The abrasive particle distribution, dynamic characteristics and the machining system vibrations also lead to the striations formation (Chen et al. 1998, 2001, 2003). Surface roughness is another disadvantage of AWJM when compared to other non-conventional machining processes; which can be eliminated or minimized with suitable selection of process parameters. Experimentally it has been reported that machining at low traverse speeds result in higher material removal rates and irregular surface morphology (Ojmertz 1996). The model developed by Deam et al. (2004) predicts the fluctuations in the local curvature of the cutting face. Fluctuations in AWJM are an inherent property of the process due to high pressures involved in cutting and these cannot be eliminated completely even after precise control of the process parameters.

1.2.3 Monitoring and Control

The demand for quality products with high productivity, reliability and flexibility is the need of today’s manufacturing. This can only be achieved with incorporating automation in manufacturing. The advancements in sensor technology

and signal processing techniques can enable a machining process to be made effective in terms of control and monitoring (Axinite and Gindy 2003). The precise control of process parameters in AWJM is required to ensure high quality and consistency in cutting performance. In view of the uncontrollable quasi-static parameters in AWJ cutting, it is necessary to compensate their variation by selection of suitable dynamic variables (Kovacevic et al. 1997). Earlier attempts were made to monitor cutting process status mainly employed single sensory systems (Kovacevic and Evizi 1990, Kovacevic 1991b, Hashish et al. 1993b). A single sensor based approach may not be effective in assessing the condition of the process since the sensitivity of the acquired signal can change with varying cutting conditions and process parameters. Therefore, multiple sensors are to be employed to assess status of the process and a framework for reliable monitoring of head of the AWJ system with multi-sensory approach is suggested by Knaupp (1993).

In order to control the process within the set limits, one need to choose suitable process parameters based on the condition of the system. For this purpose, the behavior of the process needs to be modelled. Usually, empirical and semi-empirical models are employed for modeling complex non-linear machining operations. With the developments in Artificial Intelligence (AI) techniques, soft computing approaches like neural networks and fuzzy logic, modeling of complex processes are getting popular than conventional methods such as multiple regression analysis in terms of building models and accuracy of prediction, etc. (Chryssolouris and Guillot 1990). However, building an intelligent abrasive water jet cutting system requires monitoring systems with suitable sensors and strategies for controlling the process within specified limits. Such systems would be useful to achieve consistent results and utilize the abrasive water jet cutting systems more effectively and efficiently.

1.3 Motivation

Some of the major advantages of abrasive water jet cutting compared to other unconventional machining techniques are ability to cut complicated shapes, high cutting rates, high cutting efficiency, omnidirectional cutting capability, cutting with close tolerances, minimal heat affected zone, absence of stresses, non-contact process with low cutting forces, environmental friendly and highly suitable for automation (Hashish

1989a). The absence of material defects due to absence of electrical and thermal energy in the process is an added advantage in AWJM. Currently Water Jets are employed in nearly all modern industries such as automotive, aerospace, construction, environment, chemical process engineering, industrial maintenance, nuclear, manufacturing and food processing. The improvements and technological advancements are still undergoing to satisfy the industrial needs (Kovacevic et al. 1997). These few advantages motivated us to work on AWJM process. Currently, in AWJM, a paradigm shift is towards understanding and making the process available to industrial applications for a variety of techniques in machining.

1.4 Research Gaps

Based on the literature review, it was observed that AWJM is a matured process for through cutting applications and the research on pocket milling has still not received much attention till date. Two most important parameters to estimate the quality of machined surfaces in AWJ milling are depth of cut tolerance and surface roughness. The tolerance and surface roughness can be achieved with suitable selection and control of process parameters like water pressure, traverse speed, abrasive flow rate, and impact angle etc. Modeling of AWJ milling is a complex phenomenon due to the presence of continuously varying dynamic variables. Since the efforts in this direction of process control are still at an infancy stage, there exists a need to look for an effective condition monitoring system for milling applications.

1.5 Aim

The research carried out in the area of milling process with AWJM is very much limited and the aim of the present research is to investigate, understand, control and monitor AWJ milling process. One of the major advantages of AWJ milling is high material removal rate which makes the process suitable for rough/stock removal. This process can be easily applied to any material irrespective of the material properties. The intensity of abrasion process can be controlled effectively by adjusting few key parameters like abrasive type, abrasive flow rate, abrasive size, etc. The work also aims to suggest the users, suitable measures to control and monitor AWJ milling with the investigations carried on forces and jet vibrations.

1.6 Objectives and scope of the work

The objectives of the present research work in the realization of the aim are as follows:

- To develop a setup for conducting statistically designed experiments to study the role of individual process parameters on mrr rate, depth and surface roughness for pocket milling; further, to develop an empirical model for volumetric material removal rate and comparison with a generic mathematical model.
- To conduct experiments for fabrication of micro-channels on the developed setup and to investigate the effect of process parameters on the geometrical parameters of the micro-channel and to develop regression models to characterize the fabricated channel.
- To develop a theoretical model for the jet impact force acting on the surface and understand the influence of process parameters on the force which affect the geometry.
- Multi-response optimization of the channel geometry and to assess the advantage of using artificial neural networks (ANN) for AWJ milling process monitoring using force and jet vibration signals.

The current research enables us to determine the proper selection of cutting conditions to obtain a milled pocket/channel with the required dimensional accuracy. The objective of the work includes finding the output parameters with the help of input process variables and their influence on the responses.

1.7 Organization of the thesis

The present work is carried in the following modules:

- Influence of input process parameters on the output parameters like material removal rate, surface roughness, and depth on pocket milling.
- Mathematical model development for mrr and the jet forces and their validation.
- Micro-channels fabrication and study and investigate the role of process parameters on the dimensional accuracies and surface characteristics. Experiments are carried to acquire force and vibration signals of the jet while

machining to enable us to understand their influence in control and process monitoring of the process.

- Multi-response optimization using Grey Relational Analysis for the channel geometry. Application of neural networks for process monitoring and control.

Chapter 2

LITERATURE REVIEW

| | |
|--|----|
| 2.1 Introduction | 9 |
| 2.2 Classification of high speed water jets | 10 |
| 2.3 Abrasive water jet injection systems | 12 |
| 2.3.1. High pressure generation system | 12 |
| 2.3.2. Water jet cutting head | 14 |
| 2.3.3. Abrasive feeding system | 15 |
| 2.3.4. Catcher unit | 16 |
| 2.3.5. CNC motion controller | 16 |
| 2.4 Theory of abrasive water jet generation | 17 |
| 2.5 Material removal mechanisms in AWJM | 20 |
| 2.6 Abrasive water jet cut surface | 22 |
| 2.7 Role of process parameters | 25 |
| 2.7.1. Hydraulic parameters | 26 |
| 2.7.2. Abrasive parameters | 27 |
| 2.7.3. Mixing parameters | 28 |
| 2.7.4. Cutting parameters | 28 |
| 2.8 Control and supervision of AWJM process | 30 |
| 2.9 Signal Processing techniques and methods | 33 |
| 2.9.1. Statistical analysis | 33 |
| 2.9.2. Time series analysis | 33 |
| 2.9.3. Fast Fourier Transform (FFT) | 34 |
| 2.9.4. Wavelet Transform | 34 |
| 2.10 Process modeling in AWJM | 35 |
| 2.11 Concept of AWJ milling: Current status | 37 |
| 2.12 Motivation for AWJ milling | 39 |
| 2.13 Summary of literature | 39 |

2.1 Introduction

Initially in the 1970s processing and cutting of soft materials like wood, plastics, rubber, etc. are done using high velocity water jets. In 1990s, abrasive particles were added to water to make this process as AWJM for cutting hard and brittle materials. Later, abrasive water jets received greater attention and various applications evolved in a variety of engineering fields, including manufacturing, but not limited to cleaning, drilling, cutting, milling, turning, threading, peening and polishing. The efforts put by researchers in the past were mainly concentrated towards the study and feasibility of AWJs for processing and cutting a range of materials including ductile and brittle; to

understand the material removal mechanism; to assess the process performance, and for optimization of the process (Hashish 1991). The present day research on AWJM is concentrating towards identifying its applications to several of manufacturing methods, to monitor and control the process for new applications (Kovacevic et al. 1997; Hoogstrate et al. 1997; Momber and Kovacevic 1998). Considerable interest has been reported on process automation to achieve the best possible output (Louis and Meier 1991; Hashish et al. 1993; Brandt and Louis 2000). Several attempts were made in development of sensors for monitoring the effect of parameters and to model for controlling of the process (Kovacevic and Evizi 1990; Kovacevic 1991a; Kovacevic et al. 1995; 1998; Chakravarthy and Babu 2000).

Attempts made by researchers in AWJM are concentrated towards the separation of the work pieces (i.e. cutting applications) only. Few literatures available in AWJ milling applications and the gaps are addressed in the current research. This chapter presents the current state of the art in milling applications with AWJM and a brief review of the literature on AWJM covering the basic aspects of the process, type of jet formation, material removal mechanisms, etc.

2.2 Classification of high speed water jets

Of late, high speed water jets have gone several improvements and it is very difficult to define a critical pressure which separates a low pressure jet and a high pressure jet. High speed water jets use pressures in the range of 60-450 MPa, with velocities going up to the order of 1000 m/sec. These systems can be classified as plain water jets, water additive jets and abrasive water jets. Plain water jets can be either continuous, discontinuous or cavitation jets. Figure 2.1 gives the classification of the water jets. In relation to the type of loading, the jet can be discontinuous if it generates a discontinuous jet on the impact side and every water jet generates discontinuous phases during impact due to pressure fluctuations and droplet formation (Momber 1998). Discontinuous jets can be artificially broken up by external mechanisms while continuous jets are not influenced by external mechanisms. All the high pressure jets available today are continuous in nature, where high pressure water is allowed to pass through sapphire/diamond orifice having a diameter of 0.05-0.5 mm.

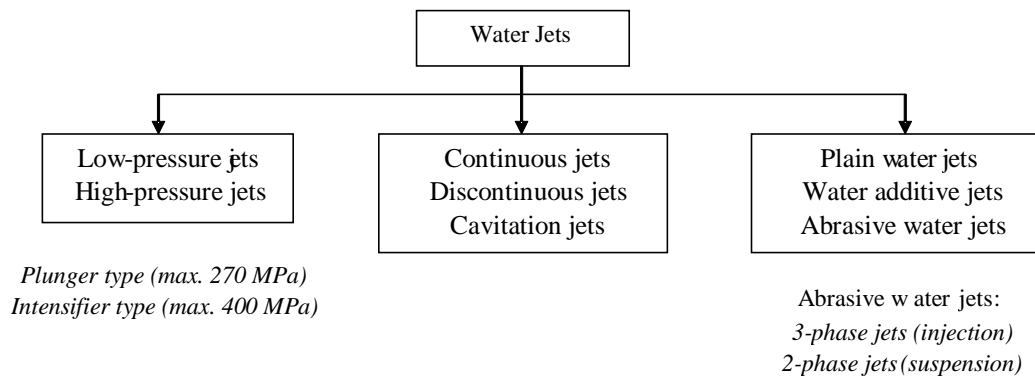


Fig. 2.1: Classification of water jets

Plain water jets are capable of cutting soft and thin materials like as rubber, wood, cardboard, etc. The cutting capability of plain water jets are enhanced with the recent developments of high pressure jets to enable for cutting metals. A mixture of additives and abrasives are added to the water jet which was the first attempt to make an abrasive water jet (Hollinger et al. 1989). Abrasive water jets are further divided according to their generation and phase composition. There exist two varieties of abrasive water jets namely Abrasive Water Injection Jets (AWIJ) and Abrasive Water Suspension Jets (AWSJ). AWIJ is produced by mixing abrasives into high velocity water jet which is usually generated through a small orifice; in a mixing chamber and then exit through a mixing tube/focusing nozzle; the schematic of AWIJ type system is shown in Figure 2.2. AWIJ is a three-phase mixture containing water (74%), abrasive (23%) and air (3%) by mass (Momber et al. 1998). The kinetic energy of water is transferred to the abrasives accelerating the particles close to 900-1000 m/sec with an inlet pressure of 350-400 MPa. In AWJM, the abrasives play a major role in the material removal mechanism, where each particle's edge acts as a single point cutting tool and the high pressure water aids for the momentum transfer to the abrasives.

In AWSJ, water at high pressure and abrasives are mixed in a high pressure chamber is discharged through the nozzle. Here, the suspension jet is a two phase mixture consisting of water and abrasives. In AWSJ, the energy estimated is 20% more than the AWIJ which allows AWSJ 5 times more effective than AWIJ in processing materials (Hashish 1991). These systems are difficult in construction and handling due to which only low pressure systems less than 70 MPa are practically in use. Due to efficient particle acceleration and jet stability, AWSJs are widely used for cutting,

mining and also micro machining applications. The present research has been carried out on a high pressure AWJM system using a continuous jet which is based on an injection type abrasive water jets.

2.3 Abrasive Water Jet Injection Systems

A schematic of the AWIJ cutting system, shown in above Figure 2.2 consists of several sub-systems namely, water preparation, pressure generation, abrasive water jet cutting head and an abrasive feeding system. Catcher tank and the CNC controller are a part of the system which is in-built within AWJM. Many times water contains total dissolved salts (TDS) consisting of Ca, Fe which tends to damage the orifice and seals working at higher pressures. The presence of salts in water is prone to formation of scales on the walls of the tubes and casings. To avoid this type of culmination, water before feeding to the high pressure generation system, is made free of the dissolved salts that can be obtained using some purification systems and then fed to the cutting head.

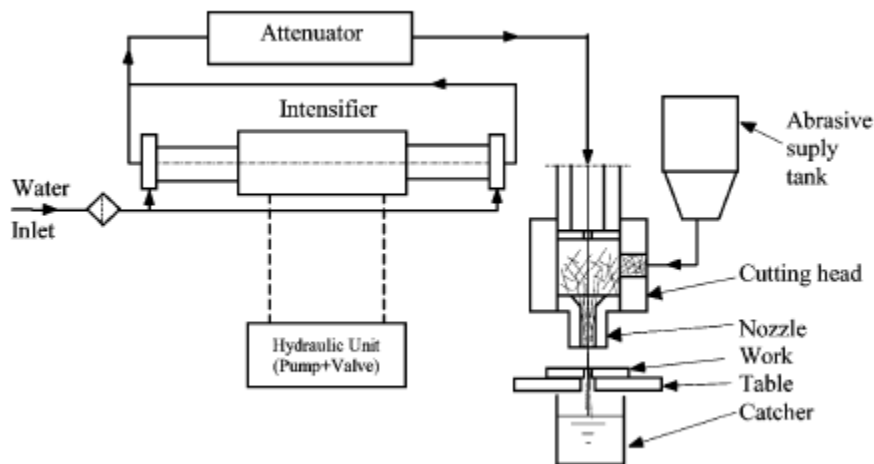


Fig 2.2: Schematic of the Abrasive Water Injection Jet System (AWIJS) (Kulekci 2002)

2.3.1. High pressure generation system

High pressure water is required to be delivered to the cutting head of the machine at a given rate, which can be achieved by the use of high pressure generation systems. Pressures up to 300 MPa are generated using plunger type pumps and an intensifier is also required to generate such high pressures. An intensifier is similar to an amplifier since it converts the energy from a low-pressure hydraulic fluid into ultra-

high-pressure water. The ratio of the pressures between the working fluid and the system fluid is known as the intensification ratio which should range from 1:10 to 1:25 if the required pressure is of the order of 400 MPa. Figure 2.3 shows the schematic of a double acting hydraulic intensifier. The operating cycle of an intensifier consists of two strokes, suction and power stroke in each reciprocating motion. There are two phases in each stroke, an acceleration phase and a superseding phase. The phase in which water is compressed and pressure is increased is known as acceleration phase. Here, the plunger moves rapidly as the fluid pressure in the cylinder at the beginning of the stroke is relatively low and the net force driving the plunger is high. Usually this phase lasts only for a few milliseconds and the duration depends on mass of the piston and its multiplication ratio.

The superseding phase is a phase where the pressure becomes stabilized (reaches its maximum pressure) and balanced with its duration depending on orifice size and geometrical parameters of the high-pressure cylinder. Therefore, a large deviation in the orifice size may affect the superseding phase of the plunger stroke. The first 15% of the piston stroke is used to pressurize and compress water in the cylinder without delivering water to the system due to compressibility of water at 350 MPa (Kulekci 2002). The undesirable pressure fluctuations in the cylinder affect the life of orifice, seals and valves due to fatigue loading. An attenuator mounted on the pressure line reduces the fluctuations during every cycle.

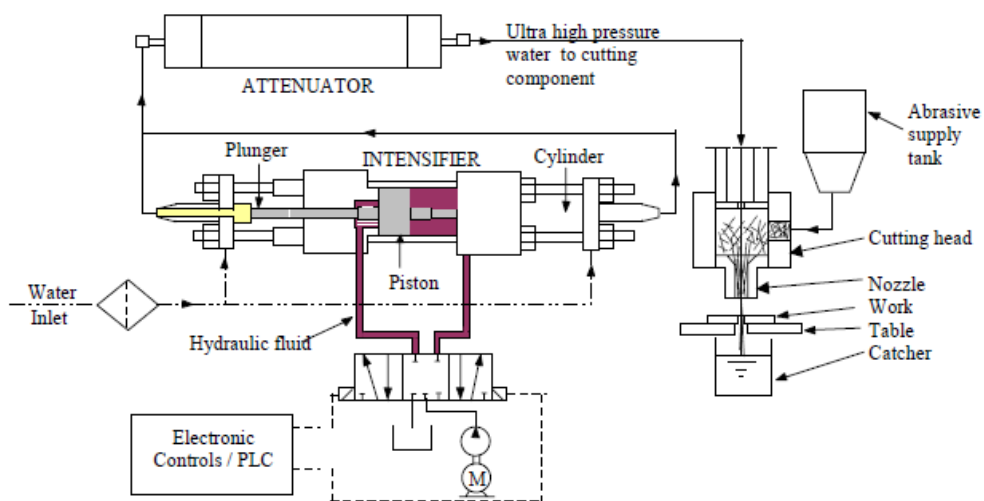


Fig. 2.3: System layout of an ultra-high pressure water preparation (Adnan 2004)

2.3.2. Water jet cutting head

Figure 2.4 shows the various parts associated with the cutting head consisting of an orifice (Figure 2.6 (b)), mixing chamber and a focusing nozzle. The cutting head can be considered as an end effector of the AWJ system to which high pressure water and abrasives are supplied to create the high velocity jet that performs the machining process. Design and the alignment of the integral parts of this unit are crucial for an efficient machining process. The cutting process can be enhanced by increasing the efficiency of abrasive particle mixing and its entry. The phenomenon of the process of abrasive mixing is very difficult to observe due to the complex turbulent nature of the process (Mendi et al. 1999). The complexity is due to the fact that particle velocities are very high (nearly 1000 m/s) with particle sizes ranging from 0.1-0.5 mm.

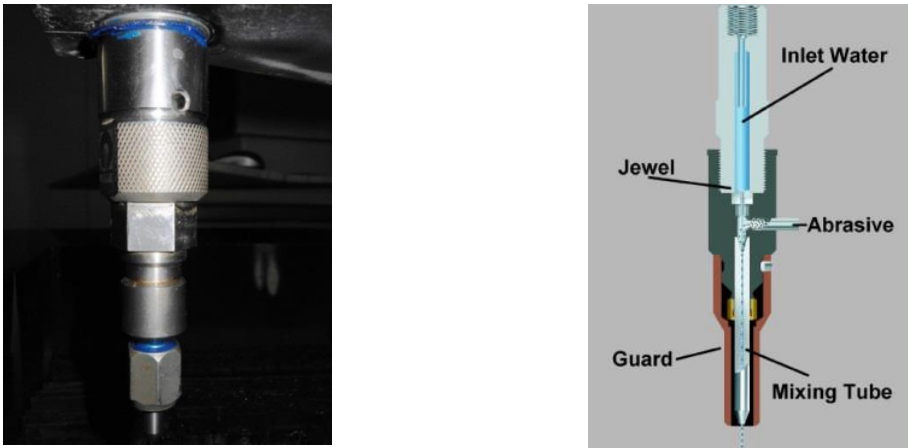


Fig. 2.4: Cutting head assembly (OMAX 2626)

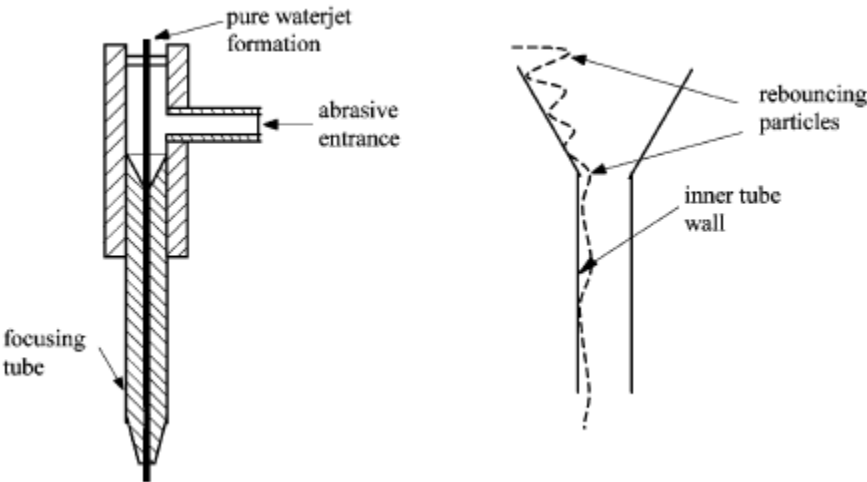


Fig. 2.5: Abrasive particle acceleration process inside the nozzle (Nanduri et al. 1996)

The theory proposed by Nanduri et al. (1996) for particle mixing predicts and compares the wear patterns of the mixing chamber and focusing tube. In AWJM, each abrasive particle enters the water jet with a negligible velocity and gets accelerated with the water jet. These particles hit the inner wall of the focusing tube, bounce back and enter the water jet again, this phenomenon continues until the velocity direction of the abrasive particles is nearly parallel to the direction of waterjet as shown in Figure 2.5.

The mixing tube performance depends on shape, inner diameter and geometry of the inlet zone. The smaller the diameter, the more concentrated is the total energy. The abrasive particle size determines the minimum inlet diameter of the focusing nozzle. For a better functioning of the process, the ratio of focusing tube diameter to the abrasive diameter is maintained to the order of five. More coherent jets are produced in longer tubes and the major disadvantage of using longer tubes is more friction with the inner wall resulting in low abrasive jet velocities.

Focusing tubes are made of advanced materials which are wear resistant and provide a reliable and stable cutting process for a long duration. The abrasive particles cause wear of the carbide tubes increasing the diameter of the tubes. This damage or change significantly influences the part being manufactured and it is not possible to make a precise cut like in a conventional machining process. Present day materials are developed to increase the life of tubes ranging up to 100 hours. The advancement of nozzle designs and materials have improved the cutting speed and precision of components manufactured through AWJM. The shape of the focusing tube is shown in Figure 2.6(a). The focusing nozzles are developed with advanced composites such as ROCTEC 100; ROCTEC 500, etc. which are the latest developments that offer a substantial improvement in the nozzle life i.e. 20 to 30 times more than the life of Tungsten Carbide tubes.

2.3.3. Abrasive feeding system

The abrasives used in the process should possess properties of high toughness and hardness when compared to the work material so that the abrasives may be used without much fragmentation. Usually, garnet is used as abrasives for processing a wide range of materials in AWJ cutting systems. The particle diameters range from 110 μm to 177 μm , which correspond to abrasive mesh size (#) 160 to 80. The abrasive

transportation to the mixing chamber is by either gravity feeding or force feeding from the hopper. Depending on the carrier medium, abrasive particles are transported like dry and wet feeding. Air is used as a carrier medium in dry feeding and in wet feeding a part of the waterjet energy is used for mixing and transportation of the abrasives.

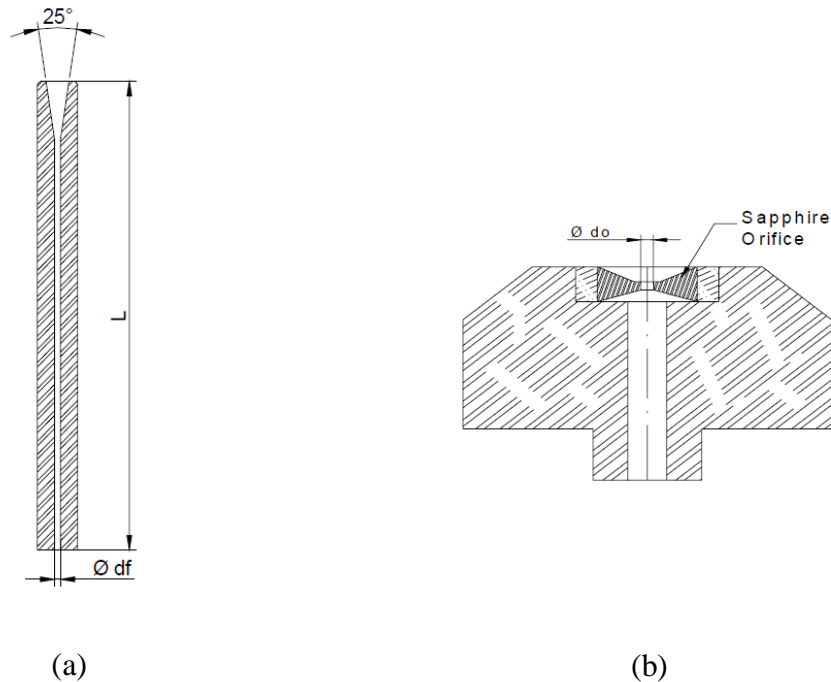


Fig. 2.6: Schematic of (a) focusing nozzle and (b) orifice (OMAX, USA)

2.3.4. Catcher unit

In quality and precision cutting operations, only 10% of the total jet energy is utilized and the remaining 90% of the energy is dissipated to the catcher unit. Catcher tanks are designed depending on the application and type of jet handling systems used.

2.3.5. CNC motion controller

The CNC controller provides the desired motion for the cutting head so as to generate the required contour on the work piece. Generally, the motion system is provided with servo drives to achieve precise motion. The number of axes controlled may vary from two to five and is chosen based on the complexity of the geometry to be cut. These are all numerically controlled by a central computer

2.4 Theory of abrasive water jet generation

The acceleration of a certain volume of pressurized water in an orifice generates high speed water jets. When high pressure water passes through an orifice, it is converted into high velocity stream of water jet. Bernoulli's law gives:

$$P_{atm} + \rho_w \frac{v_o^2}{2} + \rho_w g h_1 = P + \rho_w \frac{v_{pipe}^2}{2} + \rho_w g h_2 \quad (2.1)$$

where P_{atm} is the pressure at the exit of the nozzle, P is the pump pressure, v_o and v_{pipe} are the velocities at the exit and entry to the orifice. ρ_w is the density of water. Considering $h_1 = h_2$ and $v_o \gg v_{pipe}$, the approximate velocity of the exit water jet is given by

$$v_{oth} = \sqrt{\frac{2P}{\rho_w}} \quad (2.2)$$

In practice,

$$v_o = \mu v_{oth} = \mu \sqrt{\frac{2P}{\rho_w}} \quad (2.3)$$

where μ is the efficiency coefficient that characterizes momentum loss due to wall friction, fluid flow disturbances and compressibility of the water. The velocity of fluid at the entry of orifice is very much less when compared to the velocity at the exit of orifice. The pressure at the nozzle exit is atmosphere pressure which is very less when compared to the water pressure at the orifice entry. The effect of water compressibility has a very small influence i.e. less than 3% on water jet velocity (Hashish 2002).

The flow rate of water Q can be obtained

$$Q = A_o v_o = A_o \mu \sqrt{\frac{2P}{\rho_w}} \quad (2.4)$$

where A_o is the cross-sectional area of the orifice. The overall efficiency coefficient μ includes coefficients of velocity (C_v), contraction (C_c) and the compressibility factor. Orifice coefficients vary with changes in pressure affecting the flow rates of water and

any increase in pressure and orifice size reduces the overall coefficient of discharge (Hashish 1989b). The efficiency of jet would be high for higher overall coefficient of discharge, which indicates efficient conversion of potential energy to kinetic energy. As the high-speed water jet leaves the orifice, the kinetic energy of the jet E_w is given by

$$E_w = \frac{1}{2} \dot{m}_w v_o^2 t \quad (2.5)$$

where \dot{m}_w is the mass flow rate of water ($\dot{m}_w = \rho_w Q$) and taking $\dot{m}_w = \frac{\pi}{4} d_o^2 v_o \rho_w$

$$E_w = \alpha \frac{\pi}{4} d_o^2 \mu^3 \left[\sqrt{\frac{2P}{\rho_w}} \right]^3 \rho_w t = \frac{\alpha \pi \mu^3}{\sqrt{2\rho_w}} d_o^2 P^{1.5} t \quad (2.6)$$

where α is a constant considering the reduction in water mass flow rate due to the change in the fluid-mechanic conditions at the orifice outlet and this reduces the jet velocity due to wall friction.

Water jets emerging out of the orifice consists of three different zones: a core zone, a transition zone and final zone as shown in Figure 2.7. In the core region, the jet expands slowly and is more coherent. The length of the jet where the diameter of the jet is less than the focusing nozzle diameter, it is known as coherent length of the jet. In this zone, very few drops of water are present around the jet. As the jet comes in contact with the atmosphere, the jet spreads in the main region, the jet width increases and an enormous amount of water droplets are formed (Yanaida 1974; Yanaida and Ohashi 1978). The coherence length of water jet can be increased by adding certain long chain polymer additives such as ‘Super - Water’.

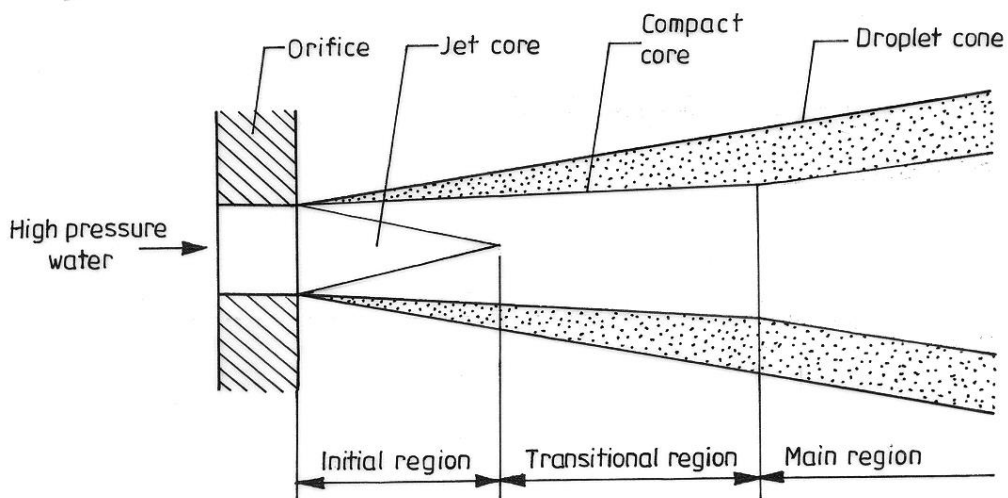


Fig 2.7: Structure of high speed water jet (Yanaida 1974)

In abrasive water jet cutting head, as the jet passes through a certain distance from the orifice, called break up point, the jet disintegrates and expands to the size of the focusing tube inner dia. Thus, it restricts the back flow of air from the tube exit creating low pressure inside mixing chamber. Jet spreading in AWJ cutting system causes adverse effects such as wear at the entry of the focusing nozzle, misalignment and also deteriorates the cutting performance. Increased jet spreading disperses the energy resulting in poor performance of jet in cutting thick specimens; besides, jet spreading enhances the suction capabilities of water jet to entrain abrasives and improves the abrasive mixing process (Hashish 1989b). Jet spreading generally increases with increase in water jet pressure and the water flow rate (Hashish 1991) and spreading changes the geometry of the orifice which changes with time (Hashish 1997) due to erosion and this plays an important role in the machining process.

As the jet emerges out of the orifice, it interacts with the surrounding air and forms a thin film of air which is carried along the walls of the focusing nozzle and creates waviness in the jet surface which results in decrease in pressure inside the mixing chamber. This partial vacuum inside the mixing chamber aids in entraining abrasives into the jet. The momentum transfer from the high velocity jet to the abrasive particles occurs in the mixing chamber and focusing nozzle. As the abrasive particles are carried by the jet due to momentum transfer, the velocity of abrasive particle in the jet is obtained by

$$v_{awj} = \eta \frac{v_o}{1 + \frac{m_a}{m_w}} = \eta \frac{v_o}{1+R} \quad (2.7)$$

where v_{awj} is the particle velocity; η is momentum-transfer parameter which is a function of process parameters such as pump pressure, abrasive flow rate (AFR) and abrasive size along with the orifice and focus geometry. R is the ratio of abrasive mass flow rate to mass flow rate of water. In general, the size of the orifice and focusing tube/nozzle is maintained at a ratio of 3:1 to 5:1 for obtaining optimum performance with abrasive water jet cutting (Chalmers 1991). If the ratio is beyond 5:1 this causes a large disintegration of jet (Hashish 1991). When the jet emerges out of the focusing nozzle, the flow pressure changes from the vapor saturation pressure to atmospheric pressure and at this region, a recompression shock occurs which causes the jet

instability disturbing the flow at the tube outlet resulting in diffusion of the jet. The total energy of the jet impacting on the work piece E_{impact} is given by

$$E_{impact} = \frac{1}{2}(\dot{m}_a + \dot{m}_w)v_{awj}^2 \frac{d_F}{v} \quad (2.8)$$

where d_F is the focus tube inside diameter and v is the traverse speed of the jet. A part of this energy is dissipated in the material and the remaining is exited into the catcher tank along with the slurry. Some part of the energy is also absorbed by the work piece material which is used for material removal and heat generation.

2.5 Material removal mechanism in AWJM

In a continuous water jet cutting system, material removal takes place due to the compressive stresses created by high velocity waterjet. In AWJs the material removal is due to the erosion caused by the impact of high velocity abrasives on the material surface. Abrasives strike the work piece at approximately one million impacts per second thus transferring the kinetic energy of the abrasive particle to the work material. The impacts caused by this high speed abrasive laden fluid damage the work material and this phenomenon is called as erosion. Bitter (1963a) described the erosion mechanism considering mechanical properties of the workpiece material. In the vicinity of the impact zone, a localized plastic deformation takes place when the impact stresses exceed the yield strength of the material. The continuous impacts create a deformed surface layer near the eroded surface, which increases the yield strength of material by strain hardening. On further deformation, the yield strength at the surface of the material will become equal to material fracture strength, thus avoiding any further plastic deformation. At this junction, the material surface becomes brittle and is fragmented on subsequent impacts. Water jets operate at macro level while abrasive water jets operate at micro level.

Crack propagation induced by macro cracking and hydro wedging is the cause for material removal in brittle machining using AWJM. The water enters the crack with high velocity generating stresses on the crack walls and when the intensity of these stresses exceeds the critical value of local material parameters such as fracture toughness, material removal takes place (Momber and Kovacevic 1998). The material

removal in brittle materials is by micro cracking, crack coalescence and micromachining as reported by Arola and Ramulu (1996). Erosion models for brittle materials are relatively well established and control of the erosion process is identified based on the indentation mechanics. These models include elastic model (Sheldon and Finnie 1966); elastic-plastic model (Evans et al. 1976) and grain ejection model (Ritter 1985). According to Hutchings (1979b), the observations through high speed photographs and SEM revealed that the material removal due to micro-cutting is defined in two modes namely ‘cutting deformation’ and ‘ploughing deformation’. Spherical particle impacts are responsible for ploughing deformation and sharp edged abrasive impacts for cutting deformation.

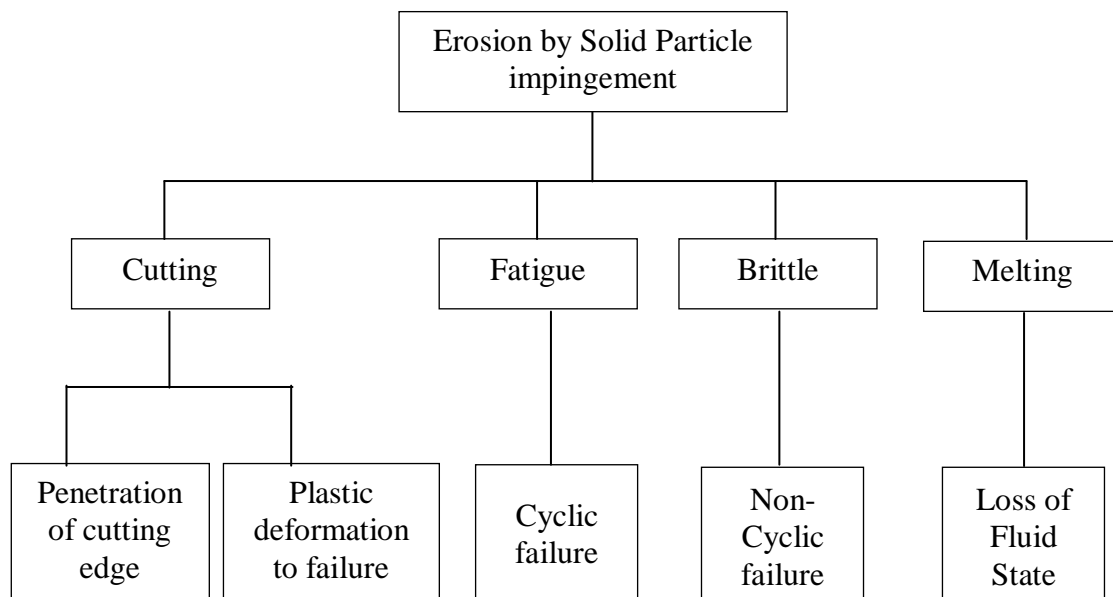


Fig.2.8: Material removal mechanisms by solid particle erosion (Meng and Ludema 1995)

Erosion of ductile materials is caused by particles shearing and cutting the surface, with material loss caused by plastic deformation. In cutting of ductile materials with this process, removal of material takes place by the displacement of target material into a crater lip where it becomes easy for further erosion or detaches material from the space (Preece 1976). While cutting ductile materials with pure water jets, the material is removed by the hydrodynamic loading, causing ‘water hammer effect’ on the surface.

In general, material removal with AWJs is effected by means of several solid particle erosion theories. Thus, material removal by abrasive water jets involves several phenomena such as erosion, fatigue, melting, plastic deformation, micro cutting and

brittle fracture. Normally, these mechanisms do not act separately but they act in combination of at least two or more phenomena (Momber and Kovacevic 1998). A consolidated material removal mechanisms by solid particle erosion is given in Figure 2.8. Despite to many limitations, Finnie's and Bitter's models are extensively used for modeling of material removal processes in AWJM process.

2.6 Abrasive water jet cut surface

In AWJM, the geometry of kerf characterizes the quality of cutting. The topography generated on the cut surface and changes in material properties around the cutting zone are also some of the important issues to estimate the quality of cut surface. Owing to the nature of AWJ cutting, the metallurgical changes in the material and changes on cut surface due to thermal effects are not significant (Hashish 1991). The different stages of abrasive water jet interaction with the work material are given shown in Figure 2.9. It is at the entry stage that the jet starts interacting with the target material. During this stage, jet spreading takes place due to wall friction whereas the jet remains relatively coherent in the upper portion. The curvature on the cutting interface increases with the advancement of the jet into the material. As the jet traverses further, it removes material to a maximum possible depth beyond which it deflects by 90° during the developed cutting stage; the cutting process is cyclic in nature. One cutting cycle is divided into two distinctive modes; the first is the material removal in cutting wear mode; here the material is subjected to shear and the abrasive particles attack and penetrate the work surface at shallow angles and remove the material. The second mode is a deformation mode, where the material is subjected to plastic deformation which is characterized by the abrasive particles impacting at large angles of attack (Hashish 1993), and the kerf curvature at depth h_c suddenly changes making a step as shown in Figure 2.9 differentiating the cutting and deformation wear mode of material removal.

The cutting process is steady in the cutting wear mode and is unsteady in the deformation wear mode. Normally, the cutting wear mode extends up to one third of the total penetration depth resulting in the striation free zone (Zeng and Munoz 1994). During the exit stage of the cutting process, the jet deflects in the traverse direction of the jet and leaves an uncut portion of the material which is of a triangular in shape. The distance between the top surface and the tip of the uncut triangle represents the steady

state cutting which is clearly shown in Figure 2.9. The jet traverse is generally slowed down to avoid the uncut triangle at the exit portion of the cut. The topography of an AWJ cut surface contains two characteristic zones, a smooth zone in the upper region of the cut surface, which is free from striations and the other a rough zone in the lower region of the cut surface, where striations are dominated due to deformation wear mode. Guo et al. (1993) explained AWJM process as three dimensional due to the nature of the jet interaction with the work material. Thus, the cut surface geometry consists of surface roughness, striations, grooves and additional external effects due to vibration of work piece or nozzle and fluctuations in jet due to the change of process parameters.

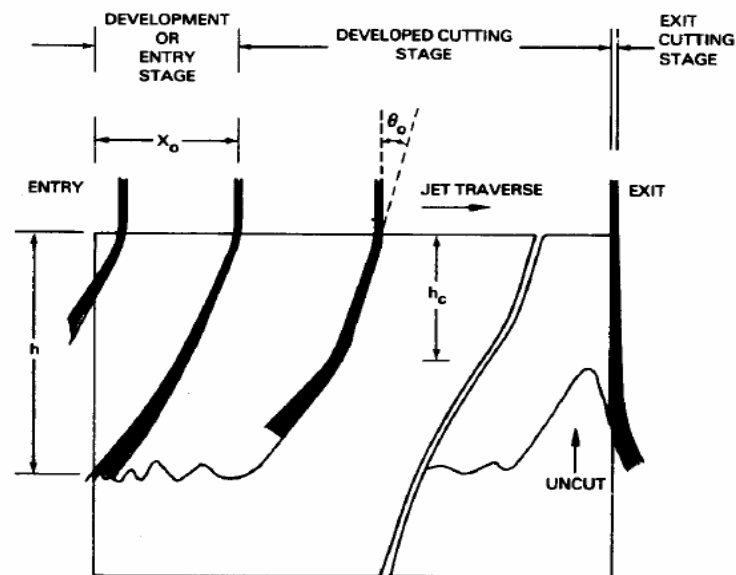


Fig. 2.9: Different stages in AWJ cutting (Hashish, 1993)

It has been reported that the four mechanisms which are significant to understand the cut surface topography are i) impact of individual abrasive particle leading to roughness formation, ii) step formation in the cutting direction that leads to striation formation, iii) jet oscillation perpendicular to the cutting direction which is responsible for groove formation, and iv) oscillation of the guiding system generates waviness. These mechanisms were observed in different materials such as Al and Ti alloys, steel and ceramic materials. Zeng and Kim (1992) proposed a two-stage impact model for explaining material removal in ductile materials in which the entire cutting process is associated with abrasive particle impacts angles.

Arola and Ramulu (1993) proposed a three-zone cutting model for explaining the material removal process. The three macro regions are the initial impact zone observed near the jet entrance into the material, cutting wear zone, which exhibits minimum roughness and the deformation wear zone, which is influenced by waviness due to deflection of penetrating jet. In AWJ cutting, striations are formed at the lower portion of the cut surfaces. The striations formation is due to the reduction in the cutting energy of the jet from top to bottom of the surface. Hence, surface roughness and striation characteristics are the major criteria to evaluate AWJ cut surface quality.

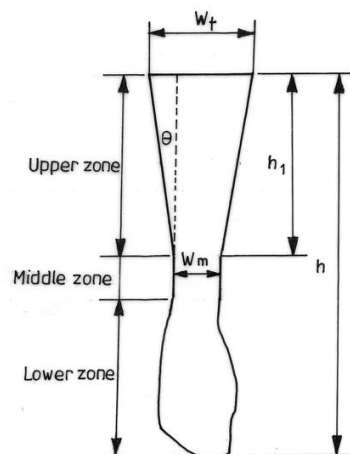


Fig. 2.10: Schematic of the kerf geometry obtained with AWJ cutting

Kerf geometry is an important characteristic in AWJ cutting. The kerf produced in cut materials with AWJs is tapered and is wide at the entry zone, which decreases down the thickness of the material. This is due to the reduction in the efficiency of jet cutting due to particle fragmentation, and energy absorption by the material along its thickness. It is observed that the entrance width is inversely proportional to the traverse speed (Gudimetla et al. 2002). At low traverse rates, the jet produces a converging kerf. The top width of kerf is greatly influenced by the focusing nozzle wear (Matsui et al. 1991). In case of cutting thicker materials, the cutting efficiency decreases with the penetration of jet into the material. It reaches a stage where the jet cannot further penetrate through the material. In such a case, the bottom of the kerf opens into a small circular groove called 'ballooning effect' and this happens due to the jet instability, deflection and the rebounding of abrasive particles. Various parameters used to characterize the kerf geometry includes width of kerf at top and bottom regions, kerf taper, width and depth of initial damage zone and total depth of cut. The kerf geometry

generated by AWJs in a through cutting process is described as shown in Figure 2.10. The top of the kerf is characterized by a small rounded corner at the top edge owing to the plastic deformation of material caused by jet impingement. The kerf is generally produced is a taper having a wider top than the bottom. The kerf is highly influenced by diameter of the focusing tube, traverse speed and standoff distance (SOD).

The velocity of the particle is assumed to vary from zero at the nozzle wall to a maximum at the jet center. This velocity corresponds to the energy distribution in the jet. The inner regions of the jet, as shown in Figure 2.11, have higher velocities and are convergent and this convergent jet results in tapered cuts on the work material. The kerf width is dependent on the effective jet diameter, which in turn depends on the jet strength and the target material. The kerf width increases in the middle of the material thickness at low traverse speeds, giving rise to a dent in the kerf. Thus, the geometry of cut is dependent on the jet energy which in turn depends on the process parameters. Hence, selection of process parameters is of considerable importance for obtaining the desired quality of cut.

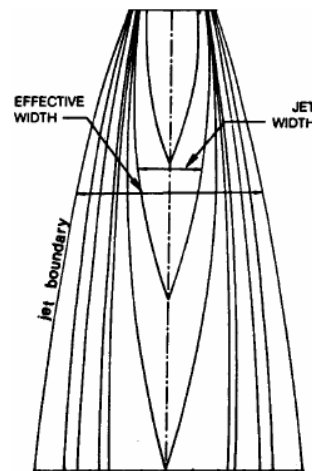


Fig. 2.11: Relative strength zones in a water jet (Hashish 1979)

2.7 Role of process parameters

The AWJ cutting process is characterized by a large set of process parameters that determines efficiency, economy, quality, etc. Process parameters optimization is a primary requirement for a successful application of AWJM. These process parameters are categorized as hydraulic, cutting, mixing and abrasive parameters as shown in Figure 2.12. The four parameters considered in the present research for AWJ milling

applications are shown with bold letters in the figure. The outputs parameters of the process are normally pocket depth and quality of kerf, which depend on the target material hardness and its composition. For identical thickness materials, the cutting rate can be different because it also depends on the traverse rate. In material removal applications, such as milling and turning, the volume of material removed is an important output parameter. Usually, the removed volume is measured by filling the generated cavities with a reference material.

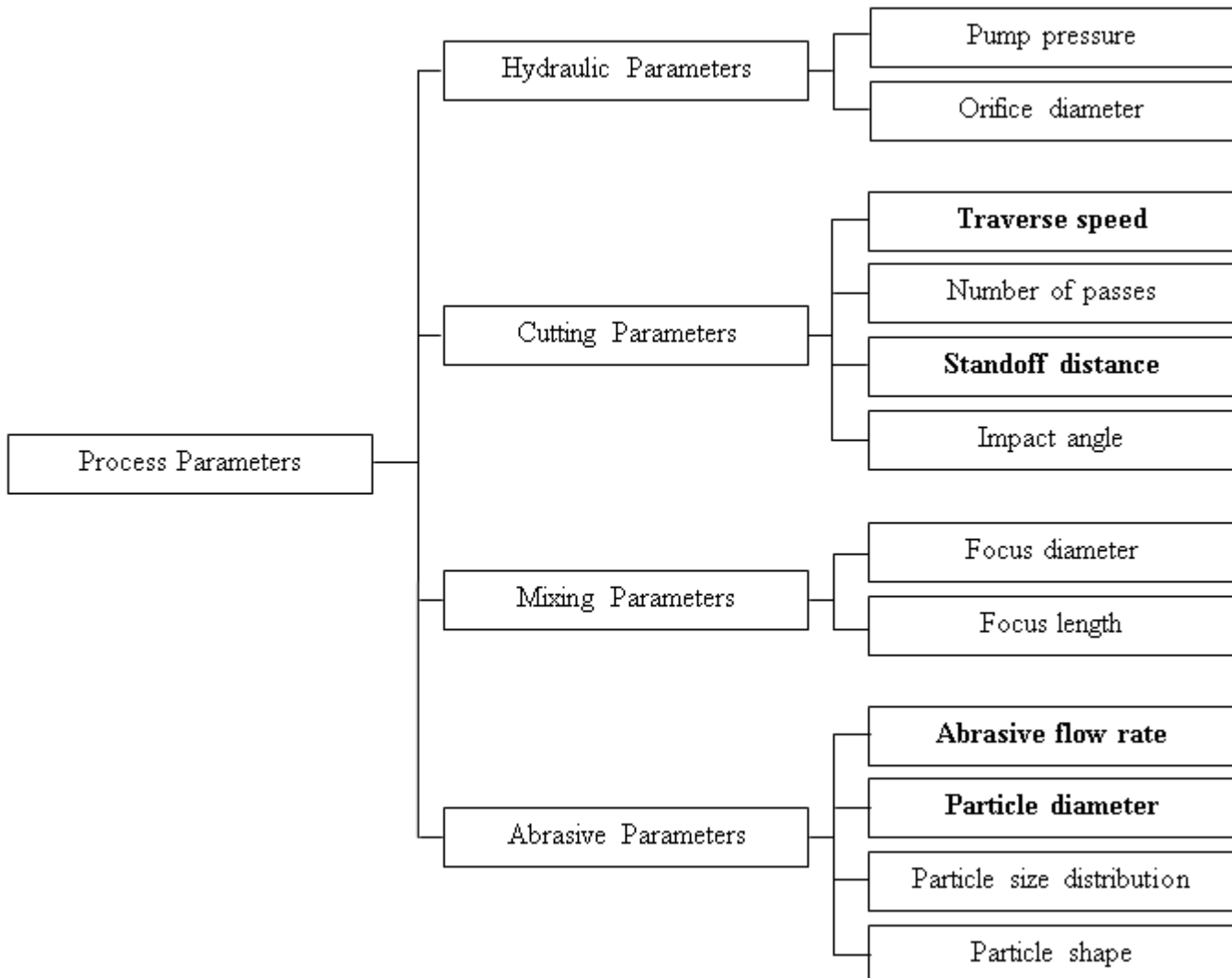


Fig 2.12: Process parameters in AWJ cutting

2.7.1. Hydraulic Parameters

The two parameters which are covered under hydraulic parameters are the pump pressure and the orifice diameter. The change in the orifice diameter and pump pressure changes the water flow rate predominantly. It also depends on the delivery capacity of the pump, which is prefixed in most of the systems. The general structure of AWJM

process is a complex phenomenon resulting in relations between the pump pressure and the process of jet formation, abrasive acceleration and mixing. Increased water jet pressure and water flow rate increases the spreading of jet (Yanaida 1974) leading to wear at the entry section of focusing nozzle and in coherence of the jet. On the other hand, jet spreading improves the suction ability of water jet thereby entraining more abrasives (Hashish 1989b). In case of smaller size of the focusing nozzle, increased water flow rate into the mixing chamber impedes the suction process due to wetting of abrasive feed line and choking of abrasives. This reduces the flow of abrasive particles into the mixing chamber. Moreover, the compressibility of water under high pressure also affects the jet velocity. The losses due to water compressibility increase with water jet pressure; however, momentum transfer efficiency improves with an increase in pressure. In contrast to this, the changes in water jet pressure vary the orifice discharge coefficients, which in turn affect the water flow rates. The orifice efficiency reduces with the increase in water jet pressure; higher water jet pressure increases the degree of abrasive particle fragmentation and affects the mixing efficiency and effectiveness of cutting (Hashish 1989b).

In general, an increase in water flow rate beyond certain limit does not show significant increase in the particle velocity (Hashish 1986a). Depth of cut decreases with an increase in water jet size due to the fact that large water jets maintain liquid (compact) core for longer distances resulting in improper mixing of abrasives and disengagement of abrasive particles in the contact region due to excess water (Hashish 1991). The cutting performance reduces with an increase in orifice diameter, i.e. beyond 0.25 mm (Guo et al. 1993). Depending on the available jet energy, the kerf is formed; convergent kerf taper is produced at low energy levels and divergent kerf taper at high energy levels (Groppetti et al. 1998). For a fixed focusing nozzle size, larger size of water jet orifice does not provide good surface quality. Hence, a proper size ratio of orifice and focusing nozzle is essential to achieve effective results in AWJ cutting (Singh et al. 1991).

2.7.2. Abrasive parameters

The abrasive size, type, shape and flow rate belong to abrasive parameters. Among them, abrasive type and abrasive size affect the abrasive feeding process. In

general, an increase in AFR increases the depth of cut. However, this trend ceases beyond a certain limit. At higher AFRs, interference between particles reduces the effective number of impacts, alters the angles of attack and also reduces the local impact velocities (Hashish 1991). Larger particles remove material faster due to higher particle inertia (Singh et al. 1991). For smooth cutting applications, fine abrasives are preferred and very fine abrasives also result in increased waviness due to reduced cutting capability and may restrict the airflow. There exists an optimum abrasive size for different types of materials (Hashish 1986a, 1991). Higher AFR increases the particle fragmentation and wear rate of focusing nozzles affecting the mixing efficiency (Hashish 1986a). An increase in the AFR improves the surface quality, i.e. reduces the surface roughness and a better surface in the cutting zone does not guarantee better finish in the deformation zone (Kovacevic 1991a; Singh et al. 1991).

2.7.3. Mixing parameters

Focusing nozzle (mixing tube) diameter and length and the inlet angle are three important factors that influence the mixing of abrasives in AWJM (Hashish 1991). Momentum transfer from water jet and acceleration of the abrasive particles takes place in the mixing tube. Hence, the diameter of mixing tube affects the power density of jet. Smaller mixing tube diameters increase the power density and larger diameters result in inefficient abrasive entrainment. The length of mixing tube affects the particle exit velocity and the jet coherency. Larger tube length increases drag force resulting in reduction in the particle velocity. Chalmers (1991) suggested a ratio of 3:1 for diameters of the focusing nozzle to orifice to achieve maximum depth of cut and beyond a ratio of 5:1 is ineffective due to entrainment of abrasives (Hashish 1986a, 1991).

2.7.4. Cutting parameters

Several other parameters like jet traverse speed, number of passes, SOD and impingement angle belong to cutting parameters. These parameters are selected based on the type of material and nature of processing the material such as cutting, turning, milling or drilling. It is seen that higher traverse rate produces convergent kerf and lower traverse rate generates divergent kerf (Niu et al. 1995). During machining with AWJs, the amount of material removed and depth of cut are reduced with an increase in

jet traverse speed. The optimum traverse rate depends on the type of cut i.e. whether it is quality cut or a separation cut. The traverse speed affects the mechanism of material removal, i.e. cutting wear at low traverse rates and deformation wear at high traverse rates. Similarly, increased number of passes increases the depth of cut. However, the trend in the rate of increase in depth of cut is not uniform with increasing number of passes as reported by Hashish (1984). As seen above, all the four categories of parameters such as hydraulic, abrasive, mixing and cutting parameters influence the performance of AWJs in cutting affecting the system operation and the machining results. In view of the large numbers of factors affecting the process results, the process is a complex and it is thus necessary to choose the parameters suitably in order to achieve the desired results during cutting.

Table 2.1: Significance of AWJ parameters on the operational and design factors (Hashish 1991)

| Operational and Hardware Factors | AWJ Parameters | | | | | | |
|----------------------------------|----------------|-------|-------|-------|-------------|-----|-------------------|
| | P | d_o | l_F | d_F | \dot{m}_a | d | Abrasive Material |
| Hydraulic efficiency | * | ** | | | | | |
| Coefficient of discharge | * | ** | | | | | |
| Jet spreading | * | ** | | | | | |
| AWJ coherency | | | * | | * | | |
| Particle fragmentation | ** | * | * | * | * | * | *** |
| Abrasive hose dimensions | ** | ** | | * | ** | * | |
| Wear of mixing tube | * | ** | * | ** | ** | ** | *** |
| Mixing efficiency | * | ** | * | ** | ** | * | |
| Equipment cost | ** | * | | | | | |
| Environmental factors | * | * | | | | | ** |
| High pressure seals | ** | * | | | | | |
| Nozzle assembly design | * | ** | | | * | * | |
| Nozzle align ability | | ** | ** | ** | | | |
| Operational reliability | ** | * | | | | * | |

(***) most significant; (**) more significant; (*) less significant; () not significant

Table 2.1 and Table 2.2 provide an overall view of the factors influencing the system design, operation, and the machining results with AWJM. In AWJ cutting, water jet pressure, orifice size and AFR are found to influence the depth of cut more prominently than the focusing nozzle diameter and abrasive particle size. The quality of cut characterized in terms of kerf width, kerf taper, surface quality which are highly influenced by the focusing nozzle diameter. The jet pressure and AFR are observed to influence the kerf quality to a lesser extent. However, the surface quality (surface roughness) is predominantly affected by the size of abrasive particles.

Table 2.2: Significance of AWJ parameters on machining results (Hashish, 1991)

| Machining results | AWJ Parameters | | | | | | |
|-------------------------|----------------|-------|-------|-------|-------------|-----|-------------------|
| | P | d_o | l_F | d_F | \dot{m}_a | d | Abrasive Material |
| Volume removal rate | *** | *** | * | ** | *** | ** | ** |
| Depth of cut | *** | *** | | ** | *** | ** | ** |
| Width of cut | * | | | *** | * | | |
| Surface waviness | ** | ** | * | * | ** | * | * |
| Surface roughness | ** | ** | | | * | *** | ** |
| Running cost of cutting | * | * | * | * | ** | | |

(***) most significant; (**) more significant; (*) less significant; () not significant

From this study, it is clear that the selection of process parameters is of considerable importance for achieving the desired results in AWJM, satisfying the criteria such as minimum utilization of energy, minimum consumption of abrasives and water, etc. During the cutting process, any change in the chosen parameters need to be monitored and compensated for maintaining the consistent performance with AWJs. Therefore selection of process parameters plays a very crucial and important role in AWJM applications.

2.8 Control and supervision of AWJM process

As in any other machining process, control and supervision of the AWJM technique improves both the efficiency and quality of the process. There are monitoring methods which can be classified as direct and indirect methods. A higher accuracy of

measurement is obtained in direct methods. Direct methods include use of sensors for measurement at appropriate locations. Even though some of these direct measurement techniques can be employed for online monitoring, they need elaborate instrumentation and large set up time for online measurement and hence are not suitable for online monitoring purposes. Monitoring can be done on the machine, tools, workpiece or the process. Appropriate sensors are to be installed at locations where a close point for measurement is available. There should be no static and dynamic stiffness reduction and also no restriction of working space and machining parameters. Further, there should not be any influence of electromagnetic and thermal changes during the process (Byrne et al. 1995). An extensive amount of efforts were put by researchers in the area of condition monitoring of cutting tools used in conventional machining processes like turning, milling and drilling. The efforts to monitor the process using forces and vibrations on the machined surface or the component have not been addressed even in conventional machining processes. On the other hand, indirect methods are less complex, cheap and more suitable for practical applications. In AWJM process, the efforts made in this research area are very limited. Reports suggest indirect methods for online sensing of AWJ cutting head were developed. Indirect approaches such as acoustics based approach and vacuum based approach were suggested to monitor the cutting process (Hashish et al. 1993).

Kovacevic (1992) considered cutting forces for online monitoring of depth of cut using different cutting parameters and reported that the vertical cutting force increases with increasing pressure, AFR and mixing tube diameter. And, the vertical cutting force decreases with increase in SOD and the effect of traverse speed on the vertical force is not very significant. A correlation between the vertical forces and surface roughness by autoregressive-moving-average (ARMA) modeling technique has been proposed by Kovacevic et al. (1995). The vertical forces are used for analyzing the energy transformation efficiency by Momber (2001).

The ratio of AFR to water flow rate affects the vertical cutting force and is very crucial in AWJM process. But, monitoring the AWJ depth of cut using online vertical cutting force measurement is expensive and safety of the dynamometer components is very important due to the erosive nature of the abrasive particles. It is always suggested to use the force dynamometer for experimental purposes based on the dynamical

LITERATURE REVIEW

characteristics of the process. The input parameters can be controlled to achieve a better product or a feature. To avoid any damage to the dynamometer components, a proper fixture is designed to accommodate the work piece in the experimental setup. To achieve more control on AWJM, it is very much essential to understand the mechanism of the material removal processes. The erosion mechanism in AWJM involves solid particles of the size of few microns striking and rebounding from the surface. Thus, the force that governs the erosion mechanism is because of the deceleration in the velocity of the striking particle during the impact. When hard particles in a medium are allowed to impinge a surface at a very high velocity (in the order of 400-500 m/s), it is expected that the solid particle erosion takes place. The transfer of kinetic energy of the abrasive water jet to the material surface causes material deformation and removal. A considerable research has been published to understand the material removal processes due to hard particle erosion on a variety of materials like ductile and brittle materials, etc. In the case of the ductile materials machining, the material deformation involve the process of crushing, ploughing and cutting. However, most of the studies include the consideration of macro-particles and only some of them take into account the effect of the velocity of the striking particles at the target surface. The erosion process by the particle impact differs with process parameters and further investigations are to be carried to understand the process.

Recent reports on micromachining of glass using abrasive air jet (AAJ) addressed the optimization of process parameters and modeling of the cut (or kerf) qualities in terms of process parameters (Fan et al. 2009; Li et al. 2009). The present investigations are carried out to study the effect of process parameters on the forces acting during machining using AWJM and correlate with the theoretical model of forces and their effect on surface roughness. The other areas of research where attempts were made in the condition monitoring include nozzle wear monitoring. Kovacevic and Evizi (1990) proposed several indirect methods employing laser based image processing systems, ultrasonic gaging of focusing nozzle thickness; vibration sensors for nozzle wear detection by thickness reduction, etc. Several attempts were made to study the variation in impact force exerted by the jet with and without abrasive particles (Kovacevic 1992 and 1994b), Zeng and Munoz (1994) to investigate the variations in the condition of the nozzle wear. Few attempts were made to monitor the AWJ cutting process such as depth of cut employing ultrasonic techniques and monitoring of sound

(Warisawa et al. 2001). Attempts in the area of process monitoring using force and vibrations during machining in AWJ milling are very much limited. Therefore, an effective way to control the process is to generate a model to adjust the process parameters using the generated signals during machining.

2.9 Signal processing techniques and methods

Signal processing deals with data acquisition and analysis to extract the relevant features. Signals can be classified as deterministic signals and random signals. Signals which can be described in a precise manner at any instant of time are known as deterministic signals and when described by explicit mathematical relations are categorized as random signals. Many signals in the real world problems such as vibration, turbulence, acoustic, etc. belong to this category. A computer is required to analyze the acquired signals from the sensor are to be converted into a digital form. The digital data is further analyzed to extract relevant information about the process. Some of the popular methods to extract features for monitoring purposes are briefed below.

2.9.1. Statistical analysis

Time domain signal is a time varying raw signal collected from the sensor. As such, this signal is not much informative to detect the status of the process. However, with the help of statistical parameters such as root mean square (RMS), arithmetic mean, standard deviation, variance, kurtosis, skewness, maximum and minimum, one can characterize the condition of the process.

2.9.2. Time series analysis

Time dependent data can be mathematically modeled as a time series model like autoregressive (AR), Autoregressive Moving Average (ARMA), etc. to characterize the signal. The modeling strategy involves fitting models in increasing order. In condition monitoring processes, the autoregressive parameters or their relations have been often used for the diagnosis of faults/failures. A major disadvantage of time series modeling is choice of the order of models that affects the quality of the signal representation. The optimum value of the order of model can be chosen by estimating the results with a sequence of models of a different order and then selecting the best order based on some

specified criteria. The time series modeling technique was employed to characterize for process monitoring using the work piece normal force signal (Kovacevic 1991a).

2.9.3. Fast Fourier Transform (FFT)

The Fourier Transform a commonly used tool for transforming the signal into frequency domain and obtain the frequency distribution of the measured signal. It is based on the fact that periodic signals can be expressed as an infinite sum of sine and cosine functions of discrete harmonic frequencies. The FFT is an efficient algorithm to compute Fourier transform of the discrete data and is widely used for obtaining spectral information from the signals. The spectral resolution of an FFT is inversely proportional to the duration of the measured signal. The Fourier transform is defined for a signal consisting of an infinite number of points but the FFT can process signals with finite number of points. FFT offers a good solution only in the frequency domain and a very bad solution in the time domain due to loss of some signal information in time domain. In AWJ cutting, Kovacevic et al. (1993, 1994a) employed spectral analysis of acoustic signal for detecting the nozzle wear. Mohan et al. (1993) employed spectral analysis of work piece normal force signal obtained in cutting for characterizing the surface.

2.9.4. Wavelet Transform

The time and frequency domains signal processing techniques are prone to noise and interference from the undesired signals; hence their use is limited in accurate assessment of machine condition. FFT is based on the assumption of stationary signals, and is inherently not suited for non-stationary and transient signal analysis. The wavelet transform (WT) can be used to analyze time series signals that contain non-stationary power at many different frequencies. The WT is an extension of the conventional spectral technique with an adjustable window size. The scaling operation in WT produces a series of wavelet functions with different window sizes, enabling multi resolution analysis suited for representing non stationary signals. A major drawback of WT is its low frequency resolution in the high frequency region (Marchant 2003) and energy to correlate the acoustic energy to the variation in the material removal rate in AWJ cutting.

2.10 Process modeling in AWJM

Monitoring and control of complex machining operations need powerful strategies to achieve effective control with optimal utilization of resources (Luttervelt et al. 1998). These strategies are models to predict the performance of the process continuously and then control the process within limits. The former requires predictive models to assess the process performance with the given conditions and the latter requires corrective models; that correct the deviations in the process performance by adjusting the process parameters. Different methods such as analytical, semi empirical, empirical, knowledge based and artificial intelligence (AI) based approaches are employed to develop models for predicting and correcting the process performance. Analytical models make use of certain theories, fundamental and derived laws to formulate the relations among the process parameters. Most of these models are built based on a large number of assumptions, as it is very difficult to capture the physics of the process through any single or may be multiple theories. Hence, they are useful only to a limited extent as far as the accurate prediction and control of the process is concerned.

Empirical models developed by formulating a suitable relation between the input and output parameters with experimental data at various conditions can be used for prediction of the process responses but are valid only in the range in which the experimental are performed (Luttervelt et al. 1998; Jain and Jain 2001). Semi empirical models developed assume an appropriate relation among the process variables and use the experimental data and regression methods to validate the response. Therefore, these models require less effort in the experimentation but more effort in determining the coefficients and exponents in the semi empirical relation.

On the contrary, the recent trends in modeling of complex processes are focused on soft computing techniques, i.e. AI based techniques such as fuzzy logic, neural networks, genetic algorithms, expert system, wavelets, complexity theory, etc. These methods consider the control of any machining process as a decision making problem and establish a suitable framework for online control of the process. Among the various available techniques, fuzzy logic, neural networks and genetic algorithms are widely employed for addressing many real world problems.

Hashish (1984) established the feasibility of AWJM technique for processing of different materials in a variety of applications such as linear cutting, milling, slotting, turning, drilling, etc. Several analytical models are developed by him considering Finnie's and Bitter's theory of erosion to predict the material removal rate and depth of cut. Kovacevic (1991a) studied the influence of process parameters on surface texture and developed an empirical model through regression analysis relating the process parameters such as AFR, traverse rate, water jet pressure, and abrasive size to measure the surface roughness. The phenomenon of erosion in ceramic materials by means of inter granular network cracking and plastic flow for the prediction of depth of cut has been attempted by Zeng and Kim (1992, 1996).

Capello and Gropetti (1993) suggested the energy balance approach model to predict depth of cut. Momber (1995) used chemical reaction kinetics in develop a model for predicting depth of cut in AWJ cutting. The model gives a concept of abrasive particle energy distribution and local energy distribution of the eroded material for estimating the depth of cut. Ramulu and Arola (1994) developed an empirical relation for predicting the surface roughness and kerf taper in terms of process parameters for cutting graphite/ epoxy laminates using Taguchi's experimental designs. Here, Analysis of Variance (ANOVA) was performed to determine the relation between the response variables (surface roughness and kerf taper) and the process parameters.

Paul et al. (1998) developed an analytical model for predicting the depth of cut in ductile and brittle materials. This work considered the specific energy of jet instead of flow strength of the material for predicting depth of cut with the variation in the width along the kerf. Blickwedel et al. (1990) developed semi empirical relation to predict depth of cut and surface quality using energy balance approach. Here, a mathematical relation was derived between the process parameters and depth of cut and surface roughness for different materials like aluminum alloy, steel, glass, etc. Chen et al. (1998) proposed a semi empirical relation for predicting depth of cut in cutting alumina ceramics. In this work, water jet pressure, AFR, traverse rate and SOD are the input process parameters, while parameters such as orifice diameter, focusing tube diameter, impact angle, size and type of abrasive were kept constant during experimentation. This study is used for the prediction of striation free depth of cut.

Chakravarthy and Babu (1997) employed dimensional analysis technique using Buckingham π theorem to develop a semi empirical model for predicting the depth of cut. This model considered several process variables like jet pressure, orifice diameter, abrasive size, AFR, abrasive density, abrasive particle velocity, traverse speed, water jet velocity, material strength and SOD

Several attempts were made to develop empirical relations for predicting the kerf geometry and quality on various materials such as metallic coated steel, composites and ceramics (Wang and Wong 1999; Wang et al. 2003). From the above, it is clear that empirical or semi empirical models are developed for different materials. As these models are built considering the experimental data for a certain range of operation, their application is limited to this range of experimentation only and might not produce reliable results.

2.11 Concept of AWJ Milling: Current status

The preliminary investigations on milling applications on Al alloy with # 80 garnets resulted in a surface roughness of 20 μm , whilst milling with # 150 grit size resulted in a surface roughness of only 13 μm (Hashish 1987). In his research, the results with # 80 and # 150 abrasive sizes for the single pass milling suggested that the use of small sized garnets produce less variation in the surface waviness depth. However, there are no details reported for a milled cavity using the above grit sizes with two depth passes. Further, the concept of milling with rotary AWJ was later attempted by Hashish (1994). This technique has been not very successful because of the improper mixing process between the abrasives and rotary water jets. It is known that several process parameters such as pump pressure, traverse speed, AFR, impact angle, etc., significantly influence the process and its efficiency. Since not much hardware was available for a real time control of parameters, the concept has become impractical during the research.

The jet traverse speed has a strong influence on surface finish. A low traverse speed results in an irregular surface morphology of the milled area (Ojmertz 1994). Ojmertz (1993) and suggested that to achieve better surface finish it requires more number of particle impacts per unit area. This can be achieved at low traverse speeds, higher AFRs or by use of smaller mixing tube or orifice ratio. However, Hashish (1987) suggested that traverse speeds should exceed a value of about 1000 mm/min to achieve

LITERATURE REVIEW

surface uniformity. Ojmertz and Amini (1994) used multi-pass linear traverse cutting strategy based on the principle of superposition of several cuts to obtain a defined cavity. The multi-pass linear traverse cutting attempted by Laurinat et al. (1993) reports that the key parameter is the lateral distance between the single kerfs.

In milling with AWJM, the prime requirement is to minimize the surface roughness and maximize mrr. This can be obtained by jet impingement angle, where a normal impingement angle gives maximum surface roughness and as the angle decreases surface finish improves. Another important target parameter to evaluate the milling performance is to generate cavities of an effective geometry and maintaining uniformity of the milling depth. A major notable difference between milling and cutting is that a small removal depth in milling, which usually ranges from microns to few hundreds of microns. In the energy dissipative process, especially damping play a minor role as the interaction time of the abrasive jet and work piece is very much less limited compared to a normal cutting with AWJM. Similar to cutting, in milling also there exists a threshold pressure for the material removal to take place. Laurinat (1993) relates the mrr to the jet power, water flow and the abrasive mass flow rates. He concludes that all these process parameters are related to the orifice diameter. Hocheng et al. (1997) found an optimum SOD for high pressure milling of fiber reinforced materials. The material removal rate increases as the AFR increases and depending on pump pressure, there exists an optimum AFR for milling applications (Laurinat 1993).

After a gap of 10 years, water jet milling has been attempted by Fowler et al. (2005). The properties of the surface obtained after milling depend on the parameters such as interaction time between the water jet and work, jet impact angle, water jet pressure and abrasive size. The levels of grit embedment and surface morphology developed in the process are observed to depend upon complex interactions of the various process parameters (Fowler et al. 2005a, 2005b, Shipway et al. 2005). Investigations on the effect of particle hardness and shape on Ti alloy milling are attempted by Fowler et al. (2009). Based on the literature it has been seen that, research published on AWJ milling is not as matured as through cutting.

2.12 Motivation for AWJ Milling

The chemical milling or machining has been used in manufacturing for many years, which is being employed for the manufacture of different kind of patterns that can be clearly seen on the 16th century suits of armor plates, while application in engineering has begun in 1900s with etching of filters and printing equipment. Chemical milling of hard to cut materials can be employed to machine conveniently. Reports (Koster and Field 1973) reveal that this process can be used to remove unwanted material from thin walled components without distortion and or unwanted stresses. However, with chemical milling it has been reported that residual stresses are induced in the material if the depth of pocket is more than 0.01mm and a residual stresses in the components made by stainless steel exhibited a reduction of 15% in fatigue life (Harris 1976). These factors motivated us for conducting research on AWJ milling process and work towards monitoring of the process using forces and vibrations of the abrasive water jet.

2.13 Summary of literature

The literature review indicates that AWJM process is a complex phenomenon influenced by a large set of process parameters. These parameters play a very significant role in the production of good quality products. Quality parameters are being characterized by pocket depth, taper, kerf width and surface roughness. The importance and optimization of the significant process parameters for through cutting is very well documented. However, for pocket milling, the significant parameters for producing a good kerf width, minimum taper, maximum depth, obtaining a better surface are not well established. The literature suggests that for pocket milling, traverse speed plays a significant role in the control of flatness and depth. There is a very little published research on the effect of abrasive size on surface roughness is available. Other research area of importance to employ milling process with AWJM is the process characteristics and controls either by use of force, vibration, etc. Thus, the research enabled us to attempt to understand the role of process parameters on the response variables and to control and monitor the process to proceed further.

Chapter 3

EXPERIMENTAL INVESTIGATIONS OF ABRASIVE WATERJET MILLING

| | |
|---|----|
| 3.1 Introduction | 41 |
| 3.2 Design of experiments | 42 |
| 3.2.1 Analysis of data | 43 |
| 3.2.2 Analysis of variance (ANOVA) | 43 |
| 3.3 Methodology | 44 |
| 3.4 Experimental setup | 44 |
| 3.4.1 Fixture and tool path strategy | 48 |
| 3.4.2 Materials | 51 |
| 3.5 Full factorial experimental design | 53 |
| 3.6 Measurement and examination of the process and pocket milling characteristics | |
| 3.6.1 Material removal rate | 54 |
| 3.6.2 Surface roughness | 54 |
| 3.6.3 Pocket depth | 54 |
| 3.7 Experimental investigations on pocket milling | 56 |
| 3.7.1 Role of traverse speed | 57 |
| 3.7.2 Effect of pressure | 57 |
| 3.7.3 Effect of standoff distance | 59 |
| 3.7.4 Influence of abrasive flow rate | 60 |
| 3.7.5 Role of abrasive size | 61 |
| 3.7.6 Effect of process parameters on pocket depth | 63 |
| 3.8 Summary and conclusions | 65 |

3.1 Introduction

As discussed in the previous chapters, the cutting performance of AWJM process is influenced by a large number of process parameters which are a part of dynamic, quasi-static and static parameters. On reviewing the literature, it was realized that some cutting and abrasive parameters are more significant in milling applications of AWJM. It was important to identify such significant parameters and investigate their effect on the process performance. Hence forth, traverse speed, standoff distance (SOD), abrasive size (mesh) and abrasive flow rate (AFR) are considered as the input parameters in the current research. It is observed from the literature that several attempts were made to analyze the AWJM performance in cutting applications by

varying the pressure, AFR, traverse rate, SOD, orifice size and focusing nozzle size (Hashish1986a; 1991).

The efforts put by researchers were directed to address the issues related to material removal rate (MRR), depth and surface roughness in through cutting processes only. In continuation to this, to the best of my knowledge, experiments were not exhaustive and systematic. To analyze a process performance in terms of input parameters and to build a suitable model to predict the performance, understanding the influence of individual process parameter on the output is very much essential. Therefore, the present study is an attempt to assess the AWJM models on the process performance in a systematic manner. In order to study the significance of process parameters, full factorial experimental design, which can statistically consider multiple factors simultaneously and is capable of detecting the interactions on the performance are applied in the present research. The information generated will be helpful to study and investigate the contribution of individual process parameters on the responses and same data may be used for modeling the process.

3.2 Design of experiments

Design of Experiments (DOE) is the process of planning the experiments considering the input process parameters at different levels. This information is useful for building statistical models to predict the process performance. In statistics a full factorial experiment is an experiment whose design consists of two or more factors each at different possible levels and whose experimental units take on all possible combinations of these levels across such factors. Such experimental designs allow studying the effect of each parameter on the response variable as well as the interactions between factors and the response variable. If the number of combinations in a full factorial design is too high, a fractional factorial design may also be considered in which some of the combinations can be omitted. When there are many factors it may lead to multiple combinations. For example, if there are, say, 10 factors at two levels, then $2^{10}=1024$ combinations would be generated. It becomes infeasible to perform such a large number of experiments due to high cost or insufficient resources. In such cases, fractional factorial designs may be used; but fractional factorial designs are less attractive if a researcher wishes to consider more than two levels. Attempts are made to

employ the full factorial design of experiments and analysis of variance approach for studying the influence of process parameters on output responses parameters.

3.2.1 Analysis of data

Analysis of the experimental data is the method of investigating, understanding, transforming and modeling the data with the goal of discovering some useful information, suggesting conclusions and supporting decision making statements. In machining, the performance of the process can be measured based on the analysis of the experimental data. In AWJM, the process performance can be measured in terms of MRR, depth, surface roughness, kerf quality, geometrical parameters, etc. The quality of AWJM process is affected by several uncontrollable parameters known as noise factors which affect the characteristics of the process. The average loss in quality can be determined from the experimental data, which is influenced by the deviation in the mean value from the target and variance. Minimization of this deviation from the target and variance reduces the average quality loss and improves the performance. Hence, the experimental analysis of the data can be carried using the techniques of analysis of means and analysis of variance.

3.2.2 Analysis of Variance (ANOVA)

The process of estimating the relative percentage contribution of individual parameter on the overall response measurement and to estimate the variance in error qualitatively, computational techniques like ANOVA is used. Thus, the significance of each parameter on the output characteristic can be obtained. A statistical ANOVA has been performed on the experimental data in order to enumerate the statistically significant parameters affecting the average response. Using this analysis, a well-established procedure by Phadke (1989) and Ross (1989) are used to estimate the sum of squares, variance and percentage contribution of linear and quadratic effects of the individual parameters and their interaction. The error variance is the ratio of sum of squares due to error to the degree of freedom for error which can be estimated by pooling the sum of squares corresponding to the parameters having the lowest mean square value. The variance ratio (F - ratio) is the ratio of the mean square due to a parameter and the error mean square value (F - test or Fisher test). The F-ratio is used to

test whether the two variances are equal or not. The magnitude of parameter effect relative to the error variance can be obtained from F - ratio. The F-ratio value is compared with the values from the statistical tables for evaluation of the process parameter. An F- ratio greater than that of the statistical table value, it suggests that the parameter has influence on the average population and those with F- ratio values lesser than the table value, have no effect on the average (Ross 1989; Phadke 1989). This ratio helps in finding the confidence level of the response parameter. ANOVA analysis has been carried for all the quality characteristics under study in AWJ milling. Based on these results, the significant parameters are identified for building a statistical model.

3.3 Methodology

The present research aims to investigate the influence of the input parameters on milling process performance with AWJM technique. The objective of AWJ milling is evaluated in terms of MRR, surface roughness, pocket depth and dimensional accuracies in terms of kerf width, taper, depth and surface characteristics. The process is also monitored using force and vibration signals. The complexity of the process and the need to understand the interdependence of the process variables on the material characteristics requires the utilization of a parametric study. Hence, a full factorial experimental design consisting of three levels of each input process parameter has been employed and Analysis of Variance (ANOVA) has been carried out to identify the statistical significance of the input parameters on the responses.

3.4 Experimental Setup

The experimental trials are conducted on a commercially available abrasive water jet machine (Model No. 2626; OMAX, USA make) as shown in Figure 3.1 The machine uses a 3-stage plunger type high pressure pump which has a capacity to generate high pressures up to 344 MPa. Figure 3.2 shows the high pressure generation system equipped with the machine consisting of filters for the water delivery system. The machine has a water discharge capacity of 2.65 liters/min at this rated pressure. The working and technical specifications of the machine are given in Table 3.1.

In the present work, two setups are developed for performing the experiments; the first setup is used for pocket milling and the second setup for machining micro

channels. The schematic of the setup for pocket milling consists of a fixture to hold the specimen as shown Figure 3.3. The fixture is mounted on a dynamometer (Kistler Make, Model-9275B) for the force measurement. Figure 3.4 show picture of the experimental setup. All the experiments are conducted at 90° jet impingement angles only. The fresh orifice and focusing nozzle are used for the experimentation; abrasives are fed into the mixing chamber using a feed pipe attached. Proper care has been taken that the wear of the nozzle does not affect the experimentation. The focusing tube is inserted into the mixing chamber which is being tightened with a screw. The focusing tube is made of tungsten carbide and the orifice is made of sapphire (Figure 3.5). The maximum traverse speed of the machine is limited to 4000 mm/min and the motion is controlled by a CNC; a motorized Z-axis for vertical movement. Fresh abrasives of the required sizes are used for every experiment. Abrasives once used for machining are collected inside the catcher tank located at the bottom of the jet. The present AWJM system has a requirement of specific water quality so that scales are not formed inside the system and also to prevent the metallic components against corrosion. A separate Reverse Osmosis (RO) water purification system is integrated with a chiller to maintain the water at temperature of $\sim 8^\circ\text{C}$.



Fig. 3.1: OMAX 2626 Unit - Experimental setup photograph



Fig 3.2: High pressure generation pumping system

Table 3.1: Technical Specifications of AWJM

| Working Specifications of the machine | | |
|---|--|------------|
| Machine | OMAX 2626, Make: OMAX Corp., USA | |
| Maximum Traverse Speed | 4500 mm/min | |
| Jet Impingement Angle | 90° | |
| Orifice Diameter | 0.33 mm | |
| Focusing/Mixing Tube Diameter | 0.762 mm | |
| Mixing Tube Length | 101.6 mm | |
| Maximum Working Pressure | 344 MPa (or 50 Ksi) | |
| Standard Specifications of the Machining center | | |
| Maximum Supported Material Load | 1,950 kg/m ² | |
| X-Y cutting travel | 737 mm x 660 mm | |
| Z- axis travel (motorized) | 203 mm | |
| Table Size | 1,168 mm x 787 mm | |
| Noise Level | Below 80 dBA for submerged cutting | |
| Accuracy of motion | Circularity | ± 0.076 mm |
| | Repeatability | ± 0.033 mm |
| Electrical specifications | 3-Phase, 380-480 VAC, 50-60 Hz | |
| Drive Description | Closed loop, digital drives, brushless servo motors, pre-loaded ball screws, recirculating ball bearings, linear bearing with hardened precision ground ways | |

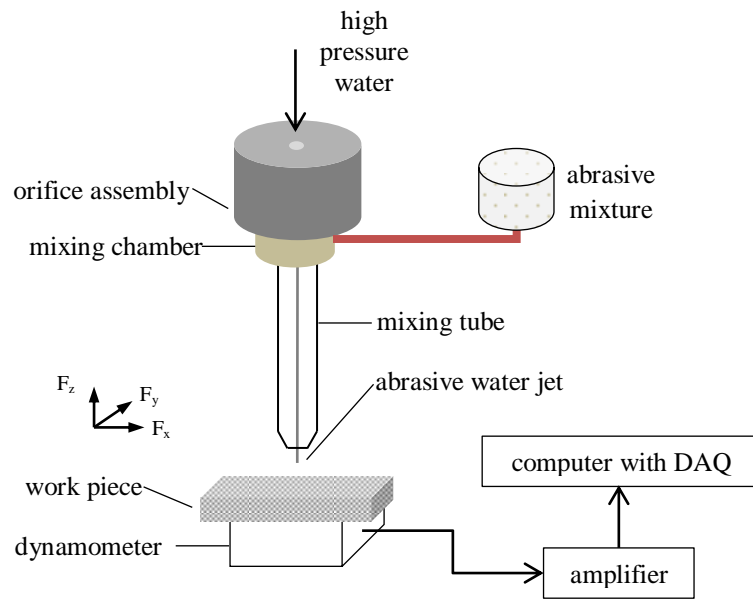


Fig. 3.3: Schematic of the experimental setup for pocket milling



Fig. 3.4: Experimental setup photograph for pocket milling

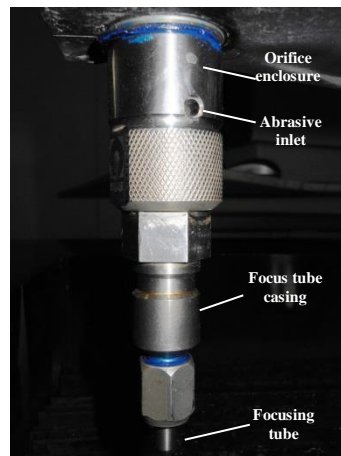


Fig. 3.5: Cutting head assembly (OMAX 2626)

3.4.1 Fixture and tool path strategy

Figure 3.6 shows a CAD model of the fixture designed and fabricated for accommodating the workpiece of size 30 mm x 30 mm x 10 mm respectively. The fixture is mounted on the force dynamometer through nuts and bolts. The experimental setup aims to make a pocket size of 20 mm X 20 mm respectively as per the design of experiments. One of the major tasks in milling process is the tool path strategy of machining. The various tool paths available in milling are raster, contour, zig-zag, etc. During the pre-experimentation phase, these strategies were tested in AWJ pocket milling process and the raster tool path strategy has been chosen in the current set of experiments. Figures 3.7(a) and 3.7(b) shows a raster tool path strategy and the sample pocket machined. The present raster tool path considers a step over of 0.4 mm (apx. half the diameter of jet). It is observed that the depth at the corners increases. This is because of the machine dynamics where the traverse speed of the jet decelerates in the areas where the jet changes its direction of motion. This deceleration results in material removal mechanism to change from milling to cutting which in turn increases the localized MRR. The localized material removal is known as digging at the corners. The typical force signal captured for pocket milling as shown in Figure 3.8 could not give conclusive information about the nature of forces acting on the workpiece during pocket milling.

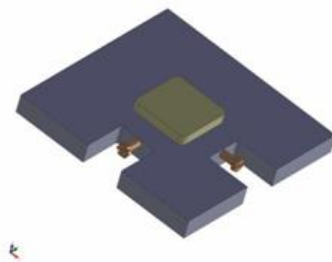


Fig 3.6: Work holding fixture

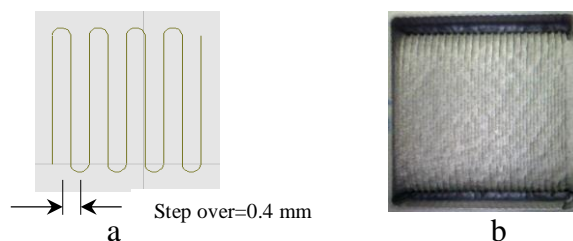


Fig 3.7: (a) Tool path strategy and (b) sample pocket image

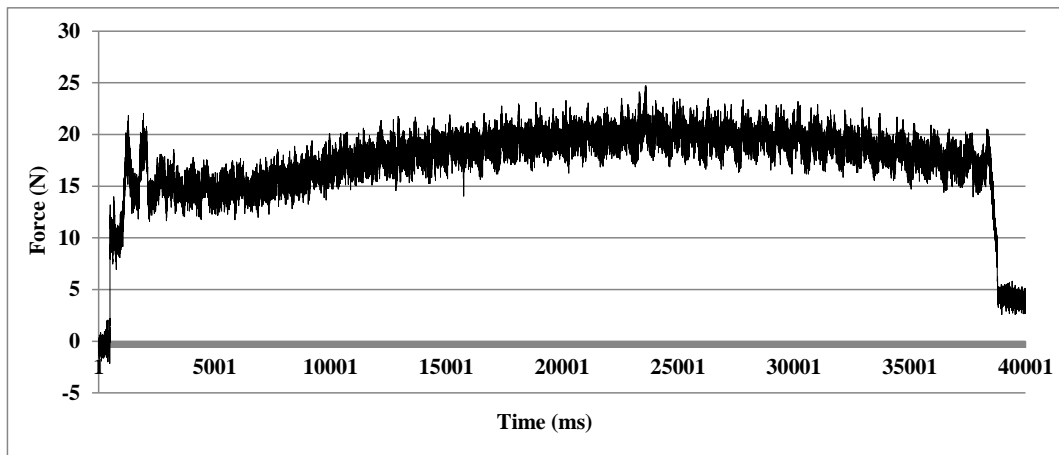


Fig. 3.8: Typical force signal for a rater tool path-pocket milling

The schematic of the experimental setup for micro-channel fabrication is shown in Figure 3.9 and Figure 3.10 shows the actual setup.

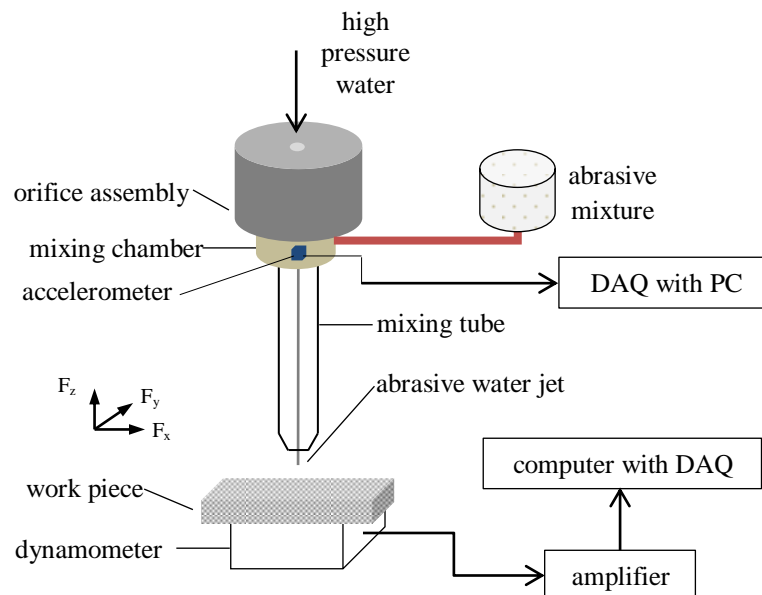


Fig. 3.9: Schematic of the experimental setup for micro-channel fabrication

The micro-channels are fabricated on SS304 plate of size 300 mm x 300 mm x 10 mm; which is mounted on the dynamometer. The force and vibration signals are captured using a dynamometer and an accelerometer. The dynamometer is integrated with an amplifier and a data acquisition system to capture force data in all three directions (x, y and z) respectively. An IEPE accelerometer (ONOSOKKI NP-3331) is used as a vibration sensor for measurement of the jet vibrations. The accelerometer has a magnetic base and is placed on the external flat surface of the mixing chamber which is just above the mixing tube assembly as shown in Figure 3.10. The vibration signals

EXPERIMENTAL INVESTIGATIONS OF ABRASIVE WATER JET MILLING

from the accelerometer are acquired through a data acquisition system (DEWE-ORION-0424) shown in Figure 3.9. The fabricated micro-channels are shown in Figure 3.11. A typical force and vibration signals of the jet during micro-channel fabrication are given in Figures 3.12 and 3.13 respectively.

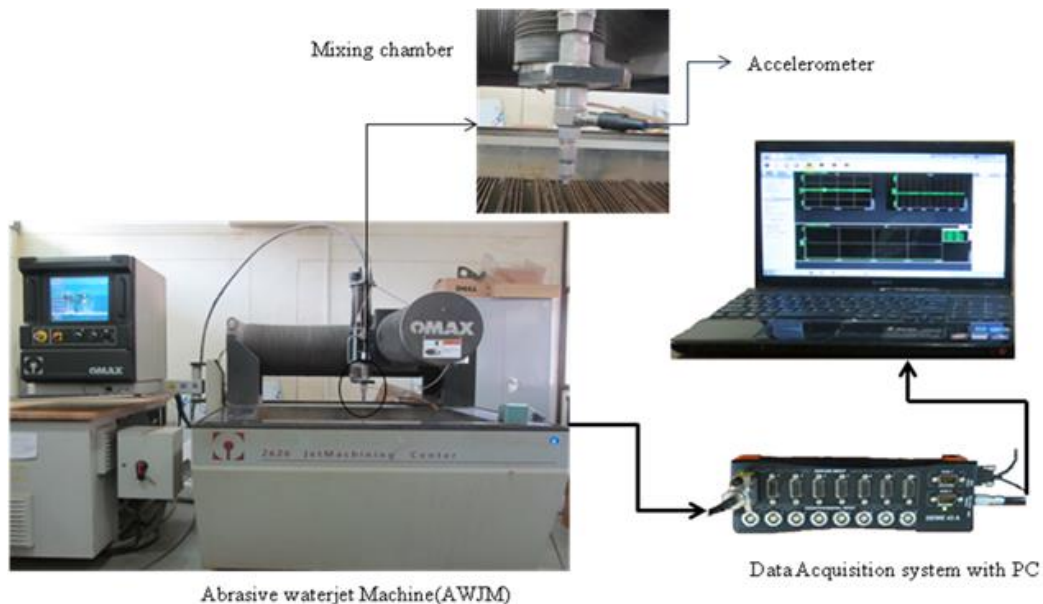


Fig. 3.10: Experimental Setup for the micro-channel preparation

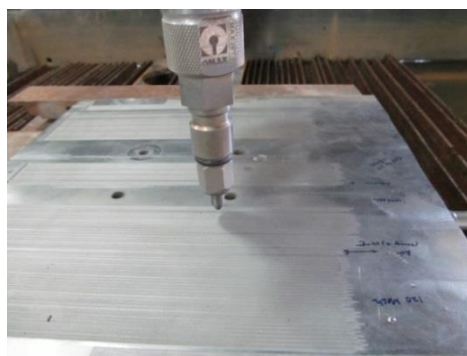


Fig. 3.11: Micro channels fabricated on SS304 plate

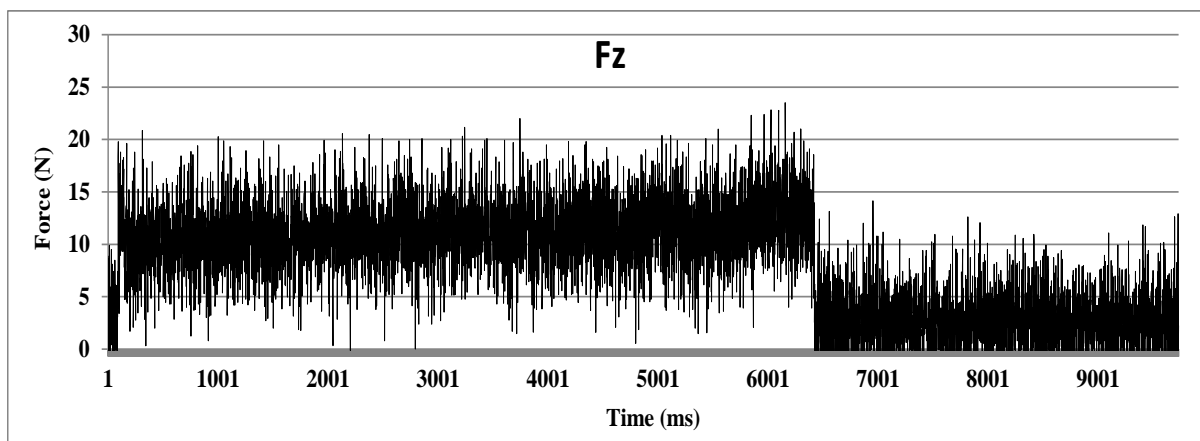


Fig.3.12: Typical force signal for a micro-channel (*Exp.No. 12*)

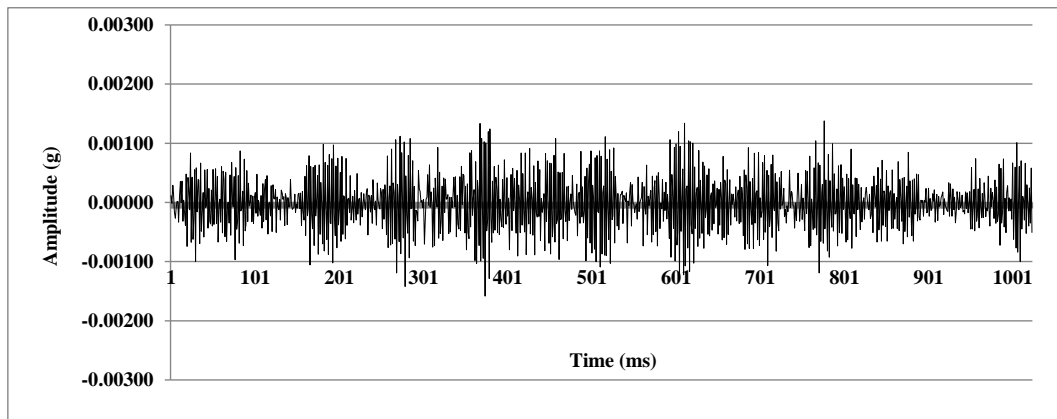


Fig.3.13: Jet vibration signal during the micro-channel fabrication (*Exp. No. 12*)

3.4.2 Materials

The target material chosen for experimentation is SS304, whose mechanical properties are given in Table 3.2. The abrasives employed in the machining process are garnets of mesh size # 80 (177 μ m), # 120 (125 μ m) and # 160 (110 μ m) respectively. The numbers in the parentheses are the abrasive particle diameters. The abrasives are supplied by M/s VV Minerals, (Tuticorin, India). The abrasive particle morphology and corresponding diameters observed through the microscope are shown in Figures 3.14 (a, b, c). Table 3.3 gives the physical and chemical properties of the garnet.

Table 3.2: Mechanical Properties of SS304

| | |
|----------------------|-------------------------------|
| Material | Stainless Steel grade (SS304) |
| Specimen Size | 30 mmx30 mmx10 mm |
| Density | 7861.093 kg/m ³ |
| Tensile Strength | 215 MPa |
| Young's Modulus | 200 GPa |
| Thermal Conductivity | 21.5 W/m ^o C |
| Melting Point | 1455 ^o C |

Table 3.3: Physical and Chemical properties of garnet

| Property | Value |
|----------------------|-----------------------|
| Specific Gravity | 4.0 - 4.5 |
| Average Bulk Density | 2.4 g/cm ³ |
| Hardness | 8.0 (mohs scale) |
| Melting Point | 1320 ^o C |

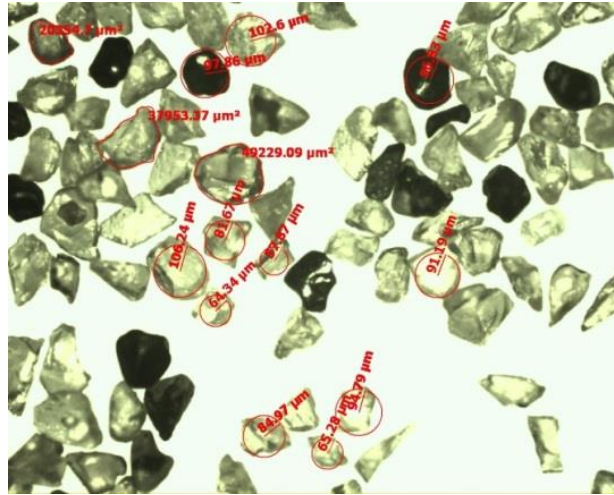


Fig. 3.14(c): Abrasive Particle photograph for # 160 abrasive

3.5 Full factorial experimental design

The input process parameters considered in the present study are traverse speed (v), SOD (h) AFR (\dot{m}_a) and abrasive size (d); each parameter is considered at 3 levels and thus, leading to a total of 81 experiments. Table 3.4 gives the range of input process parameters and their values at different levels. The parameters traverse speed and AFRs are chosen based on the limitations of the machine. SOD has been taken as per the available literature and the abrasive sizes are chosen based on the availability in standard sizes. All the experiments are conducted to acquire force and vibration data during the process of machining.

Table 3.4: Range of input process parameters

| Process Parameter (units) | Range of Values | | |
|---------------------------------|-----------------|----------------|----------------|
| | <i>Level 1</i> | <i>Level 2</i> | <i>Level 3</i> |
| Traverse Speed (mm/min) | 3000 | 3500 | 4000 |
| Standoff distance (mm) | 3 | 4 | 5 |
| Abrasive Flow Rate (Kg/min) | 0.27 | 0.38 | 0.49 |
| Abrasive Mesh Size (dia. in mm) | 80 (0.177) | 120 (0.125) | 160 (0.110) |

For pocket milling, the performance is evaluated based on the output parameters in terms of MRR, surface roughness and pocket depth. The response parameters for the micro channel fabrication are width, depth, taper and surface roughness. This chapter

deals with the investigations carried on the role of process parameters on pocket milling which are further discussed in detail in the later sections. Table 3.5 gives the consolidated experimental data for the pocket milling process.

3.6 Measurement and examination of the process and pocket milling characteristics

3.6.1 Material removal rate

The mass of the workpiece specimen is weighed before and after the experiment using an electronic balance having a resolution of 0.01 g. the specimen is weighed in dry condition before experimentation. After the pocket is milled, the abrasive particles are washed off; the cut specimen is cleaned with compressed air and completely dried before being weighed again. MRR is calculated as the ratio of weight loss to the total cutting time.

3.6.2 Surface roughness

There are a number of techniques employed to measure surface roughness. The method adopted to measure the surface roughness during the present investigation is Ra (the Arithmetic Mean of the peaks and valleys from the mean line though a sampling length). It is the most widely used and internationally employed parameter for the measurement of surface roughness. The surface roughness is measured using a Rugosurf 10, roughness measuring instrument.

3.6.3 Pocket depth

A height gauge instrument is used to measure the pocket depth. The gauge is kept at ten different locations of center of the pocket and average of these readings is taken as pocket depth.

Table 3.5: Experimental Data for pocket milling

| <i>Exp. No</i> | <i>v</i> (<i>mm/min</i>) | <i>m_a</i> (<i>kg/min</i>) | <i>d</i> (<i>mm</i>) | <i>h</i> (<i>mm</i>) | <i>MRR</i> (<i>mm³/sec</i>) | <i>Ra</i> (<i>μm</i>) | <i>Depth</i> (<i>mm</i>) |
|----------------|-------------------------------|---|---------------------------|---------------------------|---|----------------------------|-------------------------------|
| 1. | 3000 | 0.49 | 0.177 | 4 | 22.653 | 5.49 | 0.88 |
| 2. | 3500 | 0.49 | 0.125 | 5 | 22.221 | 4.42 | 0.76 |
| 3. | 3500 | 0.38 | 0.110 | 4 | 21.575 | 6.36 | 0.74 |

| | | | | | | | |
|-----|------|------|-------|---|--------|------|------|
| 4. | 3500 | 0.38 | 0.177 | 4 | 22.224 | 5.23 | 0.74 |
| 5. | 3500 | 0.27 | 0.177 | 3 | 22.394 | 5.45 | 0.79 |
| 6. | 3500 | 0.38 | 0.177 | 5 | 22.427 | 5.01 | 0.71 |
| 7. | 3000 | 0.49 | 0.125 | 4 | 20.319 | 4.86 | 0.85 |
| 8. | 4000 | 0.38 | 0.177 | 3 | 22.202 | 5.05 | 0.61 |
| 9. | 4000 | 0.38 | 0.177 | 4 | 20.965 | 5.89 | 0.67 |
| 10. | 3000 | 0.27 | 0.177 | 5 | 22.258 | 5.40 | 0.85 |
| 11. | 3000 | 0.27 | 0.110 | 4 | 21.758 | 4.61 | 0.92 |
| 12. | 3000 | 0.49 | 0.110 | 4 | 21.866 | 7.00 | 1.02 |
| 13. | 3000 | 0.38 | 0.177 | 3 | 22.590 | 5.80 | 0.82 |
| 14. | 4000 | 0.49 | 0.177 | 4 | 22.223 | 4.39 | 0.64 |
| 15. | 3500 | 0.38 | 0.177 | 3 | 22.104 | 5.92 | 0.59 |
| 16. | 3500 | 0.49 | 0.125 | 4 | 22.058 | 4.68 | 0.75 |
| 17. | 4000 | 0.49 | 0.110 | 4 | 21.310 | 6.41 | 0.71 |
| 18. | 3500 | 0.27 | 0.110 | 5 | 21.189 | 6.28 | 0.79 |
| 19. | 3000 | 0.27 | 0.177 | 3 | 22.526 | 6.19 | 0.90 |
| 20. | 3500 | 0.27 | 0.125 | 3 | 22.357 | 5.26 | 0.83 |
| 21. | 4000 | 0.27 | 0.177 | 4 | 22.168 | 5.54 | 0.60 |
| 22. | 4000 | 0.27 | 0.125 | 3 | 21.744 | 5.65 | 0.65 |
| 23. | 4000 | 0.49 | 0.125 | 3 | 22.079 | 5.12 | 0.61 |
| 24. | 4000 | 0.38 | 0.177 | 5 | 22.315 | 5.33 | 0.50 |
| 25. | 3000 | 0.27 | 0.125 | 4 | 19.459 | 4.74 | 0.88 |
| 26. | 4000 | 0.38 | 0.110 | 5 | 21.083 | 5.26 | 0.71 |
| 27. | 3500 | 0.49 | 0.177 | 4 | 22.420 | 5.69 | 0.70 |
| 28. | 4000 | 0.38 | 0.110 | 3 | 21.343 | 5.06 | 0.77 |
| 29. | 3000 | 0.49 | 0.177 | 3 | 22.953 | 4.71 | 0.71 |
| 30. | 3000 | 0.38 | 0.110 | 4 | 22.077 | 4.02 | 0.93 |
| 31. | 3000 | 0.38 | 0.110 | 3 | 21.836 | 5.48 | 0.99 |
| 32. | 3000 | 0.38 | 0.110 | 5 | 22.324 | 5.70 | 1.06 |
| 33. | 4000 | 0.49 | 0.125 | 5 | 22.288 | 5.23 | 0.59 |
| 34. | 3000 | 0.38 | 0.177 | 5 | 22.849 | 5.25 | 0.87 |
| 35. | 3500 | 0.49 | 0.177 | 3 | 22.717 | 5.31 | 0.62 |
| 36. | 3000 | 0.38 | 0.125 | 3 | 22.473 | 5.51 | 0.85 |
| 37. | 4000 | 0.49 | 0.177 | 5 | 22.404 | 5.56 | 0.59 |
| 38. | 3500 | 0.27 | 0.177 | 5 | 22.577 | 5.52 | 0.65 |
| 39. | 4000 | 0.27 | 0.177 | 3 | 22.579 | 5.79 | 0.63 |
| 40. | 3000 | 0.27 | 0.125 | 5 | 22.558 | 5.54 | 0.85 |
| 41. | 4000 | 0.38 | 0.125 | 5 | 25.344 | 3.39 | 0.65 |
| 42. | 4000 | 0.38 | 0.125 | 3 | 22.086 | 4.51 | 0.62 |
| 43. | 3000 | 0.38 | 0.177 | 4 | 22.966 | 6.01 | 0.77 |
| 44. | 3500 | 0.49 | 0.110 | 4 | 21.692 | 6.21 | 0.76 |
| 45. | 3500 | 0.27 | 0.110 | 3 | 21.537 | 5.15 | 0.87 |
| 46. | 3000 | 0.27 | 0.125 | 3 | 22.735 | 5.89 | 0.96 |
| 47. | 4000 | 0.38 | 0.125 | 4 | 21.908 | 4.51 | 0.71 |
| 48. | 4000 | 0.27 | 0.110 | 4 | 21.356 | 6.15 | 0.66 |

EXPERIMENTAL INVESTIGATIONS OF ABRASIVE WATER JET MILLING

| | | | | | | | |
|-----|------|------|-------|---|--------|------|------|
| 49. | 3500 | 0.27 | 0.125 | 4 | 22.440 | 5.08 | 0.78 |
| 50. | 4000 | 0.49 | 0.110 | 3 | 21.181 | 5.56 | 0.70 |
| 51. | 3000 | 0.49 | 0.177 | 5 | 22.754 | 6.00 | 0.92 |
| 52. | 3000 | 0.49 | 0.110 | 3 | 21.595 | 5.21 | 0.95 |
| 53. | 3500 | 0.27 | 0.110 | 4 | 21.641 | 5.27 | 0.77 |
| 54. | 4000 | 0.27 | 0.125 | 4 | 22.223 | 4.55 | 0.67 |
| 55. | 3500 | 0.38 | 0.125 | 4 | 22.520 | 4.20 | 0.77 |
| 56. | 3500 | 0.49 | 0.110 | 5 | 21.473 | 5.09 | 0.76 |
| 57. | 4000 | 0.27 | 0.110 | 3 | 21.310 | 5.21 | 0.68 |
| 58. | 3000 | 0.49 | 0.110 | 5 | 21.776 | 3.33 | 0.89 |
| 59. | 3000 | 0.38 | 0.125 | 5 | 22.508 | 4.76 | 0.85 |
| 60. | 3500 | 0.38 | 0.125 | 3 | 22.420 | 5.06 | 0.71 |
| 61. | 4000 | 0.27 | 0.125 | 5 | 22.397 | 3.43 | 0.55 |
| 62. | 4000 | 0.49 | 0.177 | 3 | 22.531 | 6.00 | 0.62 |
| 63. | 3500 | 0.27 | 0.125 | 5 | 22.440 | 4.99 | 0.76 |
| 64. | 3500 | 0.38 | 0.110 | 3 | 21.537 | 7.21 | 0.79 |
| 65. | 4000 | 0.49 | 0.110 | 5 | 21.246 | 5.27 | 0.66 |
| 66. | 3500 | 0.49 | 0.177 | 5 | 22.723 | 5.65 | 0.75 |
| 67. | 4000 | 0.27 | 0.177 | 5 | 22.483 | 5.90 | 0.38 |
| 68. | 3500 | 0.38 | 0.110 | 5 | 21.562 | 5.65 | 0.74 |
| 69. | 4000 | 0.49 | 0.125 | 4 | 22.182 | 5.38 | 0.68 |
| 70. | 3500 | 0.27 | 0.177 | 4 | 22.797 | 4.69 | 0.69 |
| 71. | 3000 | 0.38 | 0.125 | 4 | 22.460 | 4.51 | 0.93 |
| 72. | 3000 | 0.49 | 0.125 | 5 | 22.520 | 4.91 | 0.91 |
| 73. | 3000 | 0.27 | 0.110 | 3 | 21.656 | 5.70 | 1.01 |
| 74. | 4000 | 0.27 | 0.110 | 5 | 21.343 | 4.71 | 0.73 |
| 75. | 4000 | 0.38 | 0.110 | 4 | 21.424 | 5.27 | 0.72 |
| 76. | 3000 | 0.27 | 0.110 | 5 | 21.836 | 4.71 | 0.93 |
| 77. | 3000 | 0.49 | 0.125 | 3 | 20.291 | 4.80 | 0.91 |
| 78. | 3500 | 0.49 | 0.110 | 3 | 20.430 | 5.12 | 0.75 |
| 79. | 3500 | 0.49 | 0.125 | 3 | 22.091 | 5.09 | 0.83 |
| 80. | 3500 | 0.38 | 0.125 | 5 | 22.524 | 4.98 | 0.80 |
| 81. | 3000 | 0.27 | 0.177 | 4 | 22.890 | 4.78 | 0.87 |

3.7 Experimental investigations on pocket milling

The milling process with AWJM is not a matured technique when compared to through cutting with little published research on the process characteristics for MRR, surface roughness and pocket depth. The following sections explain the experimental investigations carried on the role of individual process parameters on the response parameters.

3.7.1 Role of traverse speed

In AWJM, traverse speed plays a dominating role in the material removal process. The major influence of the traverse speed on the process is the local exposure time, in which the abrasive water jet interacts with the work material. Figures 3.15-3.19 illustrate the effect of traverse speed on surface roughness, MRR and pocket depth with pump pressure, SOD, AFR and abrasive (mesh) size respectively. At low traverse speeds the material removal takes place mainly due to cutting wear mechanism and results in higher surface roughness. The higher surface roughness is due to damping effect of the abrasive particles on the surface and further due to higher interaction time of the jet with the material, higher MRR are observed. At high traverse speeds, the energy density of the particle impacting the surface reduces which results in lower pocket depth and an improved finish. The graphs reveal that the MRR decreases at higher traverse speeds because of the smaller interaction time. Reports on surface roughness (Hashish 1991, Ojmertz 1993) have indicated that non-uniformity in depth exists on components machined with AWJM and it cannot be removed, but instead would be exaggerated by subsequent passes. So, to improve the surface roughness, the traverse speed has to be increased. In this case, the kinetic energy transferred to the work piece by the abrasive water jet is inversely proportional to the traverse rate.

3.7.2 Effect of pressure

The general structure of AWJM process is a result of complex relations between the pump pressure, process of jet formation, acceleration and mixing of the abrasives. It is evident from the basic principles that the water jet velocity increases with the rise in pump pressure. The efficiency parameter and the compressibility factor decreases with rise in the pump pressure. The influence of pump pressure on the mixing process is similar to the complex process of AWJM. All the parameters that influence the average velocity of the abrasive particles depend on the pump pressure. In AWJM process, a threshold pressure exists above which the material removal takes place and this depends on the abrasive mass flow rate, traverse speed and orifice diameter for a given target material.

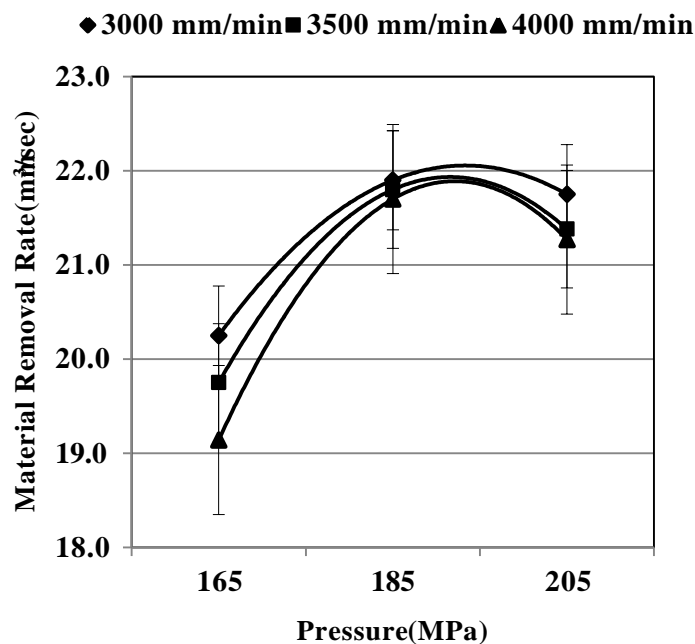


Fig 3.15: Effect of Pressure and Traverse speed on MRR (SOD 4mm, AFR 0.38 kg/min, # 80 abrasive size)

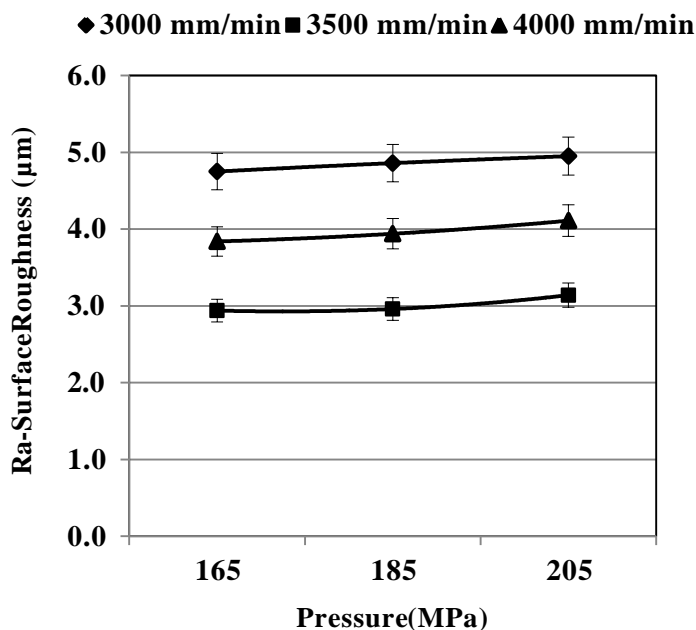


Fig 3.16: Effect of Pressure and Traverse speed on Ra (SOD 4mm, AFR 0.38 kg/min, # 80 abrasive mesh)

The preliminary experiments with varying pressure on MRR as plotted in Figure 3.15 shows that a non-linear relationship exists between the pump pressure and MRR,

where the efficiency of the cutting process decreases with an increase in the pump pressure (Momber et al. 1996) after a critical pressure. Again this depends on the type of target material and other parameters like AFR, abrasive size, etc. Figure 3.16 shows that no significant influence of pressure on surface roughness is observed for pocket milling applications.

3.7.3 Effect of standoff distance

The distance between the tip of the nozzle and target work surface is termed as SOD. It is another important parameter in AWJM process. In case of low SODs, the abrasive flow is damped or decelerated by the target surface which leads to generation of a poor surface and increased MRR. An increase in SOD increases the jet diameter leading to decrease in the energy density. The decrease in energy density generates more random peaks and valleys on the pocket surface leading to higher surface roughness and reduced MRR. Figure 3.17 illustrates the influence of SOD on surface roughness and MRR.

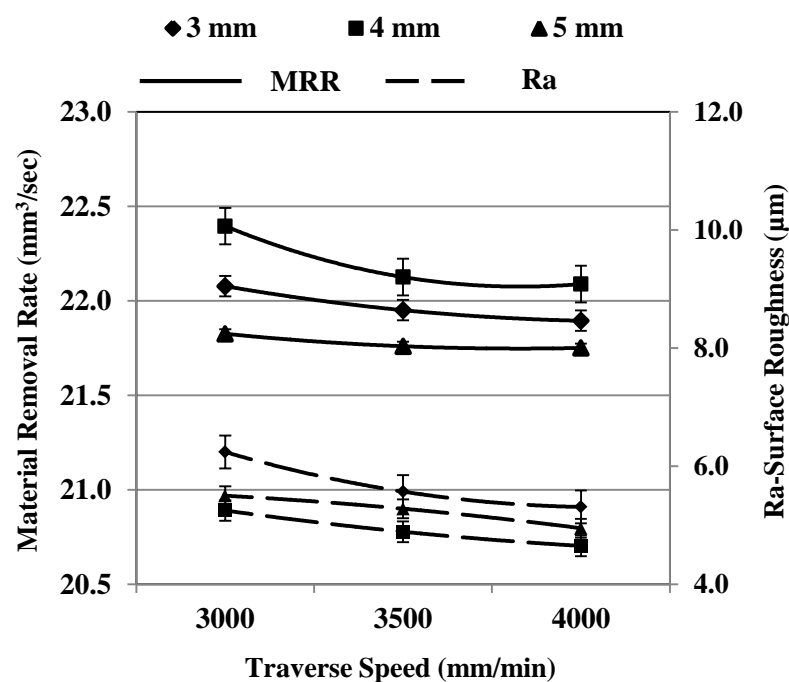


Fig 3.17: Effect of SOD and Traverse speed on MRR and Ra (Pressure 241 MPa, AFR 0.38 kg/min; # 120 abrasive mesh)

Experimentally, it is observed that at SOD of 3mm, the surface roughness is more at low traverse speeds, and on increasing the SOD to 4 mm, the surface finish is

improved. The decrease in the MRR at SOD 3 mm when compared to SOD 4 mm is due to the upward deflection of the jet. At SOD 4 mm, it is found that the MRR is high and surface finish is better. This is due to the stabilization of the jet. It is further observed that at SOD of 4 mm, the material removal mechanism is predominantly of cutting wear mode till at a traverse speed of 3500 mm/min is achieved and then the cutting mechanism changes to deformation mode. On increasing the SOD to 5 mm, the surface roughness increases. Similar trends were observed while cutting metallic coated steel sheets (Wang et al. 1999), laminates (Ramulu et al. 1994) and cutting ceramics (Chen et al. 1998).

In general, SOD has more influence on the penetration depth than the MRR. This is also clearly reflected from the rate of change of material removal, which is not that significant in comparison to surface finish. This could be due to the fact that at higher SODs, the radial expansion of the abrasive water jet yields a larger exposed area. The general increase in the width of cut with increase in the SOD also expresses this effect.

3.7.4 Influence of abrasive flow rate

AFR is another process parameter which influences the machining process. A typical AFR is a result of several effects which determines the number of impacting particles and their kinetic energies. At high AFR, larger number of particles is involved in mixing and cutting. Assuming there is no contact within the abrasives during the mixing, an increase in AFR leads to a proportional increase in the depth of cut and the phenomenon of no contact is predominant at low AFRs only.

At higher values of AFR, the particle collisions occur inside the mixing chamber, during accelerating inside the focusing tube and during cutting. At high AFR, a limited amount of kinetic energy of jet gets distributed over a large number of particles which leads to decrease in kinetic energy of the individual particle and this also leads to increase in the turbulence. As the AFR is increased, initially MRR increases and then decreases due to reduction in the abrasive flow velocity. Further increasing the AFR does not contribute to any notable change in the MRR. At lower AFRs, the mode of material removal is primarily micro-cutting and depending on the

shape of the abrasive particle the material removal modes in micro cutting are cutting deformation and ploughing deformation.

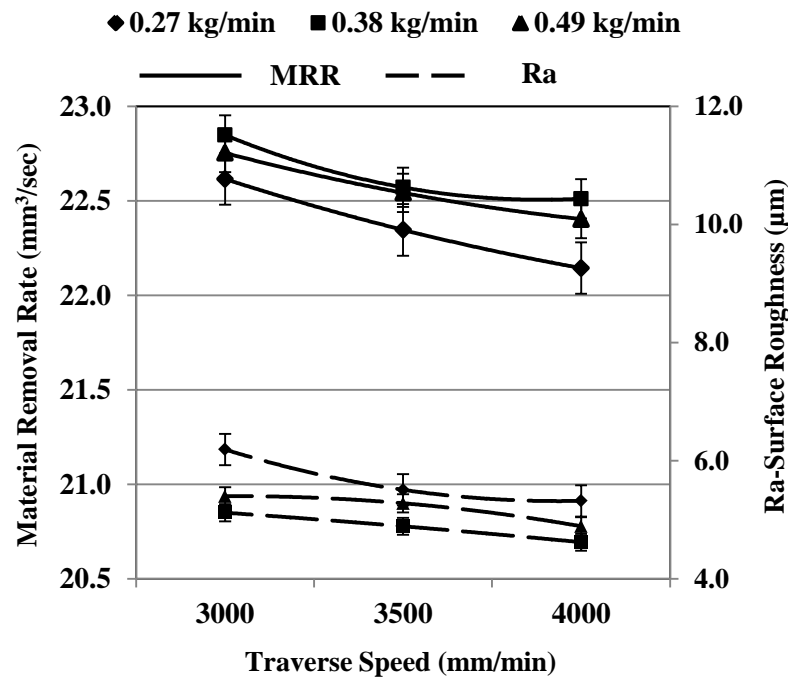


Fig 3.18: Effect of AFR and Traverse speed on MRR and Ra (Pressure 241 MPa, SOD 3 mm, # 120 abrasive mesh)

The influence of AFR with traverse speed on MRR and surface roughness is plotted in Figure 3.18. At low AFRs (0.27 kg/min), the quantity of abrasive particles impinging the surface is less and the material removal mechanism is predominantly deformation mode than cutting mode. At a given AFR, the surface roughness increases with increase in traverse speed, while the MRR decreases. On increasing the AFR to 0.38 kg/min, better surface finish and higher material removal rates are obtained. Further increase in the AFR to 0.49 kg/min results in poor surface due to collision within the particles. As the AFR increases, the surface roughness increases due to the jet instability. These instabilities are attributed to factor such as fluctuations, vibrations in the abrasive distribution.

3.7.5 Role of abrasive size (mesh)

In a through cutting process with AWJM, the size of the abrasive is not very significant, while in milling it is an important process parameter and including the shape of the particle. The surface structure of the pocket plays a vital role in AWJ

EXPERIMENTAL INVESTIGATIONS OF ABRASIVE WATER JET MILLING

milling process. The microscopic details like voids, micro cracks and details of micro structure are very crucial which depend on the engagement of abrasive particle with the work surface. With large diameter particles, higher MRR or the depth are obtained since the kinetic energy of the jet increases. This effect is clearly shown in Figure 3.19.

On the other hand, an increase in the particle diameter reduces the number of abrasives for the same AFR. Pocket machining with higher abrasive sized particles, the formation of drag lines on the surface increases which results in a poor surface. Here the surface finish initially improves with an increase in the traverse speed and then deteriorates. Bigger diameter particles tend to defragment during mixing and this is also one of the possible causes for poor finish. As shown in the Figure 3.19, # 80 abrasives gives higher MRR and higher surface roughness while a # 160 abrasives improves the finish with reduced MRR. Erosion involves high strain rate and large total strain with small depth of cut. All these factors tend to increase the flow stress and further with smaller abrasives the increased ratio of surface to mass will alter the cutting condition and increases the amount of material removal. Fine abrasives involve deformation mode of material removal at high strain and strain rates which improvement in surface finish.

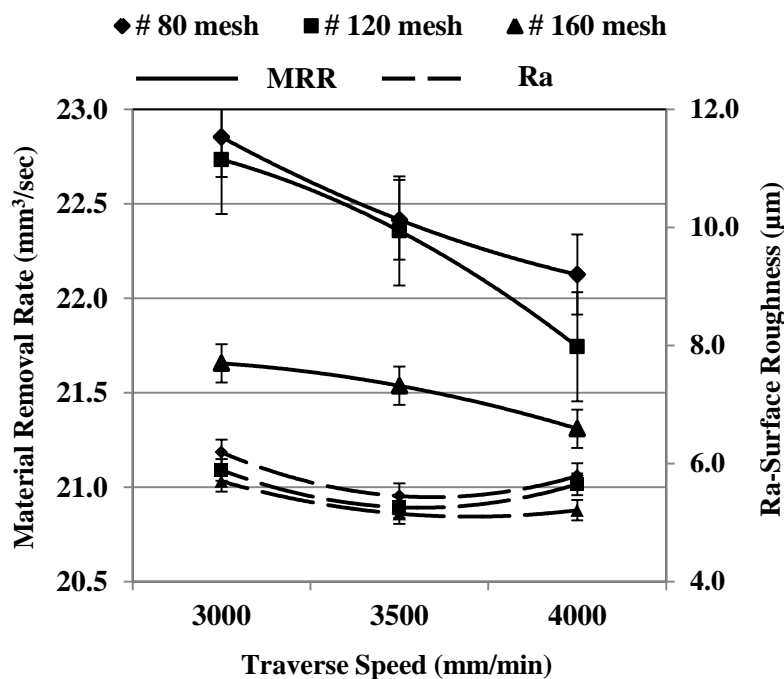


Fig 3.19: Effect of Abrasive size and Traverse speed on MRR and Ra (Pressure 241 MPa, AFR 0.38 kg/min; SOD 3mm)

3.7.6 Effect of process parameters on pocket depth

Apart from the MRR and surface roughness, pocket depth is also a significant parameter to be observed. The experimental results plotted in Figure 3.20 shows a decrease in pocket depth with increase in SOD. With increase in SOD, the energy density of the jet decrease due to the entrainment of the air present in the atmosphere and the jet loses its focus resulting in an improper machining which leads to decrease in the pocket depth.

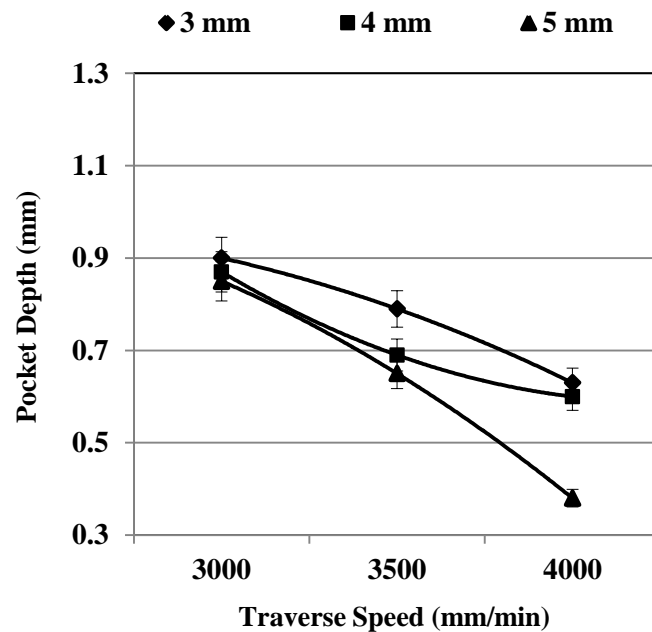


Fig. 3.20: Effect of SOD and Traverse speed on pocket depth (Pressure 241 MPa, AFR 0.38 kg/min; # 120 abrasive mesh)

A higher AFR leads to increased number of impacting abrasive particles and higher kinetic energies and the role of abrasive particles becomes more significant in mixing and cutting. As AFR is increased the pocket depth increases, but it decreases with the traverse speed as show in Figure 3.21. In general, at higher AFR some of the abrasives will land on flat faces and does no cutting and other abrasive particles cut into the surface and remove the material in a manner similar to milling cutter or grains on a grinding wheel. The plots also reveal that at lower traverse speeds the depth is not much affected with AFR, since at low traverse speeds, more number of particles gets involved at the same location irrespective of the AFR and intermixing of abrasives also take place.

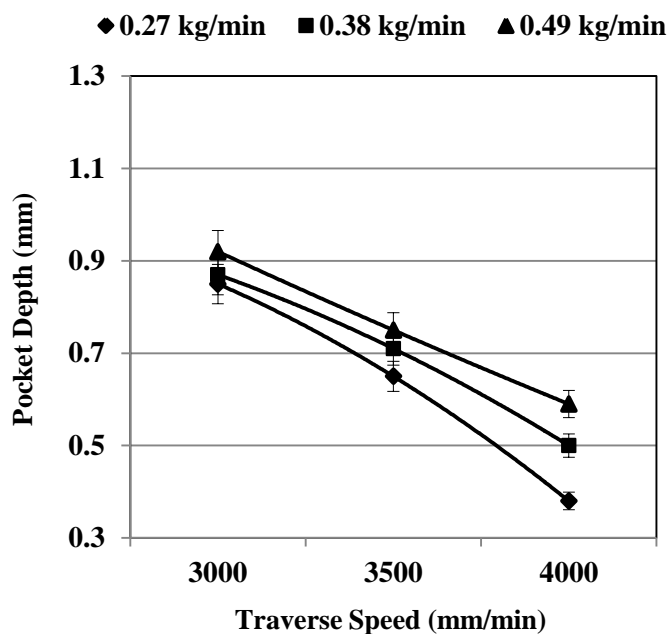


Fig. 3.21: Effect of AFR and Traverse speed on pocket depth (Pressure 241 MPa, SOD 3mm, # 120 abrasive mesh)

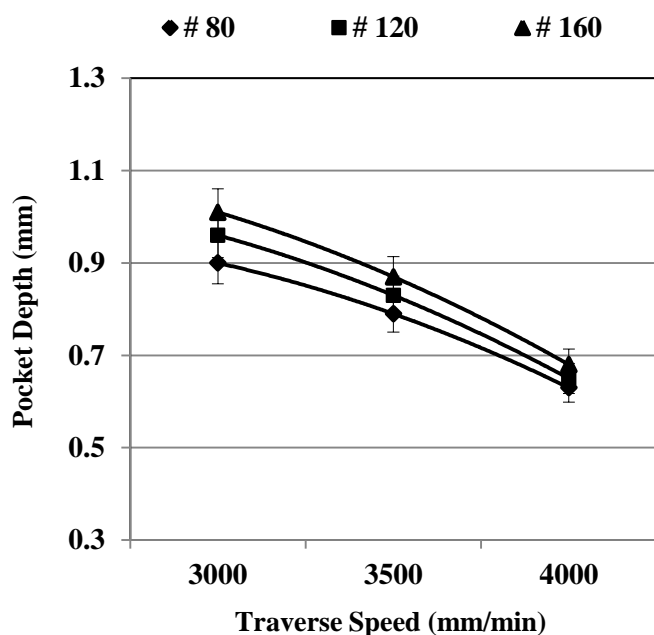


Fig. 3.22: Effect of Abrasive size and Traverse speed on pocket depth (Pressure 241 MPa, AFR 0.38 kg/min; SOD 3mm)

The penetration depth of an indenting edge depends on size of the abrasive. The pocket depth decreases with increase in the particle diameter. This is because that at a given AFR, the number of grains impacting the surface is reduced for large diameter

abrasives and also the large sized abrasives are less accelerated due to its mass. Thus, the jet stream energy gets reduced. The reduction in the abrasive particle velocities are also due to inertia of the particle. The influence of abrasive size on the cutting process has higher probability of impact fracture leading to lesser MRR with traverse speed. This influence is clearly seen in Figure 3.22 and also reveals that at higher traverse speeds, the influence of particle size is not significant.

3.8 Summary and conclusions

The present work makes an attempt to investigate the feasibility of obtaining a milled pocket, so as to reduce the weight of the structure or component without loss of its strength; as practiced in the space and defense sectors, apart from other applications. In AWJ milling process, traverse speed has more influence than any other process parameter. Higher traverse speeds are very much essential to obtain better surface finish. While considering the traverse speed with process parameters, an optimum traverse speed has to be chosen keeping the requirement of MRR and the pocket dimensions.

It has been observed that in the present experimental set, the material removal mechanism is essentially because of cutting wear mode which is predominant at SOD of 4 mm, AFR of 0.38 kg/min and a mesh size of 80. As the traverse speed increases the material removal mechanism changes from cutting wear mode to deformation wear mode due to insufficient time available for the material removal to take place during the jet and work interaction. The increase in SOD leads to higher surface roughness due to fluctuations within the jet and decrease in MRR are because of loss of focus of the jet. As the AFR increases, the surface roughness initially increases and then decreases and similarly the MRR also follows the same trend, this is due to collisions occurring within the particles in the process of mixing in the mixing chamber. This phenomenon occurs in AWJM process as reported by Hashish (1979, 1986a). Coarse abrasive particles give a more material removal and poor finish and a finer particle impact gives a better finish.

Chapter 4

EMPIRICAL AND THEORETICAL MODELING

| | |
|---|----|
| 4.1 Introduction | 67 |
| 4.2 Material removal by an individual abrasive particle | 68 |
| 4.3 Dimensional analysis for material removal rate | 69 |
| 4.3.1 Predictive model for material removal rate | 72 |
| 4.3.2 Nomenclature | 72 |
| 4.3.3 Predicted vs. experimental data | 73 |
| 4.4 Theoretical modeling of forces | 75 |
| 4.4.1 Calculation of abrasive water jet velocity | 78 |
| 4.4.2 Experimental validation and conclusions | 80 |
| 4.5 Theoretical calculations for MRR | 85 |
| 4.6 Summary | 89 |

4.1 Introduction

Many researchers worked in the field of AWJM and developed variety of empirical models for a range of process parameters and responses. Their works have been outlined in the previous chapters. These empirical models are restricted to cutting applications of metals, non-metals, composites, ceramics, etc. As per the best of our knowledge, there is no literature that reports the development of predictive models for controlled depth cutting or milling applications. The development of material removal rate (MRR) models considering a host of operating parameters is enormously difficult. Further, various phenomena associated in AWJ cutting like particle interference and fragmentation, were not very well understood and we could not find any published research focusing on the mathematical models developed to represent this. As a result, development of a theoretical model for the material removal is possible either with only a few process parameters, else very complicated equations would have to be developed with many unknown parameters which may make the model unrealistic for any practical use.

Dimensional analysis is a powerful analytical technique to describe the relation between the physical engineering quantities like MRR and other independent variables.

This can be used to develop mathematical equations in terms of the process variables, while the constants can be determined from the experimental data. In this technique, all variables appearing in the problem can be assembled into small number of independent dimensionless products (π groups). The requirement of this technique is that a mathematical relation must have the same dimensions regardless of the choice of units of individual variables. The relationships connecting the individual variables can be determined by algebraic expressions relating to each π group, thus reducing the total number of variables.

4.2 Material removal by an individual abrasive particle

The impact of a single solid particle is the basic event in the material removal by AWJs. A compressed review on the material removal erosion by a solid particle is expressed in Chapters 2 and 3. Although, a large number of variables affect the material removal process, there are a few dominating process parameters which govern the MRR as per the literature. Basic material removal mechanisms are either by cutting, fatigue, brittle fracture and melting. A combination of these mechanisms generally acts for the material removal to take place. The contribution of a particular erosion process depends on several factors, such as impact angle, particle kinetic energy, particle shape, target material properties and environmental conditions.

Zeng and Kim (1996a) incorporated a host of workpiece material properties in their model of machining brittle materials, including the ratio of dynamic hardness to the elastic modulus. In another work by Zeng and Kim (1996b), flow stress of the material is considered in view of the fact that material removal in AWJ involves flow of the material, which is nothing but shear deformation of the work material during machining.

The dominant set of parameters considered in the present research is outlined in the previous chapter. They are abrasive size which relates the individual particle mass; number of particles impacting per unit time, known as abrasive flow rate (AFR); velocity of the abrasive water jet, governed by water jet pressure; distance between the work surface and nozzle tip known as the standoff distance (SOD) and the jet interaction time determined by the traverse speed of the jet. The experimental MRR data presented in Table 3.5 is used for further analysis.

4.3 Dimensional analysis for material removal rate

AWJM process being influenced by a variety of variables for the material removal process to take place and though the literature reveals the dominating parameters in the process, the work presented considers only a few parameters. Their ranges are specified in Table 3.4. The MRR can be expressed as a function of input process parameters and material properties as follows:

$$\dot{V} = f(\dot{m}_a, h, v, d, P, H_w) \quad (4.1)$$

Where, \dot{V} is the volumetric MRR, \dot{m}_a is the AFR, h is SOD, v traverse speed, d diameter of the particle, P is the jet pressure, H_w is the Vickers's hardness expressed in pressure units. The variables in Equation 4.1 can be expressed in terms of the three fundamental dimensions, i.e. length L, mass M, and time T respectively. Here, the total number of variables is seven while three are repeating variables.

$$\dot{V} = M^0 L^3 T^{-1}$$

$$\dot{m}_a = M^1 L^0 T^{-1}$$

$$h = M^0 L^1 T^0$$

$$v = M^0 L^1 T^{-1}$$

$$d = M^0 L^1 T^0$$

$$P = M^1 L^{-1} T^{-2}$$

$$H_w = M^1 L^{-1} T^{-2}$$

According to the Buckingham π -theorem, \dot{m}_a, d, v are selected as the repeating variables and the difference between the total number of variables and number of repeating variables gives the total number of dimensionless groups. In the present case, there are $7 - 3 = 4$ dimensionless groups ($\pi_1, \pi_2, \pi_3, \pi_4$) which are expressed as:

$$\pi_1 = \dot{V}(\dot{m}_a^{x_1})(d^{y_1})(v^{z_1}) \quad (4.2)$$

$$\pi_2 = h(\dot{m}_a^{x_2})(d^{y_2})(v^{z_2}) \quad (4.3)$$

$$\pi_3 = P(\dot{m}_a^{x_3})(d^{y_3})(v^{z_3}) \quad (4.4)$$

$$\pi_4 = H_w(\dot{m}_a^{x_4})(d^{y_4})(v^{z_4}) \quad (4.5)$$

Solving the individual dimensional group as follows:

$$\pi_1 = L^3 T^{-1} (M T^{-1})^{x_1} (M^0 L^1 T^0)^{y_1} (M^0 L^1 T^{-1})^{z_1}$$

$$M^0 L^0 T^0 = L^3 T^{-1} (M T^{-1})^{x_1} (M^0 L^1 T^0)^{y_1} (M^0 L^1 T^{-1})^{z_1}$$

Equating the dimensional terms in π_1 we get,

$$x_1 = 0 \quad (\text{for terms of } M) \quad (4.6)$$

$$y_1 + z_1 = -3 \quad (\text{for terms of } L) \quad (4.7)$$

$$-x_1 - z_1 = 1 \quad (\text{for terms of } T) \quad (4.8)$$

Solving equations 4.6-4.8 for x_1 , y_1 , z_1 the following values are obtained

$$x_1 = 0; \quad y_1 = -2; \quad z_1 = -1$$

Substituting these values in π_1 ,

$$\pi_1 = L^3 T^{-1} (M T^{-1})^0 (M^0 L^1 T^0)^{-2} (M^0 L^1 T^{-1})^{-1}$$

This leads to

$$\pi_1 = \dot{V}(\dot{m}_a)^0 (d)^{-2} (v)^{-1} \quad (4.9)$$

$$\pi_1 = \frac{\dot{V}}{vd^2}$$

Similarly solving equations π_2, π_3, π_4 we can obtain

$$\pi_2 = h(\dot{m}_a)^0(d)^{-1}(v)^0 \quad (4.10)$$

$$\pi_2 = \frac{h}{d}$$

$$\pi_3 = P(\dot{m}_a)^{-1}(d)^2(v)^{-1} \quad (4.11)$$

$$\pi_3 = \frac{Pd^2}{\dot{m}_av}$$

$$\pi_4 = H_w(\dot{m}_a)^{-1}(d)^2(v)^{-1} \quad (4.12)$$

$$\pi_4 = \frac{H_w d^2}{\dot{m}_av}$$

According to dimensional analysis, the relation between the dimensionless groups (Equation 4.9-4.12) can be expressed as,

$$\pi_1 = f(\pi_2, \pi_3, \pi_4) \quad (4.13)$$

Therefore, Equation 4.13 can also be expressed as:

$$\dot{V} = vd^2 \left\{ \left(\frac{h}{d} \right)^{X_1} \left(\frac{Pd^2}{\dot{m}_av} \right)^{X_2} \left(\frac{H_w d^2}{\dot{m}_av} \right)^{X_3} \right\} \quad (4.14)$$

Taking log on both sides,

$$\ln \left(\frac{\dot{V}}{vd^2} \right) = \left\{ X_1 \ln \left(\frac{h}{d} \right) + X_2 \ln \left(\frac{Pd^2}{\dot{m}_av} \right) + X_3 \ln \left(\frac{H_w d^2}{\dot{m}_av} \right) \right\} \quad (4.15)$$

In the above equation X_1, X_2, X_3 are the dimensionless constants and the MRR is expressed as a function of the independent variables considered in developing the relation. The mathematical models developed in the above equations are in generic

form considering the input process parameters for the pocket milling using AWJM. However, before proceeding for further analysis, the constants in the models are to be determined. For this purpose, regression analysis of the experimental data obtained in Chapter 3 is performed. Using the technique the constants in the Equation 4.15 can be obtained as described below. Equation 4.15 is rewritten in a simplified form as:

$$A = BX_1 + CX_2 + DX_3$$

where

$$A = \ln\left(\frac{\dot{V}}{vd^2}\right) \quad B = \ln\left(\frac{h}{d}\right) \quad C = \ln\left(\frac{Pd^2}{\dot{m}_a v}\right) \quad D = \ln\left(\frac{H_w d^2}{\dot{m}_a v}\right)$$

4.3.1 Prediction of MRR for pocket milling

Since the expression is generic and is valid for any material machining with AWJM. To establish a relation and develop a model which could predict the behavior of the pocket milling process, the constants in the above expression are to be found with the pocket milling experimental data. For this purpose, the experimental data obtained in Chapter 3 has been utilized. Since the above set of experiments are conducted at constant pressure and the same material is same; pressure and hardness are considered as constant values. Considering the pressure and workpiece material properties On performing linear regression analysis of the experimental data, the values of X_1 , X_2 , X_3 are obtained as $X_1 = -0.5301$; $X_2 = 2.185$; $X_3 = -1.0497$, which support in expressing the MRR for pocket milling as:

$$\dot{V} = (1.5003 \times 10^{-14}) \frac{\dot{m}_a^{1.1353} P^{2.185} d^{4.8007}}{h^{0.5301} v^{0.1353} H_w^{1.0497}} \quad (4.16)$$

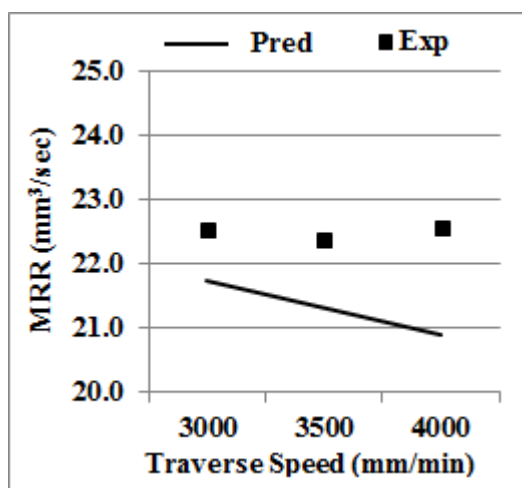
4.3.2 Nomenclature

The units for the parameters used in the above expression are as follows:

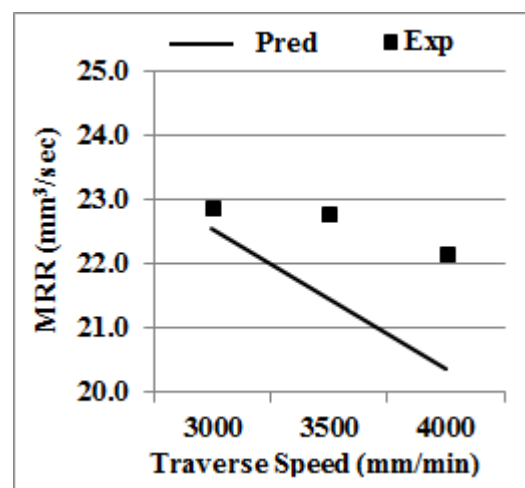
| | |
|--|---|
| d : average particle diameter (microns) | P : pressure (MPa) |
| h : standoff distance (mm) | \dot{m}_a : Abrasive flow rate (kg/min) |
| H_w : Vickers Hardness (kg/mm ²) | v : Traverse speed (mm/min) |
| MRR : Material Removal Rate | \dot{V} : Volumetric MRR (mm ³ /min) |

4.3.3 Predicted vs experimental results

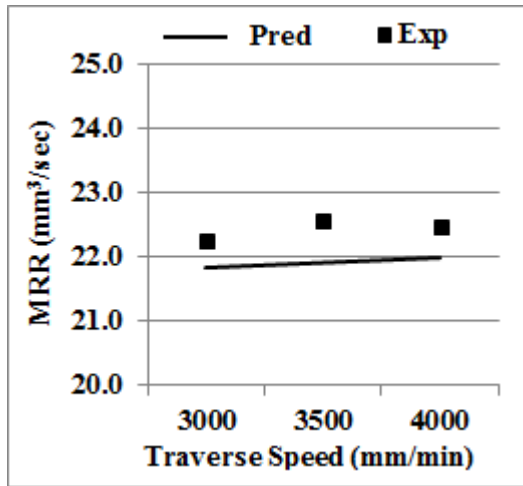
Equation 4.16 is valid for pocket milling on SS304 material within the range of the machining conditions and can help to predict the MRR for other parametric values within the specified limits. Here, H_w, P are not varied during experimentation and are considered as constants. The units of the process variables are converted to the units mentioned in the nomenclature, and accordingly a constant is obtained in the predicted equation. It is interesting to note that exponents of the process variables are in conjunction to the dependence of the process variables. The values of the exponents tell us how much quantitatively each individual parameter influences the response parameter and would change with pressure and work material combination. A quantitative assessment of the models has been carried out based on the percentage deviation of the predicted model with the experimental results. The plots in Figure 4.1-4.3 show the comparison. The difference observed in the MRR values is in the range of 0.1-0.5 mm^3/s ; however the trend in the predicted model with parameters is consistent. The variations observed are might be due to the fact that, the model is developed for a set of process parameters only. The plots in Figures 4.1 (d), 4.2 (d), 4.3 (d) show the percentage deviation of the predicted model with experimental results. Deviations of 0.2 -8.5 % for SODs; 0.2 -12% for AFRs and 0.1-7.0 % for abrasive sizes are observed.



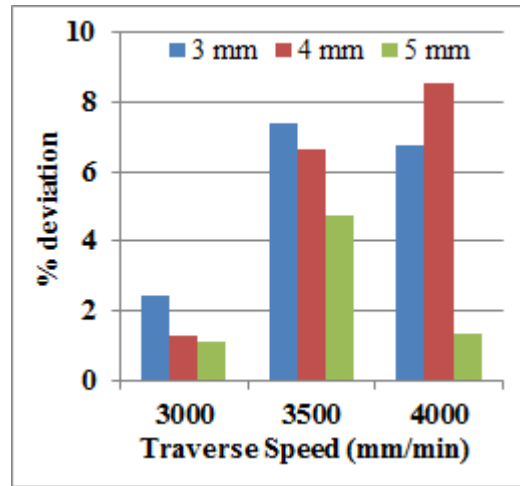
(a)



(b)

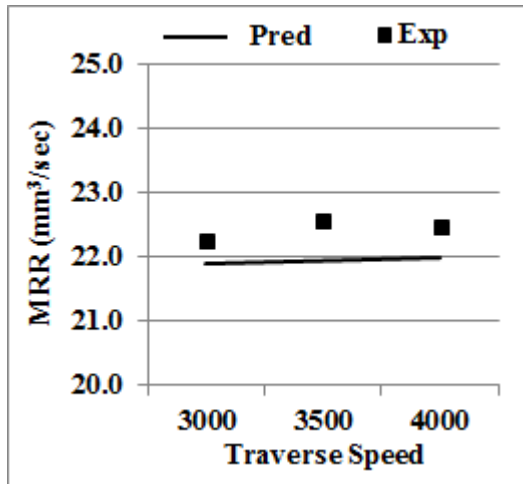


(c)

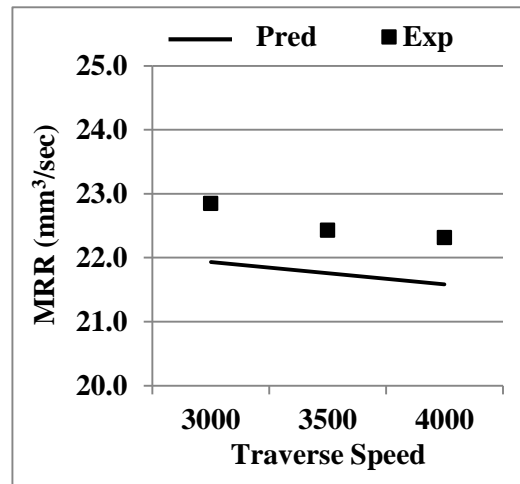


(d)

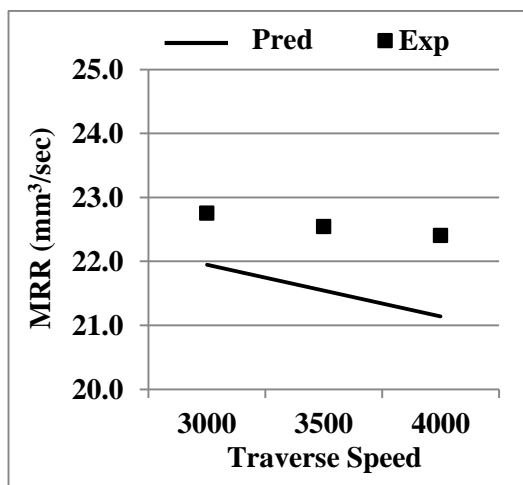
Fig. 4.1: Comparison between predicated vs experimental values for MRR at SOD (a) 3 mm (b) 4 mm (c) 5 mm (d) % deviation



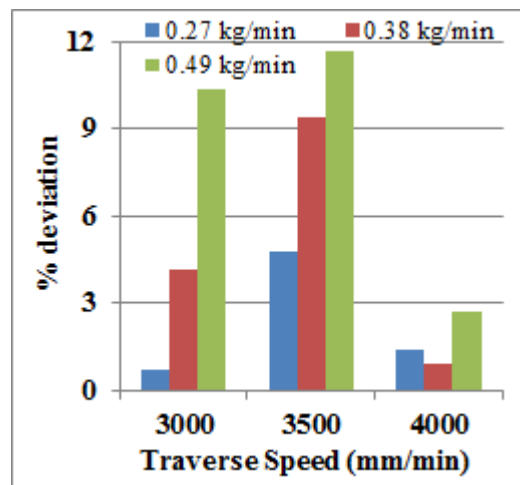
(a)



(b)



(c)



(d)

Fig. 4.2: Comparison between predicated vs experimental values for MRR at AFR (a) 0.27 kg/min (b) 0.38 kg/min (c) 0.49 kg/min (d) % deviation

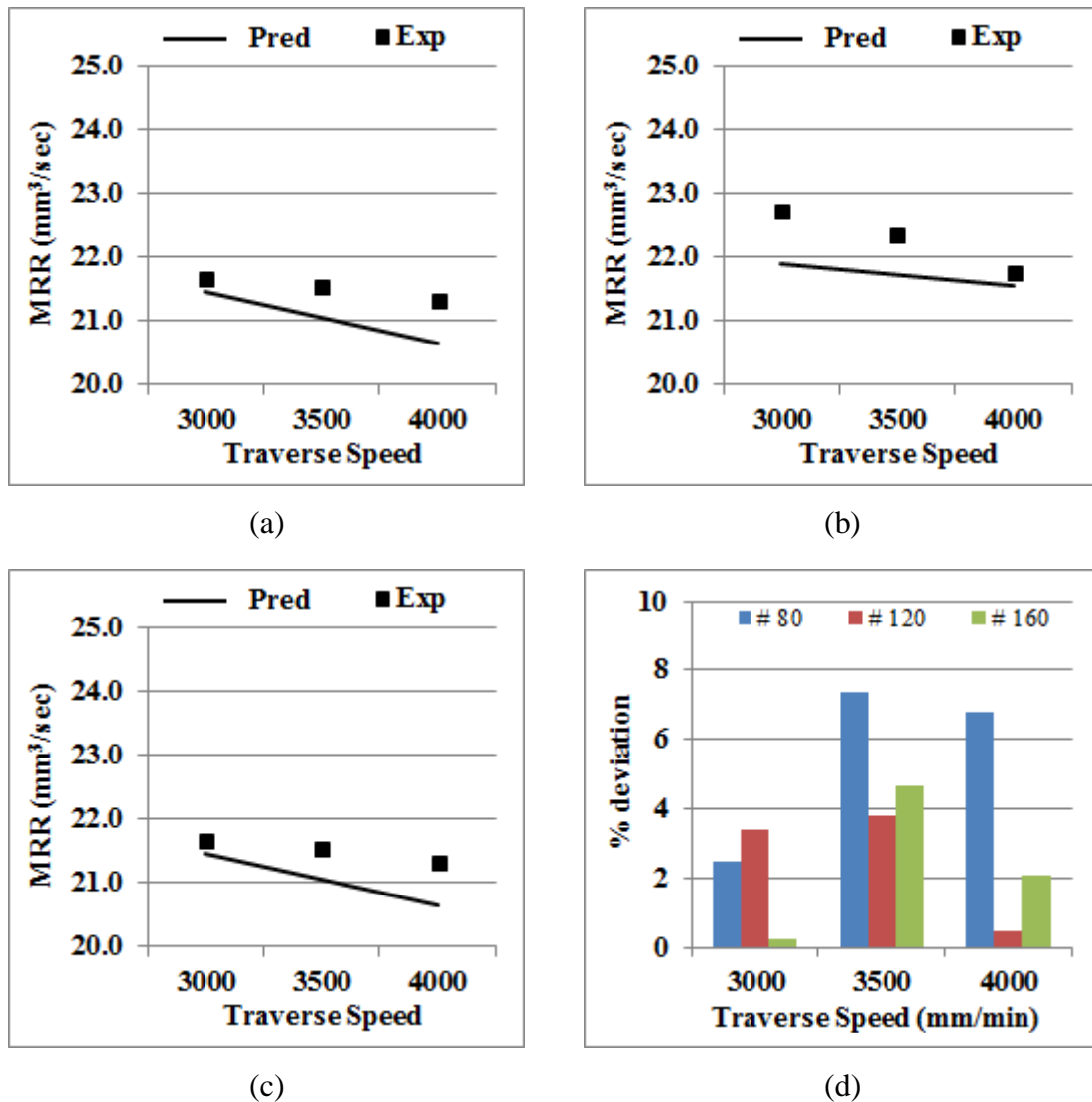


Fig. 4.3: Comparison between predicted vs experimental values for MRR at (a) # 80 abrasive (b) # 120 abrasive (c) #160 abrasive (d) % deviation

4.4 Theoretical modeling of forces

Consider an abrasive particle moving with a velocity v_p which is approximating equal to the velocity of the abrasive water jet, v_{awj} and flowing through a focusing tube having an exit area of 'A', (as in Figure 4.4) hits the target surface and the material removal takes place due to the particle impact.

$$\text{Area of the focusing tube is } A = \frac{\pi}{4} d_F^2 \quad (4.17)$$

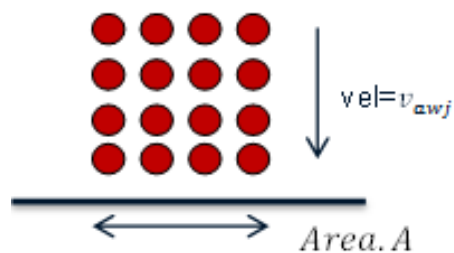


Fig.4.4: Schematic of the abrasives impacting the surface

Using the principles in theory of momentum we proceed as follows:

Momentum per particle,

$$M_1 = m_p v_{awj} = \rho V_p v_p \quad (4.18)$$

where, V_p is volume of the individual spherical abrasive particle,

$$M_1 = \frac{\pi}{6} \rho d^3 v_p \quad (4.19)$$

Considering a raster tool path as shown in Figure 4.5,

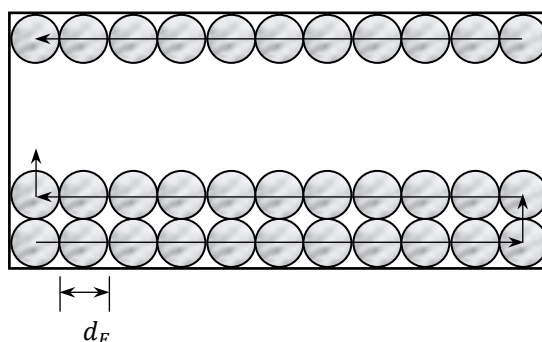


Figure 4.5 Traverse tool paths of the focusing tube.

If Δt is the exposure time of the jet, then $\Delta t = l/v$

Here, l and v is length of the tool path and traverse speed of the jet. Figure 4.6 shows the schematic of the cross-section of the abrasive particle distribution in the focusing tube.

The focusing tube interaction time with work surface is given as $\Delta t_F = d_F/v$

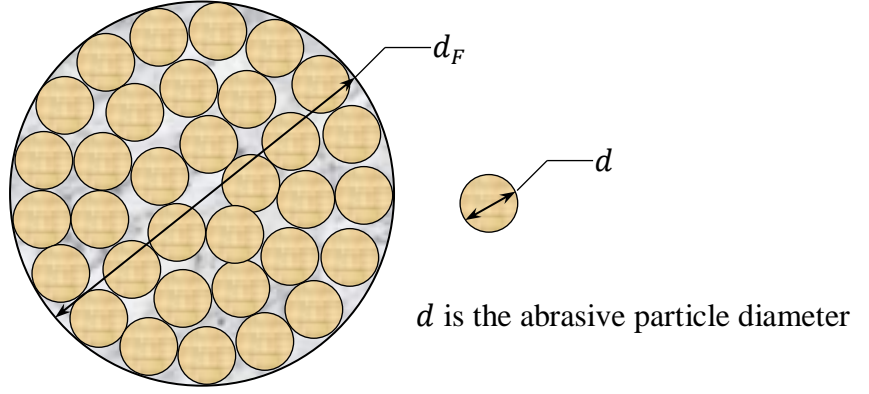


Figure 4.6 Particle distributions on the exit focus diameter.

Number of abrasive particles (N) impacting per unit time is given as:

$$N = \frac{\dot{m}_a}{m_p} = \frac{\dot{m}_a}{\frac{\pi}{6}\rho d^3} \quad (4.20)$$

$$\text{No. of particles interacting at time } \Delta t_o = N \times \Delta t_F \quad (4.21)$$

Cross-sectional area of abrasive particles in the focusing tube during the interaction

$$\text{time} = \left(\frac{\dot{m}_a}{\frac{\pi}{6}\rho d^3}\right) \times \frac{\pi}{4} d^2 \times \Delta t_F = \frac{3\dot{m}_a}{2\rho d} \times \Delta t_F$$

Therefore, the total number of layers of abrasives available for a given AFR is:

$$\frac{\frac{3\dot{m}_a}{2\rho d} \times \Delta t_F}{\frac{\pi}{4} d_F^2} = \frac{6\dot{m}_a(\Delta t_F)}{\rho \pi d d_F^2} \quad (4.22)$$

The time available per particle is = $\frac{\text{focus tube interaction time}}{\text{no. of abrasives}}$

$$\Delta t = \frac{\left(\frac{d_F}{v}\right)}{\left(\frac{6\dot{m}_a(\Delta t_F)}{\rho \pi d d_F^2}\right)} = \frac{\rho \pi d d_F^2}{6\dot{m}_a} \quad (4.23)$$

Force per particle is the rate of change of momentum = $F = M_1/\Delta t$

$$\text{Total force per interaction is } F = \frac{\left(\frac{\pi}{6}\rho d^3 v_p\right)}{\left(\frac{\rho \pi d d_F^2}{6\dot{m}_a}\right)} = \frac{d^2 v_p \dot{m}_a}{d_F^2} \quad (4.24)$$

The total theoretical force during the entire interaction time is

$$F \cong \frac{d^2 v_p \dot{m}_a}{d_F^2} \times \left(\frac{\pi d_F^2}{4} \right) = \dot{m}_a v_p \quad (4.25)$$

As per the literature, the percentage of abrasives by mass in the abrasive water jet mixture is approximately 23-25% of total mass of the jet.

$$\text{So the Force measured is } F = \frac{\dot{m}_a v_p}{\chi} = \frac{\dot{m}_a v_{awj}}{\chi} \quad (4.26)$$

where χ is the mass percentage of abrasives in the abrasive water jet.

4.4.1. Calculations of abrasive water jet velocity

In order to calculate the abrasive water jet velocity, the velocity of water is required. The acceleration of a certain volume of pressurized water in an orifice generates high speed water jets. In this case, Bernoulli's law gives

$$P_{atm} + \frac{\rho_w}{2} v_{oth}^2 + \rho_w g h_1 = P + \frac{\rho_w}{2} v_{pipe}^2 + \rho_w g h_2$$

where P_{atm} is the pressure at the exit of the nozzle, P is the pump pressure, v_o and v_{pipe} are the velocities at the exit and entry to the orifice, ρ_w is density of water. Considering $h_1 = h_2$ and $v_o \gg v_{pipe}$, the approximate velocity of the exit water jet is given by

$$v_{oth} \cong \sqrt{\frac{2P}{\rho_w}}$$

In practice

$$v_o = \mu v_{oth} = \mu \sqrt{\frac{2P}{\rho_w}}$$

Where, μ is an efficiency coefficient that characterizes momentum losses due to wall friction, fluid flow disturbances and the compressibility of the water. The process of abrasive-particle acceleration in an injection-abrasive water jet is momentum transfer

from the high velocity water jet to the abrasive particles that are injected at comparatively low velocities and the air sucked with the abrasive material. An impulse balance gives

$\Sigma F = \text{constant}$, and this leads to

$$(\dot{m}_a v_{po} + \dot{m}_w v_o + \dot{m}_L v_L) = (\dot{m}_a + \dot{m}_w + \dot{m}_L) v_{awj} \quad (4.27)$$

\dot{m}_L, v_L are the mass and velocity of air present in the jet and v_{po} is the initial velocity of the abrasive particle. The amount of air present on the entire mass of the abrasive water jet is about 3%. For simplification purposes, amount of air is neglected. Another simplification is to neglect the slip between water and abrasive particles if they leave the focusing tube. Neglecting the input velocity of the abrasive particle, since $v_{po} \ll \ll v_o$. The process of abrasive particle acceleration is the momentum transfer from the high velocity water to the abrasive particles that are injected at comparatively low velocities. The losses during the acceleration process are characterized by the parameters related to the momentum transfer losses during the acceleration process and is characterized by a momentum-transfer parameter η .

Thus,

$$v_{awj} = \eta \frac{v_o}{1 + \frac{\dot{m}_a}{\dot{m}_w}}$$

Then the velocity of abrasive water jet is given by

$$v_{awj} = \eta \frac{v_o}{1+R} \quad (4.28)$$

here R is ratio of mass flow rate of abrasive and water and is given by $R = \frac{\dot{m}_a}{\dot{m}_w}$

So, theoretical force (impact force only) can be calculated as:

$$F = \left(\frac{\mu\eta}{\chi} \right) \left(\frac{\dot{m}_a}{1+R} \right) \left(\sqrt{\frac{2P}{\rho_w}} \right) \quad (4.29)$$

4.4.2. Experimental validation and conclusions

In AWJ cutting, surfaces and the features is characterized using static and dynamic characterization techniques. The dynamic workpiece normal force in AWJM is influenced by a large set of process parameters such as fluctuations in water jet pressure, vibration of the position system, abrasive size, traverse speed, nozzle diameter, etc. A stochastic model characterization as a dynamic modeling technique with forces provides an insight into the high energy jet machining process. The purpose of force modeling is to investigate the feasibility of using the dynamic work piece reaction force as a parameter for online monitoring of the channel dimensions. The methods reported in the literature (Evans 1979, WJTA 1987) are used to calculate the reaction force, but are limited only to reaction force from a plain water jet and do not report any change in the forces when abrasives are mixed into the water jet. Most of the methods to measure velocity of the water jet are done through photographic methods only. So, the force calculations in an AWJM process are very much limited due to various constraints like proper fixtures, placement of dynamometer, etc. To validate the force model, experimental trials performed on a SS304 plate for linear cut micro channels. Table 4.1 gives the experimental results of the dynamometer forces measured for the micro-channels. The forces specified are the impact forces in the vertical direction and the forces in the other directions are neglected. The maximum contribution to the material removal is due to the impact force. Although, it is not possible to draw consistent conclusions from the data, but it can be clearly seen that the forces calculated theoretically are valid to a certain extent of the AFR and the error is exaggerated at higher AFRs which is being explained further.

Table 4.1: Typical experimental data of the impact forces

| <i>Exp. No</i> | <i>v</i> (mm/min) | \dot{m}_a (kg/min) | <i>d</i> (mm) | <i>h</i> (mm) | <i>Force</i> (N) |
|----------------|----------------------|-------------------------|------------------|------------------|---------------------|
| 1 | 3000 | 0.49 | 0.177 | 4 | 10.33 |
| 2 | 3500 | 0.49 | 0.125 | 5 | 11.60 |
| 3 | 3500 | 0.38 | 0.110 | 4 | 11.63 |
| 4 | 3500 | 0.38 | 0.177 | 4 | 10.47 |
| 5 | 3500 | 0.27 | 0.177 | 3 | 10.91 |
| 6 | 3500 | 0.38 | 0.177 | 5 | 10.35 |
| 7 | 3000 | 0.49 | 0.125 | 4 | 11.89 |

| | | | | | |
|----|------|------|-------|---|-------|
| 8 | 4000 | 0.38 | 0.177 | 3 | 10.94 |
| 9 | 4000 | 0.38 | 0.177 | 4 | 10.17 |
| 10 | 3000 | 0.27 | 0.177 | 5 | 10.86 |
| 11 | 3000 | 0.27 | 0.110 | 4 | 10.47 |
| 12 | 3000 | 0.49 | 0.110 | 4 | 8.50 |
| 13 | 3000 | 0.38 | 0.177 | 3 | 11.07 |
| 14 | 4000 | 0.49 | 0.177 | 4 | 11.04 |
| 15 | 3500 | 0.38 | 0.177 | 3 | 10.93 |
| 16 | 3500 | 0.49 | 0.125 | 4 | 11.84 |
| 17 | 4000 | 0.49 | 0.110 | 4 | 8.94 |
| 18 | 3500 | 0.27 | 0.110 | 5 | 10.58 |
| 19 | 3000 | 0.27 | 0.177 | 3 | 10.45 |
| 20 | 3500 | 0.27 | 0.125 | 3 | 11.14 |
| 21 | 4000 | 0.27 | 0.177 | 4 | 10.51 |
| 22 | 4000 | 0.27 | 0.125 | 3 | 11.34 |
| 23 | 4000 | 0.49 | 0.125 | 3 | 11.42 |
| 24 | 4000 | 0.38 | 0.177 | 5 | 10.89 |
| 25 | 3000 | 0.27 | 0.125 | 4 | 10.88 |
| 26 | 4000 | 0.38 | 0.110 | 5 | 10.92 |
| 27 | 3500 | 0.49 | 0.177 | 4 | 9.82 |

The variation of the forces for with AFRs for different abrasive sizes is shown Figure 4.7. The calculated force increases with an increase in the AFR according to the Equation 4.29. The equation do not account other input process parameters like traverse speed, SOD, abrasive size, etc. The plots show that the experimental force initially decreases with increase in the AFR till 0.38 kg/min and further any change in the AFR does not influence the jet impact force. The reduction in the overall reaction force is due to increase in the absorption energy of the abrasives and also this can be attributed to the higher number of particles available which leads to possibility of particle fragmentation which reduces the energy level of the abrasive water jet. At lower AFRs, the difference in the measured and calculated forces range from 6-9%. At higher AFR the error increases to the order of 11% as Figure 4.8.

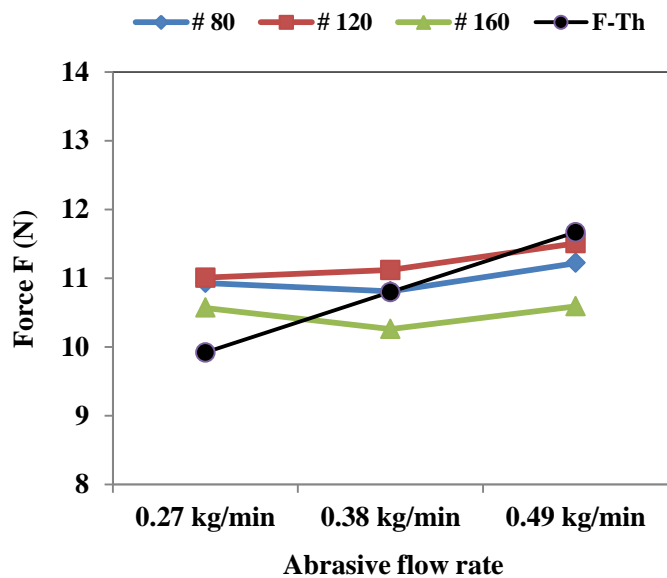


Fig. 4.7: Theoretical and experimental forces for different abrasive sizes

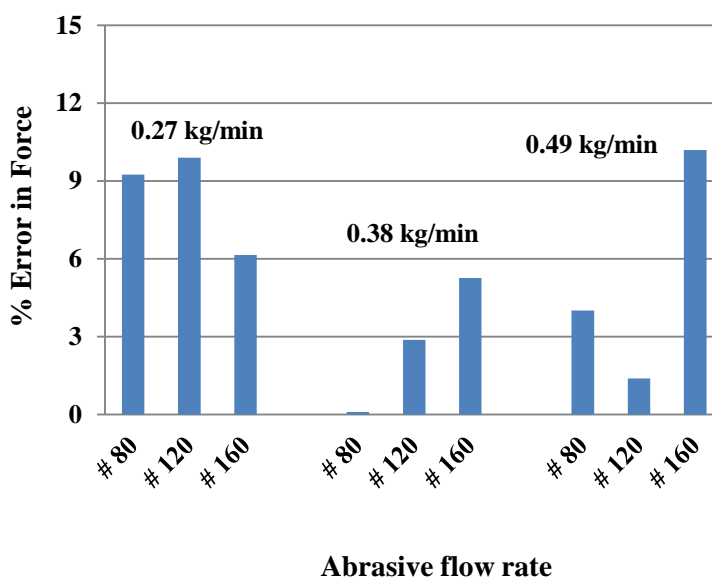


Fig. 4.8: % Error in experimental and theoretical forces for various abrasive sizes and AFRs

As shown in Figure 4.9, the force at 3 mm SOD is higher compared to other SODs. At low SODs the emerging jet directly interacts with the workpiece creating more impact force whereas at higher SODs, the energy dissipation occurs and this reduces the reaction force. In this case, the calculated forces and the measured forces are following similar paths till 0.38 kg/min and further increase in the AFR to 0.49 kg/min, SOD has not effecting the measured force. The % error in Figure 4.10 shows a deviation of about 12% with the theoretical force at 0.49 kg/min.

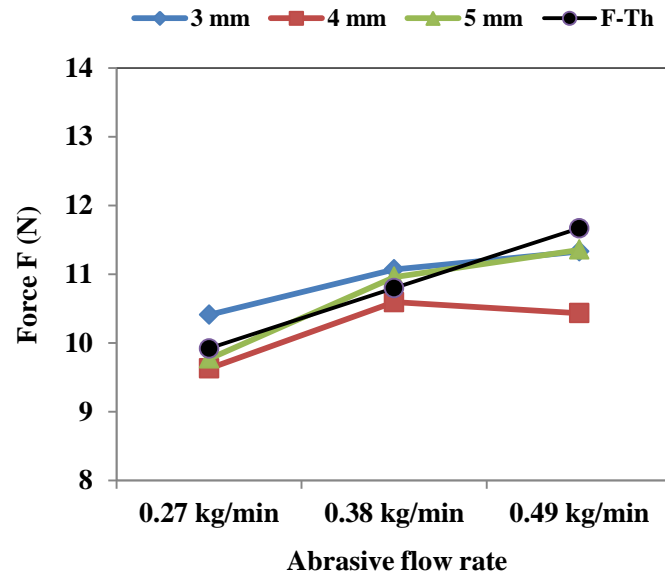


Fig. 4.9: Theoretical and experimental forces for different SOD

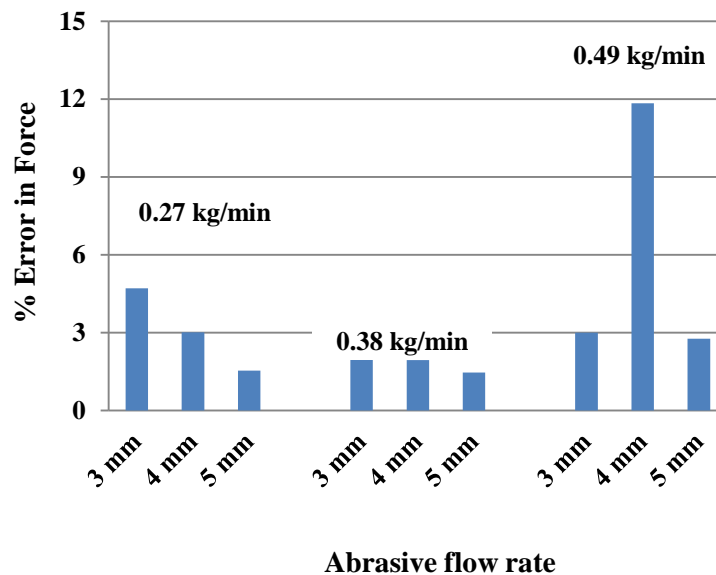


Fig. 4.10: % Error in experimental and theoretical forces at various SODs and AFRs

The influence of traverse speed on the impact force is plotted in Figure 4.11. The graph shows that at low traverse speeds of 3000 mm/min and low AFR the measured forces are more than the calculated forces. The increase in the AFR beyond 0.38 kg/min to 0.49 kg/min shows no influence on the forces. It was also experimentally shown that beyond an AFR, the material removal decrease due to crushing of the particles.

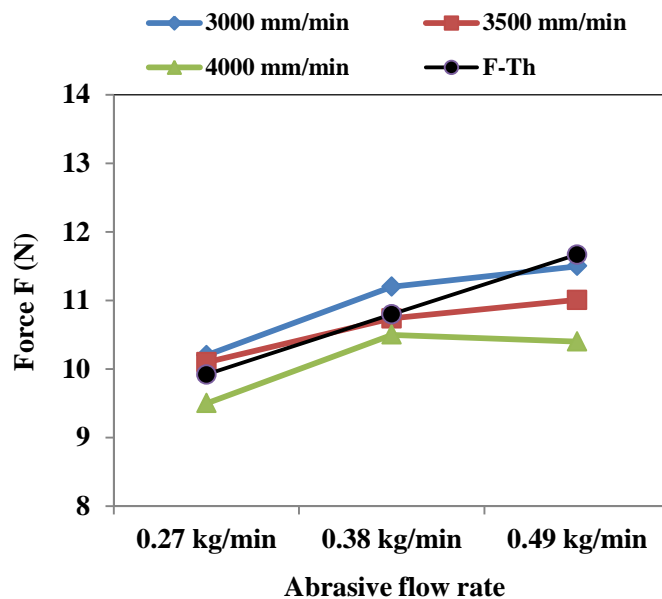


Fig. 4.11: Theoretical and experimental forces for different traverse speeds

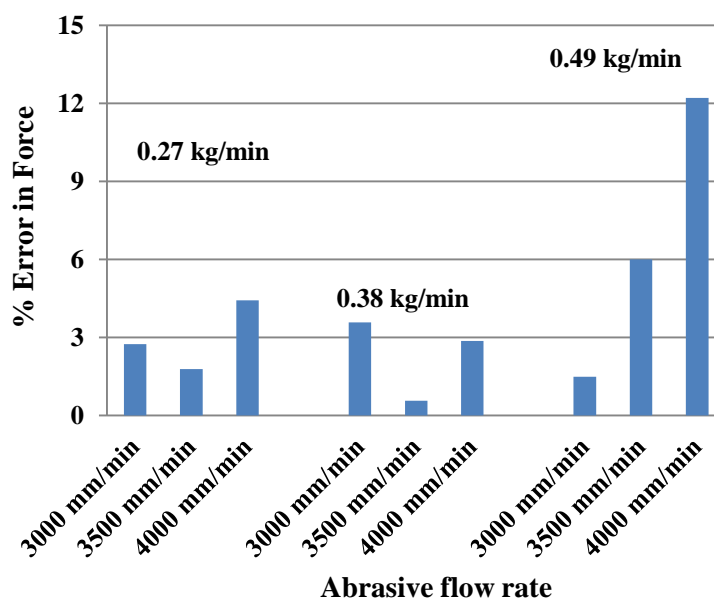


Fig. 4.12: % Error in experimental and theoretical forces at various traverse speeds and AFRs

At high traverse speeds, the specific material removal energy drops due to the reduced kinetic energy of the particle and the particle exposure time with the target material. Increasing the AFR allows the abrasives to penetrate into the surface properly. In general, high AFR should be preferred in milling applications, since majority of the abrasives do perform cutting operation due to disturbances. The percentage error is high compared to other process parameters as shown in Figure 4.12, which reveals that traverse speed has a greater role to play.

4.5 Theoretical calculations for MRR

The impact of a single solid abrasive particle is considered as the basis for material removal by abrasive water jets. Meng and Ludema (1995) analyze the state of the art modeling of particle erosion phenomena for MRR calculations. The four sub-mechanisms by which solid particles separate the material from the target surface are cutting, fatigue, melting and brittle fracture. However, all four mechanisms are observed during abrasive water jet cutting and at least three of them are applied for material removal modeling of the process. Several theories were developed to calculate the volumetric MRR using erosion phenomena. An early and often considered material removal by micro cutting is given by Finnie (1958). In the micro cutting process, it has been assumed that the plastic response of the material is determined by the flow stress of the material. Considering the trajectory of a single particle during the removal process, the volumetric MRR is given as:

$$\dot{V} = \frac{\dot{m}_a v_{awj}^2}{\sigma_f K \psi} f(\alpha) \quad (4.30)$$

$$f(\alpha) = \sin(2\alpha) - \frac{6}{K} \sin^2 \alpha \quad \text{for } \tan(\alpha) < \frac{K}{6}$$

$$f(\alpha) = \frac{K}{6} \cos^2(\alpha) \quad \text{for } \tan(\alpha) > \frac{K}{6}$$

$$K = \frac{F_Y}{F_X} \cong 2; \quad \psi \cong 2$$

where, σ_f is the material flow stress, F_Y, F_X are the jet vertical (impact) force and the horizontal force, ψ is the ratio of cut length to depth of penetration, α is the jet impingement angle.

In general the flow stress of the material is difficult to measure and it has been replaced with the hardness of the eroded workpiece material. The major disadvantages of Finnie's model are the problems concerning the flow stress of the material, particle velocity exponent, particle shape and also applicability of the model at 90° impingement angle. Later, Bitter (1963a, 1963b) divided the entire material removal process into two modes, cutting wear and deformation wear modes. This cutting wear happens at low impact angles and deformation wear occurs at high impact angles. The volume of material removed by both forms of wear is given as:

$$V_{Cutting} = \frac{m_a [v_{awj}^2 \cos^2(\alpha) - K_1 (v_{awj} \sin(\alpha) - v_{el})]^{3/2}}{2\varepsilon_{Mcut}} \quad \text{cutting wear mode,} \quad (4.31)$$

$$V_{Deformation} = \frac{m_a [v_{awj} \sin(\alpha) - v_{el}]^2}{2\varepsilon_{Mdef}} \quad \text{deformation wear mode} \quad (4.32)$$

where K_1 is a parameter that depends on the properties of target material and abrasive combination; the properties include size of the abrasive, Young's modulus and density of workpiece and abrasives, ε_M is the specific erosion energy.

Though the models proposed by Finnie, Bitter, Hashish and Kim are very comprehensive and provide the physics of the material removal mechanism; these models require substantial information on different aspects of the process parameters and their interactions within themselves which may not be readily available. A working group in TU Delft, Netherlands proposed a reliable model based on simple analogy to predict the volume of material removed. This model is presented in the later part of this section.

Practically, in AWJM, the amount of material removed depends on the power of jet; which is the responsible for the kinetic energy of the jet that can be calculated from the first principles. The following section elaborates the theoretical MRR considering the power of abrasive water jet.

$$Power = \varepsilon \times MRR \quad \varepsilon \text{ is the specific energy required for material removal.}$$

$$MRR \propto P_{awj} \propto c_d \times \frac{\pi}{4} d_o^2 \times \sqrt{\frac{2P^3}{\rho_w}} \quad (4.33)$$

$$MRR = \frac{c_d \times \frac{\pi}{4} d_o^2 \times \sqrt{2P^3}}{\varepsilon} \sqrt{\rho_w} \quad (4.34)$$

Power of abrasive water jet is:

$$P_{awj} = \frac{1}{2} \dot{m}_a v_{awj}^2 \quad (4.35)$$

Considering the abrasive water jet velocity based on the relations developed in the previous section of the chapter,

$$P_{awj} = \frac{1}{2} \dot{m}_a \left[\eta \left(\frac{1}{1+R} \right) v_o \right]^2 \quad (4.36)$$

$$P_{awj} = \frac{1}{2} \dot{m}_w R \left[\eta \left(\frac{1}{1+R} \right) v_o \right]^2 \quad (4.37)$$

$$P_{awj} = \frac{1}{2} c_d \times \frac{\pi}{4} d_o^2 \rho_w v_o R \left[\eta \left(\frac{1}{1+R} \right) v_o \right]^2 \quad (4.38)$$

$$P_{awj} = \frac{1}{2} c_d \times \frac{\pi}{4} d_o^2 \rho_w R \eta^2 \left[\left(\frac{1}{1+R} \right) \right]^2 v_o^3 \quad (4.39)$$

$$P_{awj} = \frac{1}{2} c_d \times \frac{\pi}{4} d_o^2 \rho_w R \eta^2 \left[\left(\frac{1}{1+R} \right) \right]^2 \left(\frac{2P}{\rho_w} \right)^{3/2} \quad (4.40)$$

$$P_{awj} = c_d \times \frac{\pi}{4} d_o^2 R \left[\left(\frac{\eta}{1+R} \right) \right]^2 \left(\frac{2}{\rho_w} \right)^{1/2} P^{3/2} \quad (4.41)$$

$$\text{As, } MRR = \frac{P_{awj}}{\varepsilon}$$

$$\text{So, } MRR = \frac{c_d}{\varepsilon} \times \frac{\pi}{4} d_o^2 R \left[\left(\frac{\eta}{1+R} \right) \right]^2 \left(\frac{2}{\rho_w} \right)^{1/2} P^{3/2} \quad (4.42)$$

Experimental validation of MRR

The above equation is used to measure the volume of material dislodged from the work surface based on power of the abrasive water jet. To validate the model for milling applications, the initial experimental results presented in Chapter 3 are used. The present case considers SS304 as the target material. The orifice co-efficient of discharge is considered as per the research carried by Hashish (1989c). The co-efficient of discharge is a non-dimensional number which considers the reduction in the water mass flow rate due to the sudden change in the fluid mechanic conditions at the orifice outlet, as well as the reduced jet velocity due to the orifice wall friction. Typically these values range from 0.60-0.85 depending on the diameter of the sapphire orifices and the AFRs. In the present investigations for the theoretical MRR calculations, the values of co-efficient of discharge are based on the work reported by Hashish (1989c). Specific

energy is an intensive quantity that characterizes the cutting resistance offered by a material similar to tensile stress and hardness characterize the strength and plastic deformation resistance of a material respectively. Specific energy is a useful concept for all material removal and deformation processes. It is the energy required to remove a unit volume of material from the stock material. In AWJM, the energy is in the form of kinetic energy of the abrasive particles. Taking the specific energy into account, calculations are done for the analytical model for validation. The specific energy required for machining SS304 material is approximately 12.5 J/mm^3 .

Figure 4.13 plots the experimental, theoretical and predicted values of MRR in the increasing order of AFR. The plot shows that at high AFR, the MRR decreases due to crushing of the abrasives during mixing and particle acceleration. In the present work on pocket milling, the increased AFR decreases the kinetic energy of the individual abrasive particle and at high traverse speeds the kinetic energy of the abrasive particles is not sufficiently utilized for the material removal. This is one of the major reasons for the decreased MRR. In AWJ milling, considerable amount of energy is lost in the rebounding of the abrasive particle which is offered by the target material surface. The present study concludes that an average error of 3.3% is obtained between the experimental and theoretical results and an error of 2.2% has been observed at low AFR.

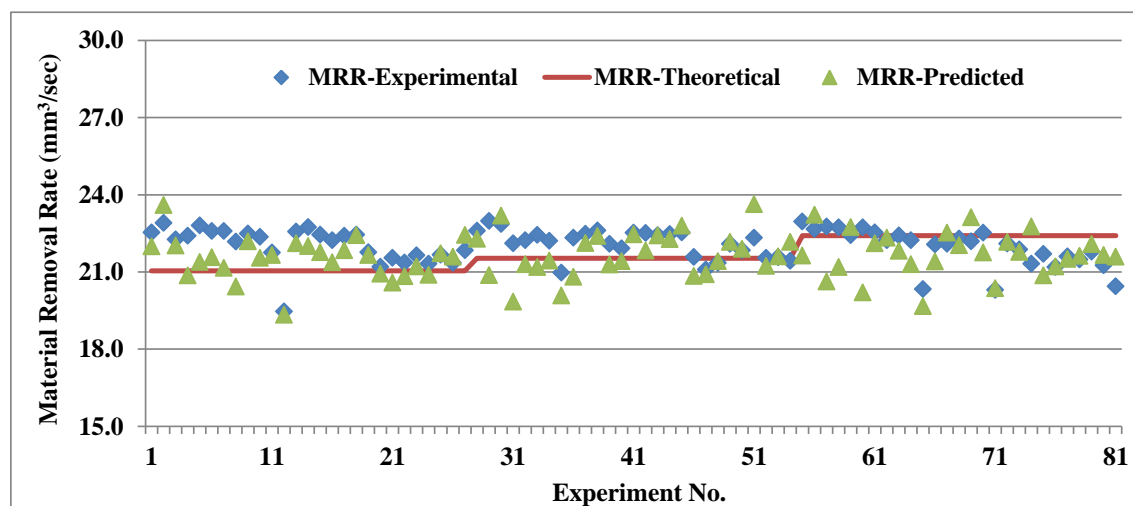


Fig. 4.13: Comparison of experimental, predicted and theoretical MRR

4.6 Summary

In continuation to the full factorial experimentation in the present work, the experimental data is used to develop a predictive model for MRR. Based on the experimental investigations and observations from the predictive model; the predictive model exhibits a deviation of 0.2-12% from the experimental results. The model has been assessed both qualitatively and quantitatively for prediction of the volumetric MRR. The objective of the first phase of the chapter is to monitor and control the MRR for a given set of parameters. This can further be used for the development of an optimized model for MRR in pocket milling. The experimental and predicated values are then compared with an energy based model for the MRR and the results show that at high AFRs the MRR less when compared to the theoretical model.

Further, the analytical model developed for the impact force, that is responsible for the material removal to take place is validated. The validation has been done for linear micro-channels on SS304. The force equation developed is well in conjunction with the experimental results up to 0.38 kg/min AFR and is being deviated at high AFRs. This could be due to the fragmentation process and improper penetration of the abrasives into the surface due to very less interaction times too. Internal collisions within the particles during mixing and machining are also the possible reasons for the deviation. The higher AFR also reduce the specific material removal energy of the abrasive particles. The calculated error is of the order of 12% at higher AFR and it ranges from 1-7% for low a low AFR.

Chapter 5

GEOMETRY AND CHARACTERISTICS OF MICRO-CHANNELS

| | |
|--|-----|
| 5.1 Introduction | 91 |
| 5.2 Cut geometry measurements | 92 |
| 5.3 Role of process parameters on channel geometry | 95 |
| 5.3.1 Influence of process parameters on channel width/depth ratio | 96 |
| 5.3.2 Effect of process parameters on channel depth | 99 |
| 5.3.3 Influence of process parameters on taper | 103 |
| 5.3.4 Role of process parameters on the channel surface roughness | 105 |
| 5.4 Regression Analysis | 109 |
| 5.5 Surface morphological studies | 110 |
| 5.6 Summary | 112 |

5.1 Introduction

Preparation of micro/macro channels using unconventional machining methods/processes on hard to cut materials is increasingly in demand in the micro manufacturing industry. AWJM is one such process that can be used for the creation of these channels. Achieving the dimensional accuracy is a big challenge since the process is influenced by a large set of process parameters. Further, in the micro-channel preparation through AWJ milling technique, attaining dimensional accuracy is more challenging than expected unlike in a conventional milling process. This chapter presents a comprehensive view of the work executed to create a channel with the input parameters as identified earlier i.e., abrasive size, flow rate, standoff distance (SOD), traverse speed. The issues related to 3D shape generation, which is an overlap of 2D channels and the variations in the dimensional accuracies of the channel for a given set of process parameters is enumerated.

Unconventional machining processes are energy in-efficient due to the presence of either thermal and/or chemical reactions in processes like laser machining, electron beam machining, electric discharge machining, electrolytic machining and chemical etching, etc. These processes cause excessive heat affected zone. While, mechanical processes like ultrasonic machining, grinding and polishing have limitations in accuracy

and productivity. AWJM process is considered to be an attractive and effective in machining hard to cut materials due to its high productivity and thin heat-affected layers caused by material removal. In view of these advantages offered by AWJM technique, it is used to fabricate these micro channels. The geometrical features of any component fabricated with AWJM are characterized by top and bottom cut width, taper, initial damage zone along depth and width, etc. (Arola 1996). The taper measured from the cut section is a non-dimensional parameter, which is the ratio of top to bottom cut widths. An alternative solution for evaluating the taper given by Chung et al. (1992) in the form of a regression model consists of traverse speed, SOD distance and focus diameter.

Characterization of the material structure, geometrical accuracies and surface quality has been used to study the material removal mechanism in milling of titanium alloy using plain water jets (Kong et al. 2010). It has been reported that at higher depths, the influence of SOD is insignificant and at higher traverse speeds the influence of other process parameters become insignificant. Preparation of micro channels on glass using abrasive slurry jets (Pang et al. 2012) characterized as a V-shaped channel (Figure 5.1) and the results reported that width of cut is decided by the SOD while the flow pattern of jet plays a critical role on the width. Here, the channel depth is affected by the transfer of kinetic energy of the abrasive particles to the target material.

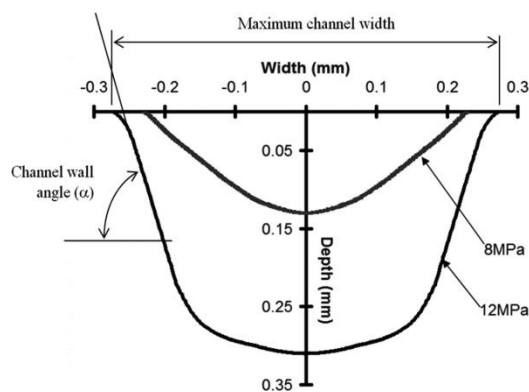


Fig.5.1: Cross-section of the profile (Pang et al. 2012)

5.2 Cut geometry measurements

The dimensions of the micro-channel are measured using a UM5-CAM digital microscope (Micro Link Technologies). The plate on which the channels are fabricated

is sectioned appropriately to measure depth, kerf width and the taper. Depth and top width of the channel are measured directly using the digital microscope. The digital image of the sectioned specimen is imported to CAD software to measure the taper. Figure 5.2 gives the comprehensive schematic of the cut geometry. In the measurements, depth is the maximum depth of the channel while kerf width is the top width of the channel. Surface roughness is measured using a roughness measuring instrument (Rugosurf 10). The measurement of the surface roughness gives the centre-line average value Ra of the channel. A sample surface roughness profile from the instrument is shown in Figure 5.3.

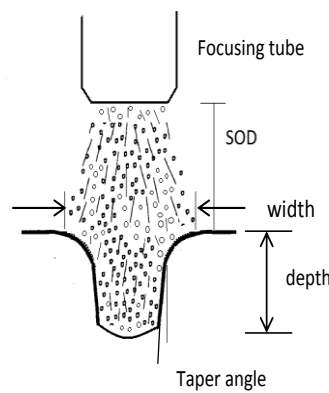


Fig. 5.2: Schematic of the cut geometry

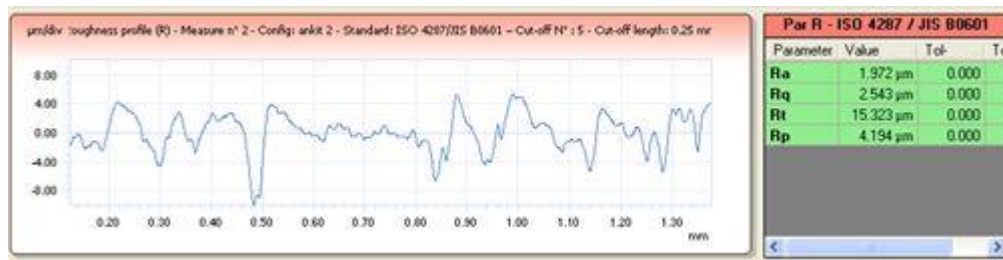


Fig. 5.3: Sample surface roughness profile of the micro-channel

In the present set of experiments, the jet traverse speeds are very high so as to achieve a micro-channel. The increase in the traverse speed makes the jet and the workpiece surface interaction time to minimum for the machining to take place. This leads to a minute jet absorption time within the material and this could be the possible reason for the deformation mode of material removal to take place. Figure 5.4 gives the micro-channel images fabricated with different abrasive sizes. The images show the material removal mode is similar to ploughing deformation. The measured width, depth, taper and surface roughness of the micro-channels is given in Table 5.1.

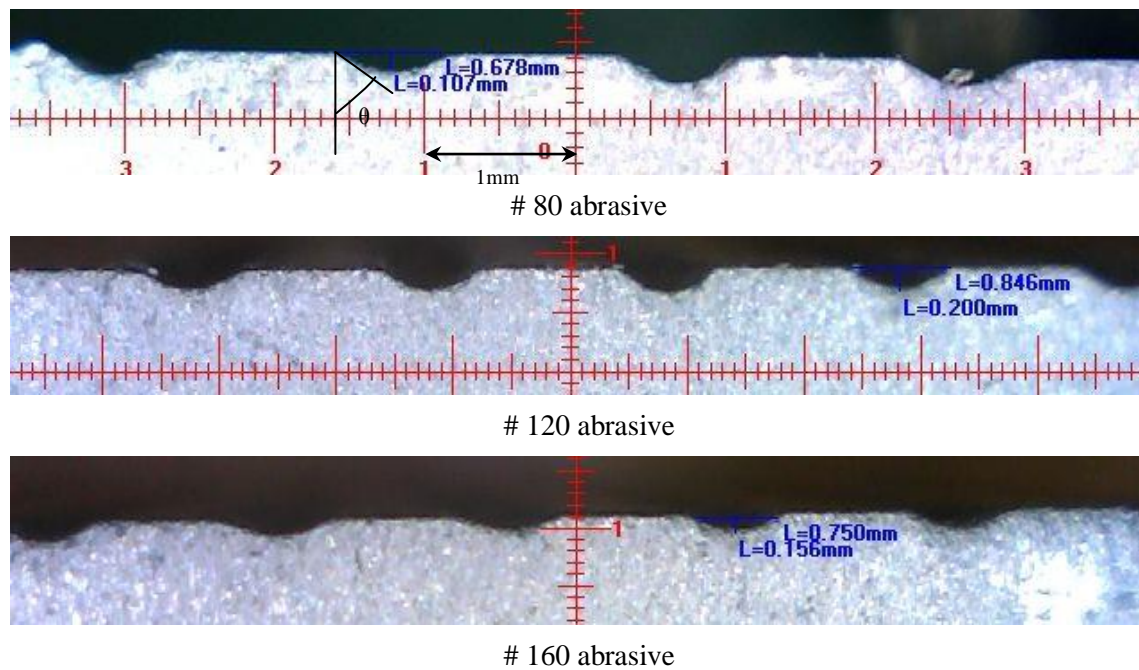


Fig. 5.4: Cut geometry photographs for different abrasive sizes

Table 5.1: Experimental data of width, depth, taper and surface roughness (*partial set*)

| Exp. No | Input Parameters | | | | Output Responses | | | |
|---------|------------------|-------------------------|-------------|-------------|----------------------------|----------------------------|----------------|----------------------------|
| | v (mm/min) | \dot{m}_a (kg/min) | d (mm) | h (mm) | Width (μm) | Depth (μm) | Taper (Deg) | R_a (μm) |
| 1 | 3000 | 0.49 | 0.177 | 4 | 785 | 225.91 | 58.90 | 3.61 |
| 2 | 3500 | 0.49 | 0.125 | 5 | 753 | 183.55 | 40.22 | 1.26 |
| 3 | 3500 | 0.38 | 0.110 | 4 | 762 | 150.00 | 50.00 | 1.09 |
| 4 | 3500 | 0.38 | 0.177 | 4 | 690 | 140.25 | 49.02 | 2.81 |
| 5 | 3500 | 0.27 | 0.177 | 3 | 690 | 160.00 | 47.21 | 2.61 |
| 6 | 3500 | 0.38 | 0.177 | 5 | 785 | 192.02 | 60.04 | 2.66 |
| 7 | 3000 | 0.49 | 0.125 | 4 | 769 | 196.79 | 51.52 | 2.30 |
| 8 | 4000 | 0.38 | 0.177 | 3 | 678 | 192.02 | 48.13 | 3.18 |
| 9 | 4000 | 0.38 | 0.177 | 4 | 595 | 186.38 | 56.38 | 1.65 |
| 10 | 3000 | 0.27 | 0.177 | 5 | 785 | 193.91 | 51.20 | 1.95 |
| 11 | 3000 | 0.27 | 0.110 | 4 | 719 | 175.08 | 63.60 | 1.97 |
| 12 | 3000 | 0.49 | 0.110 | 4 | 812 | 208.02 | 60.56 | 1.26 |
| 13 | 3000 | 0.38 | 0.177 | 3 | 702 | 257.91 | 54.20 | 3.08 |
| 14 | 4000 | 0.49 | 0.177 | 4 | 678 | 126.13 | 66.21 | 1.74 |
| 15 | 3500 | 0.38 | 0.177 | 3 | 725 | 162.85 | 66.19 | 1.81 |

| | | | | | | | | |
|----|------|------|-------|---|-----|--------|-------|------|
| 16 | 3500 | 0.49 | 0.125 | 4 | 876 | 205.20 | 50.26 | 1.56 |
| 17 | 4000 | 0.49 | 0.110 | 4 | 812 | 205.20 | 61.51 | 1.22 |
| 18 | 3500 | 0.27 | 0.110 | 5 | 734 | 180.73 | 59.35 | 1.94 |
| 19 | 3000 | 0.27 | 0.177 | 3 | 809 | 186.38 | 54.49 | 2.53 |
| 20 | 3500 | 0.27 | 0.125 | 3 | 861 | 193.91 | 50.05 | 2.18 |
| 21 | 4000 | 0.27 | 0.177 | 4 | 690 | 143.08 | 57.19 | 2.36 |
| 22 | 4000 | 0.27 | 0.125 | 3 | 846 | 159.08 | 47.64 | 2.14 |
| 23 | 4000 | 0.49 | 0.125 | 3 | 629 | 153.43 | 32.20 | 3.13 |
| 24 | 4000 | 0.38 | 0.177 | 5 | 773 | 186.38 | 54.60 | 1.46 |
| 25 | 3000 | 0.27 | 0.125 | 4 | 815 | 211.82 | 49.35 | 2.01 |
| 26 | 4000 | 0.38 | 0.110 | 5 | 688 | 153.43 | 60.65 | 1.61 |
| 27 | 3500 | 0.49 | 0.177 | 4 | 713 | 171.32 | 56.60 | 2.20 |

5.3 Role of process parameters on channel geometry

The geometry of the kerf produced in the channel preparation not only limits the ability to meet the geometric tolerances of the feature but also influences the strength and life of the components. The effect of different input parameters (v, h, \dot{m}_a, d) and their interactions on the output responses (channel depth, kerf width, taper and surface roughness) are analyzed in the preceding sections. An interaction is the variation among the differences between means for different levels of one factor over different levels of another factor under consideration. The trends in the performance variation with the parameter values are obtained from the average responses graphically. The percentage contribution of individual and interaction parameters on the responses from ANOVA and F-test results are analyzed. F value is the ratio of variance of the parameter to the variance of the average population. If the F- ratio is greater than the statistical table value, it means that the parameter has influence on the average population and those with F- ratio values lesser than the tabulated value, reveals that there is no effect on the average population. Based on these results, the significant parameters which affect the performance are identified. The purpose of the study is to examine and empirically model the dominant channel features in AWJM created micro-channels on SS304 material. General regression techniques are used to model the geometrical characteristics of the channel.

5.3.1 Influence of process parameters on channel width/depth ratio

In a general AWJM process, the width and depth of cut are influenced by traverse speed significantly due to the local exposure time of the jet with the work surface. The width of cut is strongly dependent on SOD which is due to the radial expansion of the jet as per the experimental proofs by researchers. Figure 5.2 shows the schematic of the influence of SOD with focus diameter to support the results. In the present work, the width to depth ratio of the micro-channel has been considered as a response parameter to be investigated. Figure 5.5 shows the influence of width to depth ratio with traverse speed at various SODs; where the ratio increases with increase in the traverse speed. A gradual increase in the ratio is observed till the traverse speed of 3500 mm/min is reached and thereafter the slope increases. This is due to the fact to that, at low traverse speeds, the increased interaction time allows more material to be removed and it is found that higher depths are possible than the width parameter. At high traverse speeds, due to faster movement of the jet, sufficient energy is not transferred to the workpiece for the material removal to take place leading to decrease in the depth.

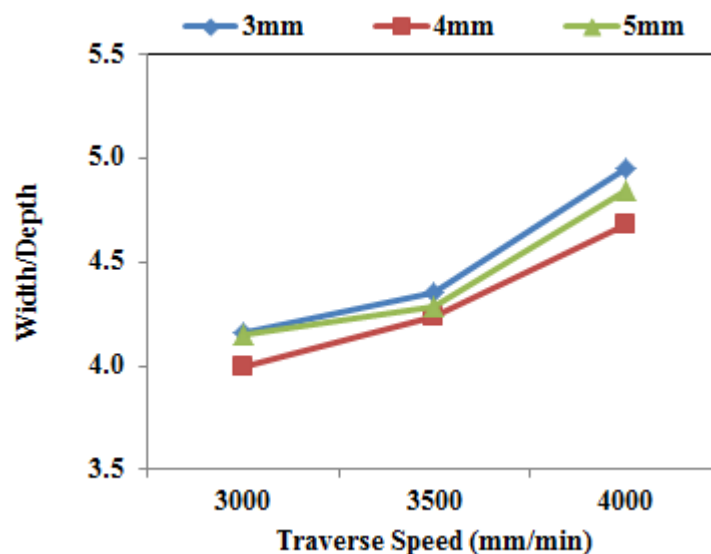


Fig. 5.5: Effect of traverse speed and SOD on kerf width to depth ratio

The ratio is less at SOD of 5 mm, when compared to SOD 3 mm. The trend at SOD 4 mm shows that width and depth are linearly related to each other. The increased SOD makes the jet losing its energy due to expansion of the jet. The ratio is less when compared at SOD 5 mm, because of that the abrasives might have attained the required momentum for the material removal to take place. In abrasive processes, there are three

phases of material removal present namely rubbing, ploughing and cutting. Here, rubbing is defined as sliding action of the abrasive particle over the work surface within the elastic limit of the material up to the onset of plastic deformation. This has a negligible influence on the material removal in AWJM process. Ploughing is the phase where the material bulges across the sides of the abrasive and accumulates continuously in front of the particle until the material removal takes place. When the piled and accumulated material could not withstand the shearing stresses, the bulged material ahead of the abrasive is then fractured from the workpiece in the form of a fine chip similar to a conventional machining process. The transition from rubbing to ploughing and ploughing to cutting depends on depth of the particle penetration into the work surface. The abrasive penetration depends on the particle interaction time with the target material, which is governed by the jet traverse speed. This is one of the major reasons why traverse speed is considered as one of the parameters affecting the kerf width. The width of cut diverges as the jet marches into the specimen at lower traverse speeds and converges at higher traverse speeds. Thus for lower traverse speeds, width of cut is larger and for higher traverse speed, vice versa.

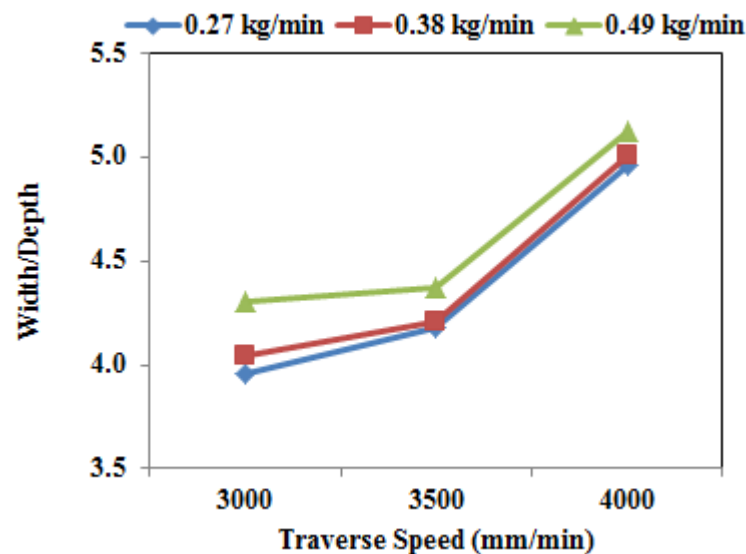


Fig. 5.6: Effect of traverse speed and AFR on kerf width to depth ratio

The effect of abrasive flow rate (AFR) on the width to depth ratio is shown in Figure 5.6. The ratio increases with the traverse speed and the reasons henceforth are explained above. The figure shows that the ratio is following the paths for till an AFR of 0.38 kg/min. As the AFR is increased to 0.49 kg/min, the variation observed is due to the shift of the material removal mechanism from cutting wear mode to deformation

wear mode. The increasing trend at 0.49 kg/min is due to the increased number of particles which tend to decrease the material removal rate. AFR is not very effective to width but is very sensitive parameter for depth and this leads the ratio to increase an increase in the AFR.

The effect of abrasive size on the width to depth ratio is shown in Figure 5.7. The plots reveal that size of the abrasive is a significant parameter on the width to depth ratio. The figure shows that at # 80, any increase in the traverse speed beyond 3500 kg/min, no effect in the ratio is observed. The trends for # 120 and # 160 are similar. At # 160 and at high traverse speeds, the depth of cut decrease, thus enabling the ratio to increase. The increased number of abrasive particles with reduced abrasive size increases the number of cutting edges thus removing more material. But at high traverse speeds, smaller abrasives do not possess sufficient kinetic energy to penetrate into the surface which reduces the channel depth, and thus increasing the ratio.

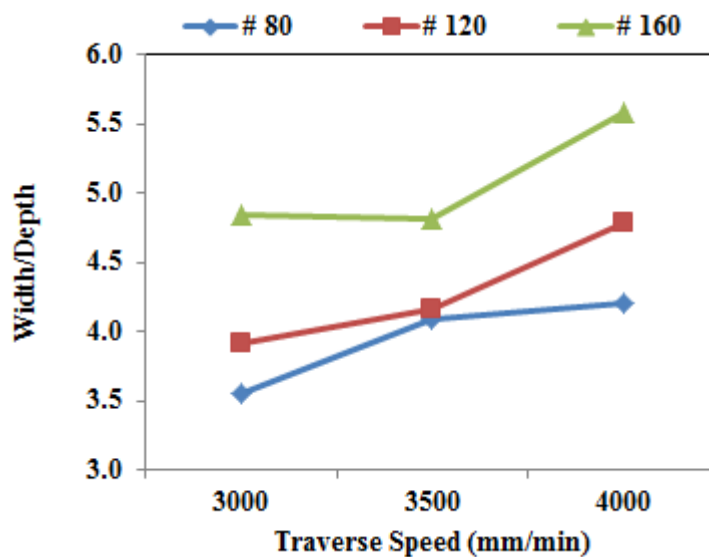


Fig. 5.7: Effect of traverse speed and abrasive size on kerf width/depth ratio

The results of ANOVA for channel width are given in Table 5.2, which suggests that the maximum contribution on the width is given by the abrasive size which is about 8.84%. The contribution by other parameters like AFR and SOD is not much as individuals, but a considerable influence of the interaction parameters on the width is observed. The combination of traverse speed, and SOD with AFR contributes about 7.94% and the interaction of AFR and abrasive size as high as 4.31% on the channel width respectively. The present analysis has been carried out at 99% confidence

intervals. Generally, the width of cut should be highly affected by SOD, but in the present study SOD is not very effective because the jet interaction time with work surface is very less due to very high traverse speeds.

Table 5.2: ANOVA analysis-channel width: ($R^2 = 78.21\%$)

| <i>Parameter</i> | <i>DOF</i> | <i>SS</i> | <i>Variance (V)</i> | <i>F-Ratio</i> | <i>Pure Sum (S)</i> | <i>Cont.(%)</i> |
|-------------------------------|------------|-----------|---------------------|----------------|---------------------|-----------------|
| v | 2 | 2478 | 1239 | 0.26 | -6926.75 | 2.01 |
| \dot{m}_a | 2 | 14975 | 7488 | 1.59 | 5570.25 | 1.61 |
| d | 2 | 39933 | 19967 | 4.25 | 30528.25 | 8.84 |
| h | 2 | 3050 | 1525 | 0.32 | -6354.75 | 1.84 |
| $v \times \dot{m}_a$ | 4 | 5638 | 1410 | 0.30 | -13171.5 | 3.82 |
| $v \times d$ | 4 | 6079 | 1520 | 0.32 | -12730.5 | 3.69 |
| $v \times h$ | 4 | 28729 | 7182 | 1.53 | 9919.5 | 2.87 |
| $\dot{m}_a \times d$ | 4 | 3920 | 980 | 0.21 | -14889.5 | 4.31 |
| $\dot{m}_a \times h$ | 4 | 12316 | 3079 | 0.65 | -6493.5 | 1.88 |
| $d \times h$ | 4 | 13758 | 3440 | 0.73 | -5051.5 | 1.46 |
| $v \times \dot{m}_a \times d$ | 8 | 37663 | 4708 | 1.00 | 44 | 0.01 |
| $v \times \dot{m}_a \times h$ | 8 | 10219 | 1277 | 0.27 | -27400 | 7.94 |
| $v \times d \times h$ | 8 | 51644 | 6455 | 1.37 | 14025 | 4.06 |
| $\dot{m}_a \times d \times h$ | 8 | 39575 | 4947 | 1.05 | 1956 | 0.57 |
| Error | 16 | 75238 | 4702 | | | |
| Total | 80 | 345215 | | | | |

5.3.2 Effect of process parameters on channel depth

The depth of the channel is a significant response parameter in AWJ milling. Figures 5.8-5.10 plots the experimental observations of the individual process parameters on depth of cut. In AWJM, indentation depth is dependent on various process parameters like, depth of cut is proportional to pressure, abrasive particle velocity and the interaction time of the workpiece with abrasive particle. Since pressure is kept constant in the present research and also experiments are conducted on a single material, depth of cut is highly dependent on the abrasive particle velocity and the traverse speed. As the traverse speed increases, the channel depth decreases due to insufficient exposure time of the workpiece to the jet. The influence of channel depth with SOD is shown in Figure 5.8. An increase in the traverse speed decreases the depth. The linear trend in the decrement is observed till 3500 mm/min and once the traverse

speed exceeds this value, a sudden decrease is observed which is due to shift in the material removal mechanism. The decreasing trend is same for all the SODs, while at SOD 4 mm, the depth of cut is more compared to SOD 5 mm. This is due to the jet stabilization and also reduced pressure fluctuations.

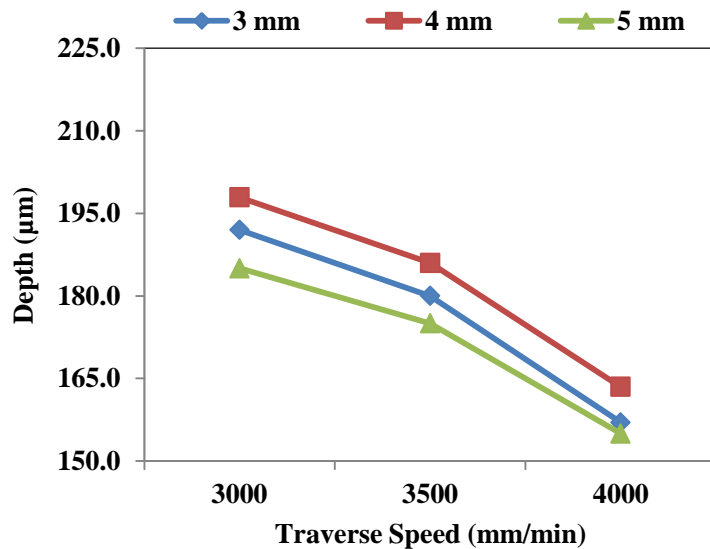


Fig. 5.8: Effect of traverse speed and SOD on channel depth

Abrasive flow rate determines the number of impacting abrasive particles and the kinetic energy of individual abrasive particle. The influence of AFR on the channel depth shown in Figure 5.9 reveals that the depth at high and low AFR follow similar trends. At low AFR the material removal is primarily because of cutting wear mode and depth of cut decreases in this mode of material removal. As the AFR is increased to 0.38 kg/min, the cutting mechanism shifts to deformation wear mode and a higher depth is obtained. Further increasing the AFR to 0.49 kg/min, depth of cut observed is decreased. This is due to the fact that erosion of a material takes place because of the very high velocity particle impacts. The continuous impacts of the abrasive particles at the same location on any metallic surface exceed the yield strength of the material in a localized plastic deformation zone within the vicinity of the impact. On the multiple impacts, plastically deformed surface layer near the eroded surface increases the yield strength of the material by strain hardening and the depth of cut is decreased. At high traverse speeds and higher AFRs, the deformation wear is dominated and shearing of the surface takes place.

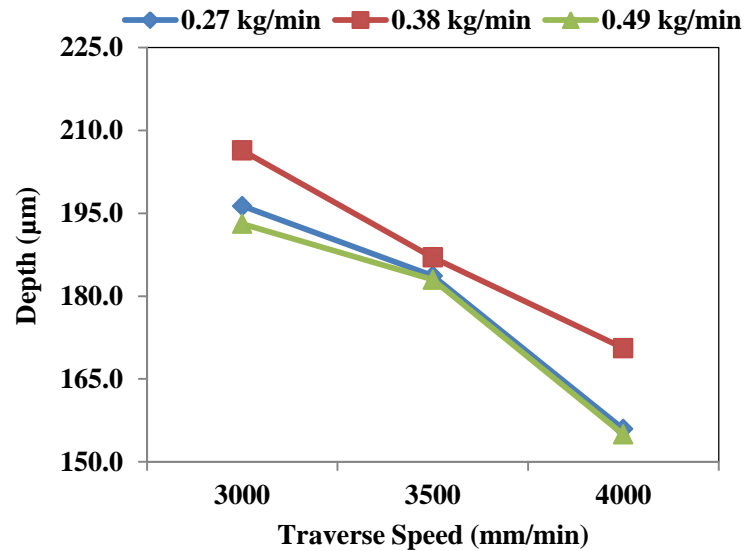


Fig. 5.9: Effect of traverse speed and AFR on channel depth

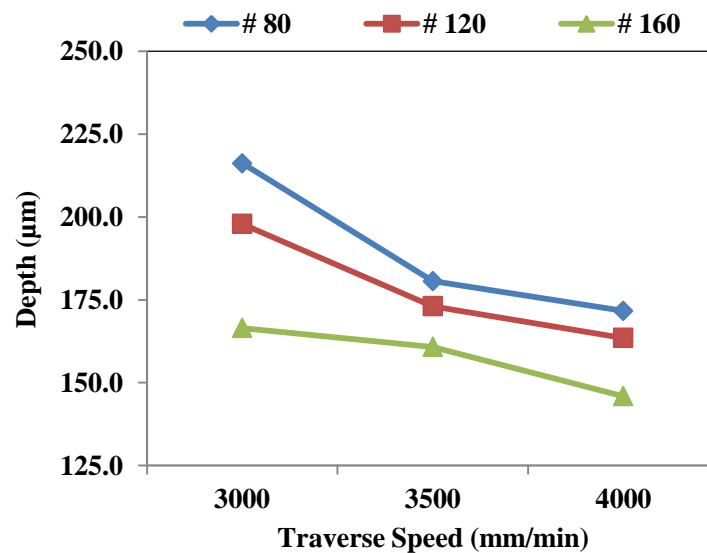


Fig. 5.10: Effect of traverse speed and abrasive size on channel depth

The abrasive size is another parameter which influences the channel depth. The increased abrasive size determines the reduction in number of particles for a given AFR. The influence of abrasive size on depth is shown in Figure 5.10. A bigger diameter (# 80) particle impact increases the area of the indented groove and a smaller particle (# 160) decreases the indentation depth. Fine abrasive particles reduce the kinetic energy of the individual particle and also the jet energy which are responsible for the low depth of cut. So, there is always a requirement of an optimum balance between the kinetic energy of the abrasive particle and the number of impacting particles. At low abrasive particle velocities we would expect that progressively more

GEOMETRY AND CHARACTERISTICS OF THE MICRO CHANNELS

particles would produce only elastic stresses in the surfaces and hence the weight loss at low velocities would decrease more rapidly.

Table 5.3: ANOVA analysis-channel depth ($R^2 = 93.08\%$)

| <i>Parameter</i> | <i>DOF</i> | <i>SS</i> | <i>Variance (V)</i> | <i>F-Ratio</i> | <i>Pure Sum (S)</i> | <i>Cont.(%)</i> |
|-------------------------------|------------|-----------|---------------------|----------------|---------------------|-----------------|
| v | 2 | 19887.8 | 9943.9 | 29.03 | 19202.6 | 24.24 |
| \dot{m}_a | 2 | 328.3 | 164.1 | 0.48 | 356.9 | 0.45 |
| d | 2 | 18306.4 | 9153.2 | 26.72 | 17621.2 | 22.25 |
| h | 2 | 83.4 | 41.7 | 0.12 | 601.8 | 0.76 |
| $v \times \dot{m}_a$ | 4 | 3420.3 | 855.1 | 2.50 | 2049.9 | 2.59 |
| $v \times d$ | 4 | 3495.3 | 873.8 | 2.55 | 2124.9 | 2.68 |
| $v \times h$ | 4 | 787.4 | 196.9 | 0.57 | 583 | 0.74 |
| $\dot{m}_a \times d$ | 4 | 702.9 | 175.7 | 0.51 | 667.5 | 0.84 |
| $\dot{m}_a \times h$ | 4 | 2801.3 | 700.3 | 2.04 | 1430.9 | 1.81 |
| $d \times h$ | 4 | 2730.8 | 682.7 | 1.99 | 1360.4 | 1.72 |
| $v \times \dot{m}_a \times d$ | 8 | 3193.1 | 399.1 | 1.17 | 452.3 | 0.57 |
| $v \times \dot{m}_a \times h$ | 8 | 3343.3 | 417.9 | 1.22 | 602.5 | 0.76 |
| $v \times d \times h$ | 8 | 9071.9 | 1134.0 | 3.31 | 6331.1 | 7.99 |
| $\dot{m}_a \times d \times h$ | 8 | 5576.2 | 697.0 | 2.03 | 2835.4 | 3.58 |
| Error | 16 | 5480.9 | 342.6 | | | |
| Total | 80 | 79209.4 | | | | |

The ANOVA results presented in Table 5.3 shows that the channel depth is influenced by traverse speed and the particle size with their contribution of 24% and 22% respectively. The contributions of both SOD and AFR are less than 1%. Based on the results, it is observed that the combination of AFR with either traverse speed or SOD has more influence on depth contributing to 2.5% and 1.8 % respectively. Further, the interaction of abrasive size and SOD with traverse speed contributes 7.99% and with AFR contributes 3.58% on depth respectively. It is understood that individual process parameters has less influence on depth, but the process parameters interactions affects the process and it is considerable. The F-test results shows that abrasive size and traverse speed are highly contributing to the average response of depth at 99% confidence interval. From the above study it is understood that, cutting parameters are more significant and influential on depth.

5.3.3 Influence of process parameters on taper

Several authors [Arola 1996, Matsui et al. 1991] used different terminology for the taper measurements. In the present work, taper is defined as the angle with which the kerf surface makes with the vertical wall of the channel. In AWJM, the jet emerging from the mixing tube is divergent in nature, creates converging cuts and this promotes taper. This convergent shape is used to measure the taper. The trends followed in the taper variation shown in Figure 5.11 are similar to the plots of width to depth ratio. At SOD 5 mm, the taper obtained is higher due to the reduced depth and increased width. A gradual increase in the taper is observed till 3500 mm/min and the variation is higher at a traverse speed of 4000 mm/min. The gradual increase in the SOD increases the impact surface is larger which reduces the coherence of the effective jet thus increasing the taper. At SOD 4 mm, the channel taper is less, compared to other SODs; due to sufficient jet energy transfer into the workpiece for the creating of the channel.

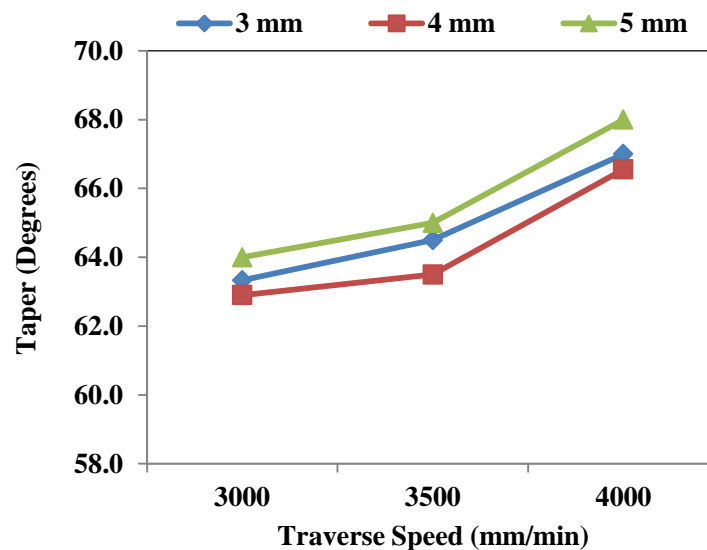


Fig. 5.11: Effect of traverse speed and SOD on taper

The variation in the channel taper with traverse speed and AFR is shown in Figure 5.12. Since the kerf width increases and depth of cut decreases with increasing AFR leads to an increase in the taper. The gradual increase in the taper initially with AFR and a steep change observed at higher AFR and high traverse speeds are due to the increased number of abrasive particles with less interaction time of the workpiece material with the abrasive for the material removal to take place. For a through cutting process, the taper changes from a convergent at higher traverse speeds and to divergent for low traverse speeds.

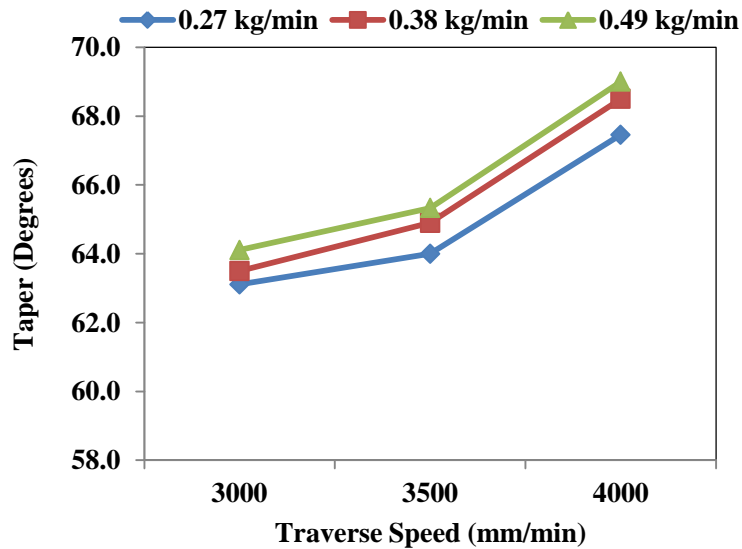


Fig. 5.12: Effect of traverse speed and AFR on taper

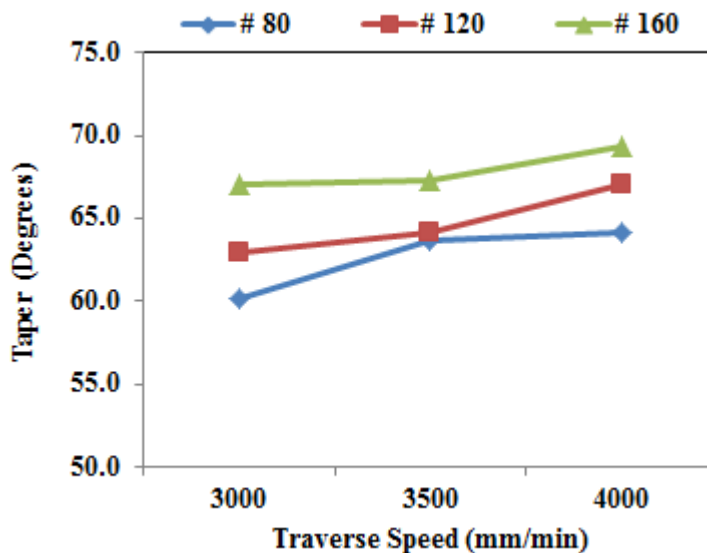


Fig. 5.13: Effect of traverse speed and abrasive size on taper

The experimental variation of taper with abrasive size and traverse speed are plotted in Figure 5.13. Similar trends were reported by earlier researchers on taper with abrasive size. In channel machining process, the abrasive size plays a critical role in achieving the geometry and accuracy. As the particle size decreases in # 160, improper machining takes place due to crushing of the particles which results in increased taper. The increasing trend in taper with reduced abrasive size is that a critical energy transfer from the jet is required to fracture the material, below which material removal does not take place.

The results of ANOVA analysis in Table 5.4 show the significant and insignificant input parameters on the taper. It is found that abrasive size is significant as an individual parameter on taper followed by SOD, traverse speed and the least being AFR. Based on the values of F-ratio AFR and abrasive size with traverse speed as interaction parameter are more significant on the taper. The abrasive size contributes to about 5.5% on taper and followed by rest of the process parameters. The interaction of abrasive particle size and AFR on SOD and traverse speed contributes to 13.4%, 12.2% respectively. The particle size and SOD with traverse speed also contributes about 10.9% on the taper.

Table 5.4: ANOVA analysis-channel taper ($R^2 = 66.48\%$)

| <i>Parameter</i> | <i>DOF</i> | <i>SS</i> | <i>Variance (V)</i> | <i>F-Ratio</i> | <i>Pure Sum (S)</i> | <i>Cont.(%)</i> |
|-------------------------------|------------|-----------|---------------------|----------------|---------------------|-----------------|
| v | 2 | 5.69 | 2.84 | 0.03 | 160.09 | 4.05 |
| \dot{m}_a | 2 | 14.55 | 7.28 | 0.09 | 151.23 | 3.82 |
| d | 2 | 384.99 | 192.49 | 2.32 | 219.21 | 5.54 |
| h | 2 | 1.34 | 0.67 | 0.01 | 164.44 | 4.16 |
| $v \times \dot{m}_a$ | 4 | 16.07 | 4.02 | 0.05 | 315.49 | 7.97 |
| $v \times d$ | 4 | 388.17 | 97.04 | 1.17 | 56.61 | 1.43 |
| $v \times h$ | 4 | 394.33 | 98.58 | 1.19 | 62.77 | 1.59 |
| $\dot{m}_a \times d$ | 4 | 233.28 | 58.32 | 0.70 | 98.28 | 2.48 |
| $\dot{m}_a \times h$ | 4 | 202.75 | 50.69 | 0.61 | 128.81 | 3.26 |
| $d \times h$ | 4 | 136.49 | 34.12 | 0.41 | 195.07 | 4.93 |
| $v \times \dot{m}_a \times d$ | 8 | 178.41 | 22.30 | 0.27 | 484.71 | 12.25 |
| $v \times \dot{m}_a \times h$ | 8 | 312.44 | 39.06 | 0.47 | 350.68 | 8.86 |
| $v \times d \times h$ | 8 | 229.96 | 28.74 | 0.35 | 433.16 | 10.95 |
| $\dot{m}_a \times d \times h$ | 8 | 131.38 | 16.42 | 0.20 | 531.74 | 13.44 |
| Error | 16 | 1326.24 | 82.89 | | | |
| Total | 80 | 3956.09 | | | | |

5.3.4 Role of process parameters on the channel surface roughness

Surface roughness gives the dimensional accuracies involved in the deviations from the target surface. The surface generation in AWJM process is based on the plastic deformation. The plastic deformation in ductile materials depends on abrasive size, number of impacting particles at high velocities. The high specific impacting forces and

the specific energy associated with the abrasives in machining is designated as ductile regime machining. Here the material removal is precisely controlled and the material removal mechanism is purely because of the material deformation. The depth of cut and surface roughness are controlled by plastic deformation in AWJM.

The influence of SOD on surface roughness is shown in Figure 5.14. The decreasing trend with traverse speed on surface roughness is due to change of material removal mechanism to deformation only. It is observed experimentally that the surface roughness is more at low SOD and low traverse speed due to cutting wear mode. An increase in the SOD leads to radial expansion of the jet yielding a larger exposed area and due to the energy dispersion level, the surface finish is poor at low traverse speeds and a better surface is obtained at higher traverse speeds.

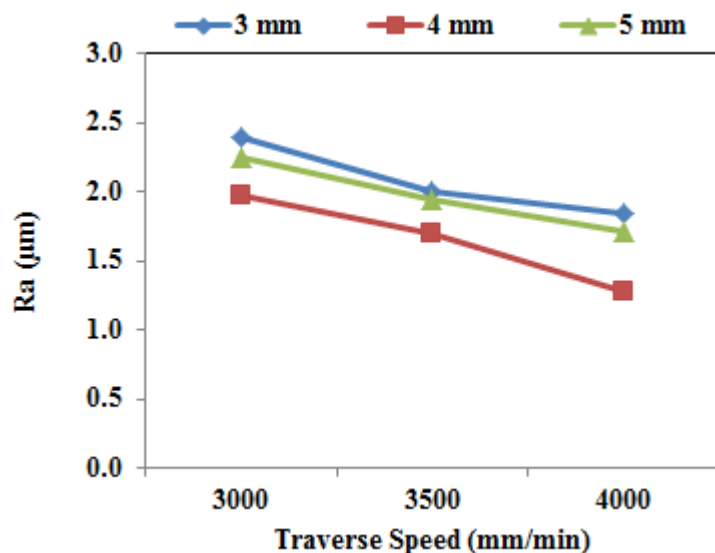


Fig. 5.14: Effect of traverse speed and SOD on surface roughness

The effect of AFR on channel roughness with traverse speed is shown in Figure 5.15. Experimental results reveal that surface roughness increases with an increase in the AFR leading to a poor finish. A higher number of abrasive particles involved in mixing increases the probability of particle collision and also decreasing the average diameter of the impacting particle due to particle defragmentation. Earlier authors, Kovacevic et al. (1988) observed that under certain low operating pressures, the roughness increases once a critical abrasive mass flow rate is exceeded. This concludes that a certain ratio between the abrasive particle diameter and number of particles is a very much essential to obtain an effective finished surface.

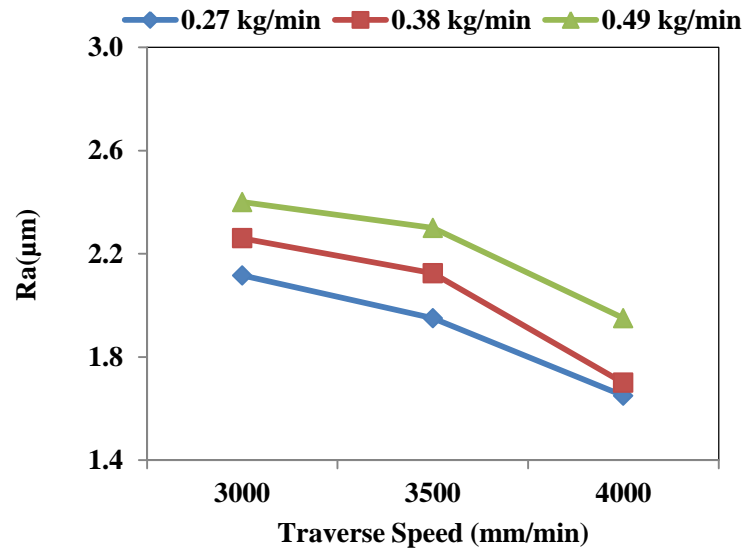


Fig. 5.15: Effect of traverse speed and AFR on surface roughness

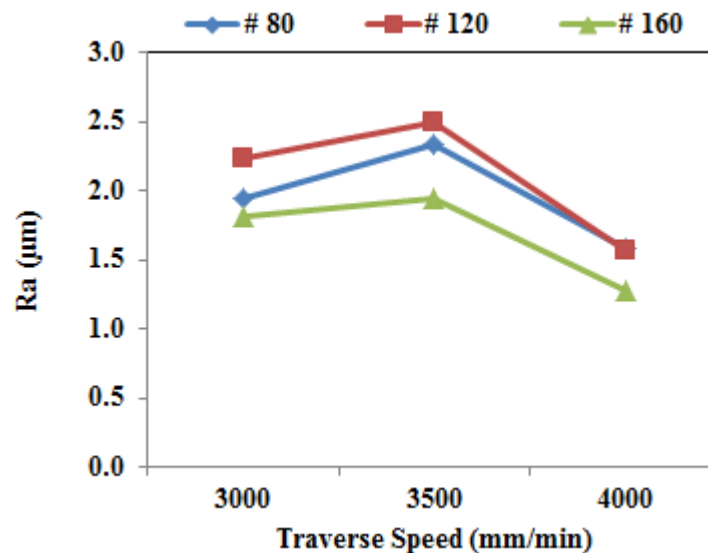


Fig. 5.16: Effect of traverse speed and abrasive size on surface roughness

Figure 5.16 shows the effect of abrasive size on surface roughness with traverse speed. It has been observed that a gradual increase in surface roughness with increase in the traverse speed till 3500 mm/min and a decreasing trend at a traverse speed of 4000 mm/min. The change in the material removal mechanism is responsible for the improved finish at higher traverse speeds. In general, surface finish improves as the particle size is reduced; this is valid for small sized abrasives. Similar trends are observed in obtaining a better finish at # 160 abrasives. The inertia of the abrasive particles for bigger sized abrasives increases the surface finish and also the jet

GEOMETRY AND CHARACTERISTICS OF THE MICRO CHANNELS

instability for higher abrasive sizes contributes to the surface structure. In order to achieve a good surface finish, an appropriate particle size distribution is very essential which can be decided based on the AFR and the target material properties.

Table 5.5 gives the ANOVA results for surface roughness, which shows the percentage contribution of process parameters on surface roughness. From these studies it is observed that the surface roughness is highly influenced by the particle size and followed by traverse speed; better surfaces are obtained at higher traverse speeds. The F-test in Table 5.6 indicates that the abrasive size is the most significant parameter on the average surface roughness, contributing to 22% which is calculated at 99% confidence intervals. It is seen that traverse speed with SOD is contributing to about 7.5% on the surface roughness, while SOD as an individual parameter the contribution is the minimum out of all process parameters.

Table 5.5: ANOVA analysis for surface roughness ($R^2 = 82.94\%$)

| <i>Parameter</i> | <i>DOF</i> | <i>SS</i> | <i>Variance (V)</i> | <i>F-Ratio</i> | <i>Pure Sum (S)</i> | <i>Cont.(%)</i> |
|-------------------------------|------------|-----------|---------------------|----------------|---------------------|-----------------|
| v | 2 | 0.9803 | 0.4902 | 2.13 | 0.52 | 2.41 |
| \dot{m}_a | 2 | 0.1139 | 0.0569 | 0.25 | 0.35 | 1.60 |
| d | 2 | 5.2048 | 2.6024 | 11.32 | 4.74 | 22.00 |
| h | 2 | 0.7220 | 0.3610 | 1.57 | 0.26 | 1.22 |
| $v \times \dot{m}_a$ | 4 | 0.6635 | 0.1659 | 0.72 | 0.26 | 1.19 |
| $v \times d$ | 4 | 1.1052 | 0.2763 | 1.20 | 0.19 | 0.86 |
| $v \times h$ | 4 | 2.5407 | 0.6352 | 2.76 | 1.62 | 7.52 |
| $\dot{m}_a \times d$ | 4 | 0.3964 | 0.0991 | 0.43 | 0.52 | 2.43 |
| $\dot{m}_a \times h$ | 4 | 0.1030 | 0.0258 | 0.11 | 0.82 | 3.79 |
| $d \times h$ | 4 | 0.6118 | 0.1530 | 0.67 | 0.31 | 1.43 |
| $v \times \dot{m}_a \times d$ | 8 | 2.7344 | 0.3418 | 1.49 | 0.90 | 4.15 |
| $v \times \dot{m}_a \times h$ | 8 | 0.6443 | 0.0805 | 0.35 | 1.20 | 5.54 |
| $v \times d \times h$ | 8 | 0.6125 | 0.0766 | 0.33 | 1.23 | 5.69 |
| $\dot{m}_a \times d \times h$ | 8 | 1.4569 | 0.1821 | 0.79 | 0.38 | 1.77 |
| Error | 16 | 3.6787 | 0.2299 | | | |
| Total | 80 | 21.5685 | | | | |

5.4 Regression analysis

Regression analysis is a statistical technique for estimating the relationships among variables. It includes techniques for modeling and analyzing several variables, when the focus is on the relationship between a dependent and one or more independent variables. Moreover, regression helps one to understand how a typical value of dependent variable changes when any one of the independent variables is varied, while keeping other independent variables fixed. In continuation to the experiments conducted according to the full factorial experimental design and further on ANOVA analysis for considering the significant and insignificant parameters on the various response variables, general linear models have been developed for predicting the geometrical parameters like depth, width, taper of cut and characteristic parameters like surface roughness. The generalized regression models developed are as follows:

Depth of cut: - ANOVA results show that traverse speed and abrasive size are significantly contributing to the channel depth when compared to SOD and AFR which were clearly shown in the plots in the previous section. The regression equation considering the process variables with the interaction effects up to first and second order is as follows:

$$\text{Depth} = 290 - 0.053v + 237\dot{m}_a - 298d - 2.1h + 0.000004v^2 + 0.0066v \times \dot{m}_a - 0.238v \times d + 0.00497v \times h - 206\dot{m}_a^2 + 726\dot{m}_a \times d - 52\dot{m}_a \times h + 4476d^2 - 15d \times h + 0.95h^2 \quad (R^2=0.925)$$

Width: - Based on the ANOVA results on the channel width, the independent variable SOD is more significant than other parameters and interaction parameters with SOD are also significant while the least significant is AFR. The regression equation considering the interaction effects and the process variables is as follows:

$$\text{Width} = 2343 - 0.423v - 106\dot{m}_a - 2489d - 213h + 0.000038v^2 - 0.047v \times \dot{m}_a + 0.419v \times d + 0.0282v \times h - 15\dot{m}_a^2 + 680\dot{m}_a \times d + 9.5\dot{m}_a \times h - 1674d^2 + 102d \times h + 12.4h^2 \quad (R^2=0.974)$$

Taper: - The regression equation considering the interaction effects of the process variables on taper is as follows:

$$\begin{aligned} \text{Taper} = & 138 - 0.0243v - 68\dot{m}_a - 398d + 1.7h + 0.000002v^2 - 0.0025v \times \dot{m}_a + 0.132v \times d - \\ & 0.00208v \times h + 19\dot{m}_a^2 + 272\dot{m}_a \times d + 7.6\dot{m}_a \times h - 832d^2 + 4.1d \times h + 0.27h^2 \\ & (R^2=0.825) \end{aligned}$$

5.5 Surface morphological studies

Several researchers carried investigations into the micro-structural alternations of abrasive water jet machined materials. Hashish (1986a) finds no distortion near the surface of aluminum and boron carbide after machining with AWJ turning. Specimens machined by laser cutting, shearing, EDM, and abrasive water jets are when compared, it has been reported that no distortions were found in the AWJ machined specimens and the surface crystallization is also minimal. The EDM cut surfaces becomes molten because of the enormous heat affected zone; while such cases are not possible with abrasive water jets.

If the process parameters are optimized, AWJ offers some quantitative advantages over conventional machining processes. Parameters like traverse speed; AFR and SOD are quantitative parameters unlike the particle size, which can be a qualitative. Assuming abrasive size has some influence on the surface characteristics; keeping other process parameters constant, samples milled with different abrasive sizes are observed using a Scanning Electron Microscope (SEM). In AWJM, abrasive particle embedding is a well know phenomenon in solid particle erosion of soft materials. Under certain operating conditions abrasive particle deposition on ductile material machining is possible. Neusen et al. (1987) carried out a detailed SEM based investigation into the particle deposition during AWJ cutting.

The sample machined with # 80 abrasive shown in Figure 5.17, when observed, bigger scratches were found on the surface which reveals a poor surface. The macrographs of the samples machined with # 120 and # 160 abrasives (Figures 5.18 and 5.19) shows that scratch widths are small and regular. This shows that machining with fine abrasives gives better surface. The width of the scratches/tracks on the surfaces is related to the abrasive size. The non-uniformity reveals the particle size distribution

after leaving the focus tube and during impacting the surface. An interesting observation is that particle embedment into the surface is clearly visible and are marked in the images. Particle embedment is more on # 160 samples as shown in Figure 5.19. For a given AFR, small sized abrasive particles are more in number which involves internal collisions during mixing. The abrasive particles get ruptured with each other and broke into finer particles embedding into the surface.

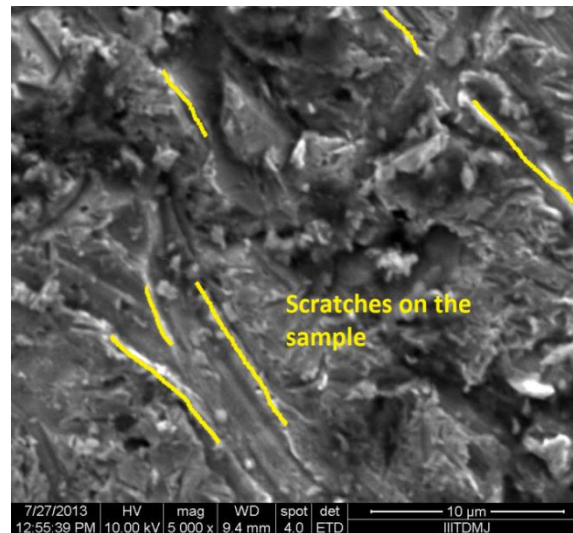


Fig. 5.17: SEM image of the experimental machined sample with # 80 abrasive

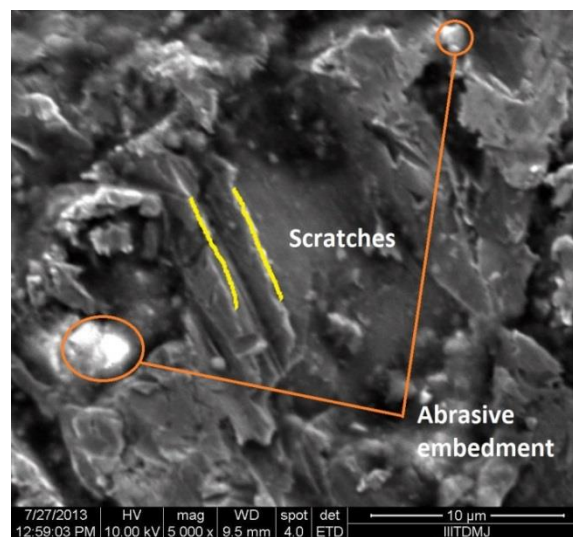


Fig. 5.18: SEM image of the experimental machined sample with # 120 abrasive

As mentioned in the previous sections of the chapter, the material removal mechanism is primarily due to deformation mode in milling in AWJM at high traverse speeds. Figures 5.17 - 5.19 shows that the ploughing action of abrasive particle is taking place during the material removal. The channel photographs reveal that micro-

machining process is involved in cutting of ductile materials which shows that the solid particle erosion process involves ploughing action of abrasive particle. The SEM images also show that the micro mechanism of the material does not change but the tracks or the scratches involved become irregular increasing the surface roughness with an increase in the diameter of the abrasive particle.

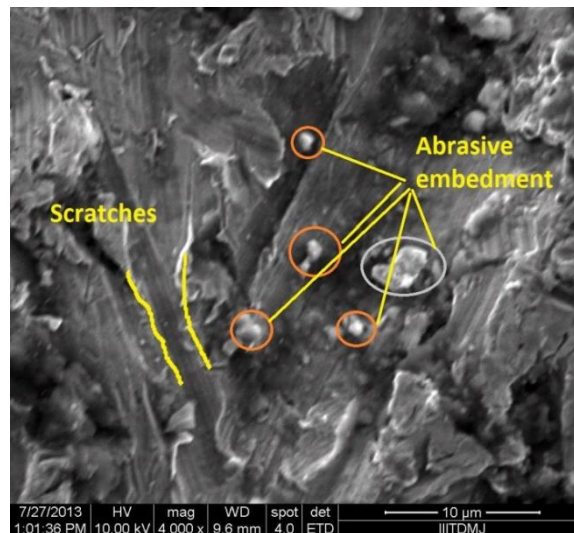


Fig. 5.19: SEM image of the experimental machined sample with # 160 abrasive

5.6 Summary

Considerable efforts were put by researchers to understand the process both mathematically and experimentally on AWJM for cutting applications on a variety of materials. Milling with AWJM technique is a recent addition to the task for reducing the weight of a component without compromising its strength. The requirement in weight reduction and high strength to weight ratio in aerospace, defense and space applications is at greater demand today. The attempts in the current research are to establish a technique in using AWJ milling process. The work presented here is to understand the process linear milling, with close dimensional tolerances and accuracies involved. In a part separation technique with AWJM, taper obtained is a predominant factor to be controlled which can be executed using a tilt jet, but to a limited extent only.

Based on the investigations carried, the depth of the channel is highly influenced by traverse speed followed by the abrasive size, while the channel width is dominated

by the jet diameter which changes with SOD. The variation in the taper is due to abrasive size in comparison to other parameters.

Conducting experiments through a full factorial experimental helped us to understand that in AWJM, individual parameters have less effect on the output and a significant influence is observed due to interaction in the parameters. ANOVA is used as a guidance to decide significant and non-significant process variables on the output; like traverse speed for depth of cut, SOD for width of cut and particle size for the taper cut respectively. An optimized model can be developed for obtaining a better surface pocket size of required width and depth with minimum taper.

Chapter 6

OPTIMIZATION, CONTROL AND ARTIFICIAL NEURAL NETWORKS

| | |
|--|-----|
| 6.1 Introduction to supervision and monitoring | 115 |
| 6.2 Optimization using Grey Relational Analysis | 117 |
| 6.2.1. Grey relational analysis for micro-channel geometry | 119 |
| 6.2.2. Results and discussion | 121 |
| 6.3 ANN for AWJM | 123 |
| 6.3.1 Preparation of training and target vector set | 125 |
| 6.3.2 Network Architecture and Training | 126 |
| 6.3.3 Results and discussion | 130 |
| 6.4 Summary | 132 |

6.1 Introduction to supervision and monitoring

As in any other machining process, control and supervision of the abrasive water jet machining (AWJM) improves both efficiency and the quality of the process. An early attempt to develop an appropriate control algorithm for linking AWJM to automated manufacturing equipment has been made by Mazurkiewicz and Karlic (1997). It is reported that it is possible to control depth of cut, width of cut and the material removal rate using the two control variables stand-off distance and traverse rate. Louis and Meier (1991) used acoustic signals to control the suction performance of an abrasive water jet system. A typical application of workpiece reaction force to control the abrasive suction process has been attempted by Hunt et al. (1987) where it was concluded that the force-signal intensity suddenly rises to a higher level and becomes stable and this corresponds to the force measured during the cutting of the materials.

Wear of the orifice is a result of the fluid conditions in the orifice which influences the jet structure. Orifice wear disturbs the jet coherence worsens which lead to irregular material removal rates and also the variation in the machining process.

There are both direct and indirect methods for the process supervision. Qualitative methods consist of direct visual inspection of the tip of the nozzle and the indirect observation is by deterioration in the quality of cut surface or the undesirable changes in the dimensions of the workpiece machined. Direct methods suffer for serious drawbacks as the process requires interruption for wear measurement which is unsuitable. Major indirect methods are based on the measurements of some parameters such as normal forces on the workpiece, noise, vibration etc.

Momber et al. (1994, 1995) used acoustic emission signals for visualization and control of the material removal rate in brittle and multiphase materials. The authors reported that these signals are capable of detecting the mode of material removal mechanism depending on the structure in the frequency-domain signals. Reports on the kerf region reveal that the presence of the rebounded abrasive particle has a damping effect on the signal. The use of workpiece reaction force to characterize the profile of surface that is generated by abrasive water jets has been attempted by Hunt et al. (1987). The reports reveal that observations are made to examine the influence of traverse speed, type of abrasives on the work piece reaction force. It shows that the force almost increases linearly with traverse speeds and it is very low for machining with hard abrasives when compared with general garnets. The authors also reported that the surface roughness can therefore be controlled by forming an error signal that is based on the difference between the desired roughness and the actual roughness obtained. Kovacevic et al. (1995) used the dynamic component of the workpiece reaction force to control the surface roughness.

The depth of cut generated by AWJM process is a complex function of a number of process parameters and the material properties. For automated machining, an online control for the depth of cut is a necessary condition. In AWJ milling, the geometry of the feature an important characteristic due to high traverse rates in order to removal a very little amount of material from the surface. The rapid movement of the jet assembly during the cut is subjected to enormous amount of vibrations which deteriorates the topology of the feature. Experimental observations show that the signals acquired for a through cutting process are entirely different in comparison to milling technique. The dimensions of the kerf width are correlated to the vibration signal in reference to the parametric set. The predicted roughness, kerf width are compared with

the desired values and if they are different, this technique can be further used to change the process parameters which can be controlled for an online monitoring process. This chapter is an attempt to correlate the force and vibration signals along with the input process parameters on the geometry using artificial neural networks.

6.2 Optimization using Grey Relational Analysis

Grey theory is a simple and accurate method for multiple attribute decision problems. Grey, when thought as a color is a blend of black and white colors. In grey analysis, black is represented as a lack of information whereas the white is full of information. Thus, the information that is either incomplete or undetermined is called as Grey. A system having incomplete information is called Grey system. The Grey relational analysis used information from the Grey system to dynamically compare each factor quantitatively. This approach is based on the level of similarity and variability among all factors to establish their relation. This kind of interaction is mainly through the connection among machining parameters and the conditions that are already known.

In grey relational analysis the optimization is carried out in different steps. The first step is data pre-processing where the original sequence is transferred to a comparable sequence. This is required because the range, unit and objective of the data sequence (for a response) vary between each other. Normalization of the data in the range between zero and one is performed using linear data pre-processing method. This is carried out in 3 different types based on the response characteristics as follows:

(a) Higher the better (HB)

$$x_i^*(k) = \frac{x_i^{(0)}(k) - \min x_i^{(0)}(k)}{\max x_i^{(0)}(k) - \min x_i^{(0)}(k)}$$

(b) Lower the better (LB)

$$x_i^*(k) = \frac{\max x_i^{(0)}(k) - x_i^{(0)}(k)}{\max x_i^{(0)}(k) - \min x_i^{(0)}(k)}$$

(c) Desired value

$$x_i^*(k) = 1 - \frac{|x_i^{(0)}(k) - x^{(0)}|}{\max x_i^{(0)}(k) - x^{(0)}}$$

where $x_i^*(k)$ is the generating value, $\min x_i^{(0)}(k)$ is the minimum value of $x_i^{(0)}(k)$, $\max x_i^{(0)}(k)$ is the maximum value of $x_i^{(0)}(k)$ and $x^{(0)}$ is the desired value.

Next step in grey analysis is to calculate the grey relational coefficient from the normalized experimental data to express the relationship between the ideal (best) and the actual experimental data. Grey relational grade is then calculated by averaging the grey relational coefficients corresponding to each performance characteristics. The term Grey relational grade, Γ is used to show the connection among original and comparative series. The procedure for calculating grey relational grade is given by Huang and Liao (2003). For a Grey relational space (X, Γ) with X collection of Grey relational factors, the comparative series, $x_i(k)$ and reference series, $x_0(k)$ are

$$x_0(k) = x_0(1), x_0(2), x_0(3), x_0(4), \dots, x_0(n)$$

$$x_i(k) = x_i(1), x_i(2), x_i(3), x_i(4), \dots, x_i(n) \in X$$

where $i = 1, 2, \dots, m$

The Grey relational grade can be calculated by Equation 6.1. Δ_{min} , Δ_{max} are the minimum and maximum value among all the Δ_{0i} values respectively. $\Delta_{0i}(k)$ is the absolute value of difference between x_0 and x_1 at the k^{th} point.

$$\Gamma_{0i} = \frac{\Delta_{min} + \Delta_{max}}{\Delta' + \Delta_{max}} \tag{6.1}$$

where,

- (1) $i = 1, \dots, m, k = 1, \dots, n, j \in i$
- (2) $x_0(k)$: reference sequence, $x_i(k)$: comparative sequences
- (3) $\Delta_{0i}(k) = |x_0(k) - x_i(k)|$
- (4) $\Delta_{min} = \min_{\forall j \in i} \min_{\forall k} |x_0(k) - x_j(k)|$
- (5) $\Delta_{max} = \max_{\forall j \in i} \max_{\forall k} |x_0(k) - x_j(k)|$

$$\Delta' = \sqrt{\sum_{k=1}^n \left(\frac{\Delta_{0i}^2(k)}{n} \right)}$$

The Grey relational grade is used for the evaluation of the experimental data for multi-response characteristics. Highest grade corresponds to the optimal level of experiments where optimization of any complicated multiple performance characteristics can be converted into a single Grey relational grade.

6.2.1. Grey Relational Analysis for AWJM micro-channel geometry

In the present work, Grey Relational Analysis has been carried on the response parameters of the micro-channels. The experimental response data in Table 5.1 is considered to perform the grey analysis for the multiple attribute decision problems to evaluate the process performance. The multiple characteristics of the process considered for grey relational analysis are surface roughness, depth, taper, width, impact force and the jet vibration. Basic requirements in fabrication of micro-channels are minimum surface roughness, maximum depth, minimum taper, and width equivalent to jet diameter, minimum impact force and minimum jet vibration to achieve the best process performance. Table 6.1 gives the grade relational coefficients for all the response parameters and the grade is given by the average of all grey relational coefficients of the concerned run. The maximum value of the grey relational grade gives the Rank for obtaining the best performance.

Table 6.1: Grey relational coefficients, Relational Grade and Rank for the micro-channels.

| Exp. No | Grey Relational Coefficients | | | | | | Grade | Rank |
|---------|------------------------------|-------|-------|-------|-------|-------|-------|------|
| | Width | Depth | Taper | Ra | F | Vib. | | |
| 1 | 0.842 | 0.607 | 0.627 | 0.333 | 0.549 | 0.516 | 0.579 | 34 |
| 2 | 0.671 | 0.533 | 0.510 | 0.884 | 0.418 | 0.806 | 0.637 | 4 |
| 3 | 0.529 | 0.552 | 0.420 | 1.000 | 0.416 | 0.903 | 0.637 | 5 |
| 4 | 0.465 | 0.430 | 0.431 | 0.423 | 0.531 | 0.532 | 0.469 | 81 |
| 5 | 0.588 | 0.430 | 0.485 | 0.454 | 0.480 | 0.518 | 0.493 | 76 |
| 6 | 0.625 | 0.607 | 0.512 | 0.445 | 0.546 | 0.533 | 0.545 | 54 |
| 7 | 0.444 | 0.568 | 0.539 | 0.510 | 0.396 | 0.760 | 0.536 | 62 |
| 8 | 0.613 | 0.415 | 0.613 | 0.377 | 0.477 | 0.399 | 0.482 | 80 |

OPTIMIZATION, CONTROL AND ARTIFICIAL NEURAL NETWORKS

| | | | | | | | | |
|-----------|--------------|--------------|--------------|--------------|--------------|--------------|--------------|----------|
| 9 | 0.513 | 0.333 | 0.717 | 0.693 | 0.571 | 0.517 | 0.557 | 45 |
| 10 | 0.520 | 0.607 | 0.518 | 0.595 | 0.486 | 0.520 | 0.541 | 56 |
| 11 | 0.492 | 0.472 | 0.510 | 0.589 | 0.530 | 1.000 | 0.599 | 24 |
| 12 | 0.567 | 0.687 | 0.539 | 0.885 | 1.000 | 0.883 | 0.760 | 1 |
| 13 | 0.719 | 0.447 | 1.000 | 0.388 | 0.464 | 0.562 | 0.597 | 25 |
| 14 | 0.684 | 0.415 | 0.403 | 0.659 | 0.467 | 0.522 | 0.525 | 67 |
| 15 | 0.499 | 0.482 | 0.470 | 0.636 | 0.478 | 0.484 | 0.508 | 72 |
| 16 | 0.430 | 1.000 | 0.490 | 0.730 | 0.400 | 0.753 | 0.634 | 7 |
| 17 | 0.408 | 0.687 | 0.531 | 0.910 | 0.833 | 0.552 | 0.653 | 3 |
| 18 | 0.576 | 0.497 | 0.516 | 0.598 | 0.517 | 0.754 | 0.576 | 36 |
| 19 | 0.471 | 0.677 | 0.482 | 0.468 | 0.533 | 0.553 | 0.530 | 66 |
| 20 | 0.478 | 0.904 | 0.471 | 0.537 | 0.458 | 0.878 | 0.621 | 16 |
| 21 | 0.519 | 0.430 | 0.438 | 0.498 | 0.525 | 0.489 | 0.483 | 79 |
| 22 | 0.409 | 0.824 | 0.406 | 0.547 | 0.439 | 0.613 | 0.540 | 58 |
| 23 | 0.588 | 0.363 | 0.511 | 0.382 | 0.432 | 0.660 | 0.489 | 78 |
| 24 | 0.510 | 0.577 | 0.504 | 0.773 | 0.483 | 0.381 | 0.538 | 61 |
| 25 | 0.551 | 0.697 | 0.549 | 0.578 | 0.483 | 0.857 | 0.619 | 17 |
| 26 | 0.586 | 0.428 | 0.467 | 0.709 | 0.479 | 0.793 | 0.577 | 35 |
| 27 | 0.641 | 0.463 | 0.502 | 0.532 | 0.628 | 0.513 | 0.546 | 53 |
| 28 | 0.497 | 0.448 | 0.412 | 0.585 | 0.645 | 0.608 | 0.532 | 64 |
| 29 | 0.461 | 0.577 | 0.626 | 0.528 | 0.405 | 0.632 | 0.538 | 60 |
| 30 | 0.631 | 0.640 | 0.380 | 0.622 | 0.663 | 0.829 | 0.627 | 11 |
| 31 | 0.414 | 0.745 | 0.467 | 0.693 | 0.628 | 0.829 | 0.629 | 9 |
| 32 | 0.455 | 0.824 | 0.451 | 0.779 | 0.526 | 0.776 | 0.635 | 6 |
| 33 | 0.489 | 0.433 | 0.555 | 0.806 | 0.443 | 0.717 | 0.574 | 37 |
| 34 | 0.516 | 0.640 | 0.561 | 0.454 | 0.449 | 0.615 | 0.539 | 59 |
| 35 | 0.561 | 0.550 | 0.489 | 0.501 | 0.391 | 0.457 | 0.492 | 77 |
| 36 | 0.411 | 0.697 | 0.642 | 0.495 | 0.452 | 0.731 | 0.571 | 40 |
| 37 | 0.520 | 0.401 | 0.499 | 0.552 | 0.530 | 0.514 | 0.503 | 73 |
| 38 | 0.429 | 0.607 | 0.588 | 0.505 | 0.349 | 0.516 | 0.499 | 75 |
| 39 | 0.506 | 0.463 | 0.536 | 0.640 | 0.461 | 0.527 | 0.522 | 69 |
| 40 | 0.515 | 0.824 | 0.541 | 0.526 | 0.487 | 0.909 | 0.634 | 8 |
| 41 | 0.429 | 0.649 | 0.463 | 0.846 | 0.451 | 0.669 | 0.585 | 31 |
| 42 | 0.505 | 0.753 | 0.429 | 0.692 | 0.413 | 0.903 | 0.616 | 18 |
| 43 | 0.495 | 0.640 | 0.583 | 0.463 | 0.452 | 0.653 | 0.548 | 52 |
| 44 | 0.505 | 0.814 | 0.402 | 0.751 | 0.668 | 0.603 | 0.624 | 14 |
| 45 | 0.469 | 0.640 | 0.427 | 0.582 | 0.582 | 0.700 | 0.567 | 42 |

| | | | | | | | | |
|----|-------|-------|-------|-------|-------|-------|-------|----|
| 46 | 0.441 | 0.904 | 0.496 | 0.564 | 0.445 | 0.918 | 0.628 | 10 |
| 47 | 0.531 | 0.568 | 0.469 | 0.584 | 0.488 | 0.700 | 0.557 | 46 |
| 48 | 0.455 | 0.597 | 0.426 | 0.870 | 0.550 | 0.865 | 0.627 | 12 |
| 49 | 0.505 | 0.904 | 0.487 | 0.467 | 0.511 | 0.724 | 0.600 | 23 |
| 50 | 0.945 | 0.472 | 0.333 | 0.487 | 0.333 | 0.871 | 0.574 | 38 |
| 51 | 0.499 | 0.607 | 0.624 | 0.447 | 0.364 | 0.546 | 0.515 | 70 |
| 52 | 0.507 | 0.687 | 0.352 | 0.753 | 0.403 | 0.704 | 0.568 | 41 |
| 53 | 0.532 | 0.448 | 0.425 | 0.839 | 0.407 | 0.592 | 0.540 | 57 |
| 54 | 0.481 | 0.753 | 0.435 | 0.686 | 0.528 | 0.803 | 0.614 | 19 |
| 55 | 0.441 | 0.454 | 0.587 | 0.570 | 0.474 | 0.784 | 0.552 | 49 |
| 56 | 0.464 | 0.687 | 0.417 | 0.582 | 0.424 | 0.684 | 0.543 | 55 |
| 57 | 0.512 | 0.527 | 0.372 | 0.559 | 0.435 | 0.789 | 0.533 | 63 |
| 58 | 0.432 | 0.428 | 0.389 | 0.754 | 0.602 | 0.693 | 0.550 | 51 |
| 59 | 0.436 | 0.697 | 0.599 | 0.490 | 0.417 | 0.925 | 0.594 | 28 |
| 60 | 0.531 | 0.649 | 0.489 | 0.559 | 0.453 | 0.680 | 0.560 | 44 |
| 61 | 0.509 | 0.649 | 0.389 | 0.723 | 0.460 | 0.844 | 0.596 | 26 |
| 62 | 0.510 | 0.577 | 0.538 | 0.604 | 0.461 | 0.500 | 0.532 | 65 |
| 63 | 0.434 | 0.568 | 0.557 | 0.472 | 0.430 | 0.844 | 0.551 | 50 |
| 64 | 0.492 | 0.497 | 0.488 | 0.607 | 0.764 | 0.542 | 0.565 | 43 |
| 65 | 0.494 | 0.597 | 0.364 | 0.887 | 0.395 | 0.837 | 0.596 | 27 |
| 66 | 0.514 | 0.640 | 0.545 | 0.460 | 0.394 | 0.454 | 0.501 | 74 |
| 67 | 0.507 | 0.762 | 0.438 | 0.722 | 0.559 | 0.333 | 0.554 | 47 |
| 68 | 0.429 | 0.527 | 0.409 | 0.557 | 0.446 | 0.943 | 0.552 | 48 |
| 69 | 0.478 | 0.604 | 0.403 | 0.376 | 0.392 | 0.802 | 0.509 | 71 |
| 70 | 0.581 | 0.342 | 0.785 | 0.676 | 0.474 | 0.571 | 0.572 | 39 |
| 71 | 0.452 | 0.904 | 0.496 | 0.494 | 0.497 | 0.809 | 0.608 | 22 |
| 72 | 0.643 | 0.824 | 0.453 | 0.589 | 0.461 | 0.780 | 0.625 | 13 |
| 73 | 0.356 | 0.527 | 0.456 | 0.642 | 0.419 | 0.750 | 0.525 | 68 |
| 74 | 0.369 | 0.993 | 0.392 | 0.945 | 0.777 | 0.588 | 0.677 | 2 |
| 75 | 0.388 | 0.814 | 0.419 | 0.540 | 0.649 | 0.931 | 0.624 | 15 |
| 76 | 0.364 | 0.527 | 0.600 | 0.575 | 0.625 | 0.803 | 0.582 | 32 |
| 77 | 0.478 | 0.697 | 0.630 | 0.621 | 0.553 | 0.703 | 0.614 | 20 |
| 78 | 0.333 | 0.561 | 0.515 | 0.632 | 0.565 | 0.941 | 0.591 | 29 |
| 79 | 0.718 | 0.697 | 0.513 | 0.578 | 0.510 | 0.635 | 0.609 | 21 |
| 80 | 0.647 | 0.604 | 0.458 | 0.502 | 0.503 | 0.813 | 0.588 | 30 |
| 81 | 0.604 | 0.342 | 0.838 | 0.476 | 0.503 | 0.730 | 0.582 | 33 |

6.2.2. Results and discussion

According to the grey relational grades from Table 6.1, experiment no. 12 has the highest grey relational grade. Thus, experiment no. 12 gives the best performance characteristics in the present experimental set to fabricate the micro-channel. The corresponding input parameters are the optimum set of process parameters. Table 6.2 gives the average response table for the grey relational grade values. Delta is the difference between the maximum and minimum grade values of the each input parameter and the significance row gives the order of influence of the process parameter. The results obtained through grey relational analysis are in agreement with the results obtained from ANOVA analysis in Chapter 5.

Table 6.2: Average Grey Relational Grade for Factor and Levels

| Levels | v (mm/min) | \dot{m}_a (kg/min) | d (mm) | h (mm) |
|--------------|-----------------|-------------------------|---------------|---------------|
| 1 | 0.5878 | 0.5705 | 0.5292 | 0.5565 |
| 2 | 0.5619 | 0.5700 | 0.5874 | 0.5844 |
| 3 | 0.5618 | 0.5710 | 0.5959 | 0.5706 |
| Delta | 0.0026 | 0.0010 | 0.0667 | 0.0279 |
| Significance | 3 | 4 | 1 | 2 |

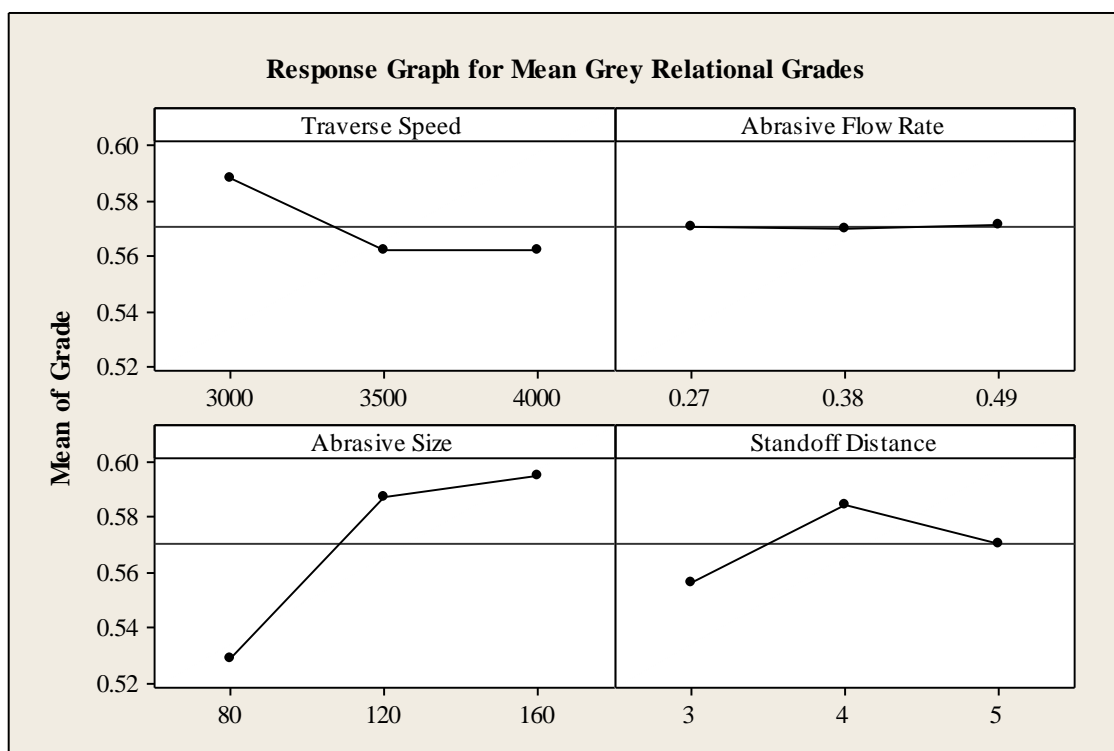


Fig. 6.1: Response graph for the mean grey relational grades

The response graph for the mean grey relational grades at different levels of the input parameters is shown in Figure 6.1. The graph indicates the optimal factorial sets like traverse speed (level 1), AFR (level 3), abrasive size (level 3) and SOD (level 2) i.e., the combination of 3000 mm/min traverse speed, 0.49 kg/min AFR with # 160 mesh abrasive size at an SOD of 4 mm gives the best possible response parametric set. Figure 6.2 gives the graph showing the corresponding grade values for the full experimental runs.

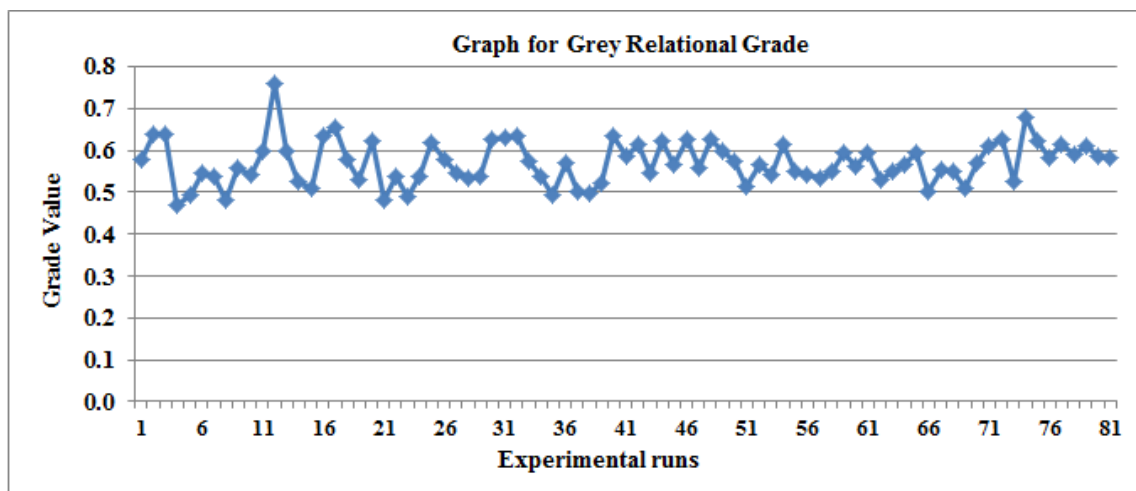


Fig. 6.2: Grey Relational Grade Graph

6.3 ANN for AWJM

An Artificial Neural Network (ANN) is a mathematical or computational model inspired by the structure and/or functional aspects of biological neural networks. It is a massively parallel, distributed processor that has capability of storing experimental knowledge. ANN tries to mimic the human brain in two ways, firstly, ANN learns by experience; secondly it stores the information in the form of synaptic weights. Modern neural networks are non-linear statistical data modeling tools. They are normally used to model complex relationships between inputs and outputs or find patterns in the given data. In most cases, an ANN is an adaptive system that changes the structure based on external or internal information that flows inside the network. Reference can be made to Hassoun (2009), for a detailed treatise on ANN.

The present work is an attempt to use ANN for process monitoring the dimensional and characteristics of the micro channel fabricated with AWJM technique. The functional aspect of the ANN developed for the AWJM process is described here.

In the present study, the network toolbox in MATLAB is utilized. Back Propagation Technique is adopted for training the network. A typical three layered Back Propagation Network is shown in Figure 6.3. Training is accomplished by sequentially applying input vector, while adjusting network weights according to a predetermined procedure. During training, the network weights gradually converge to values such that each input vector produces the desired output vector.

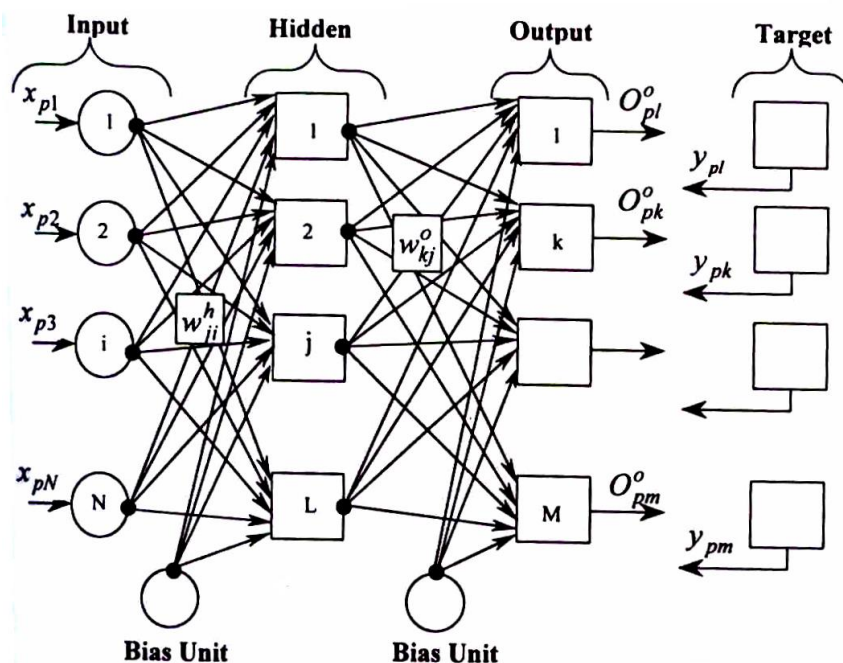


Fig. 6.3: A typical 3-layer Back Propagation Network

The neural network architecture, number of layers, nodes, transfer function and the training pattern chosen in the present study are shown in Table 6.4. Tangent sigmoidal functions are used for all layers and the percentage validation of the architectures considered is specified in Table 6.4.

Neural Network Toolbox of MATLAB provides fifteen different learning functions. In the present study *Trainlm* is used as network training function. *Trainlm* is a network training function that updates weight and bias values according to Levenberg-Marquardt optimization (Kenneth 1944).

6.3.1 Preparation of training and target vector set

As investigated in the previous chapters, the channel geometry and roughness are a function of input process parameters. In the present work, the jet impact force and jet vibration are considered as the influencing parameters along with the input process parameters that affects the surface topology of the channel. It is similar to a conventional metal cutting process where the cutting tool vibration and the cutting force influence the machining process that affects the surface roughness. Hence, the training vector consists of traverse speed (v), SOD (h) AFR (\dot{m}_a) and abrasive size(d), impact force (F) and the jet vibration (g). Accordingly the typical input and target data are presented in Table 6.3. The input and target parametric values are normalized while performing training and testing the networks.

Table 6.3: Typical input and output data for the neural networks.

| Exp. No | Input | | | | | | Target | | | |
|---------|-----------------|-------------------------|-------------|-------------|------------|---------------|---------------------|---------------------|----------------|---------------------|
| | v (mm/min) | \dot{m}_a (kg/min) | d (mm) | h (mm) | F (N) | $accn$ (g) | Width (μ m) | Depth (μ m) | Taper (Deg) | R_a (μ m) |
| 1 | 3000 | 0.49 | 0.177 | 4 | 10.33 | 0.000552 | 785 | 225.91 | 58.90 | 3.61 |
| 2 | 3500 | 0.49 | 0.125 | 5 | 11.60 | 0.000382 | 753 | 183.55 | 40.22 | 1.26 |
| 3 | 3500 | 0.38 | 0.110 | 4 | 11.63 | 0.000349 | 762 | 150.00 | 50.00 | 1.09 |
| 4 | 3500 | 0.38 | 0.177 | 4 | 10.47 | 0.000538 | 690 | 140.25 | 49.02 | 2.81 |
| 5 | 3500 | 0.27 | 0.177 | 3 | 10.91 | 0.000551 | 690 | 160.00 | 47.21 | 2.61 |
| 6 | 3500 | 0.38 | 0.177 | 5 | 10.35 | 0.000537 | 785 | 192.02 | 60.04 | 2.66 |
| 7 | 3000 | 0.49 | 0.125 | 4 | 11.89 | 0.000400 | 769 | 196.79 | 51.52 | 2.30 |
| 8 | 4000 | 0.38 | 0.177 | 3 | 10.94 | 0.000692 | 678 | 192.02 | 48.13 | 3.18 |
| 9 | 4000 | 0.38 | 0.177 | 4 | 10.17 | 0.000551 | 595 | 186.38 | 56.38 | 1.65 |
| 10 | 3000 | 0.27 | 0.177 | 5 | 10.86 | 0.000548 | 785 | 193.91 | 51.20 | 1.95 |
| 11 | 3000 | 0.27 | 0.110 | 4 | 10.47 | 0.000323 | 719 | 175.08 | 63.60 | 1.97 |
| 12 | 3000 | 0.49 | 0.110 | 4 | 8.50 | 0.000355 | 812 | 208.02 | 60.56 | 1.26 |
| 13 | 3000 | 0.38 | 0.177 | 3 | 11.07 | 0.000513 | 702 | 257.91 | 54.20 | 3.08 |
| 14 | 4000 | 0.49 | 0.177 | 4 | 11.04 | 0.000547 | 678 | 126.13 | 66.21 | 1.74 |
| 15 | 3500 | 0.38 | 0.177 | 3 | 10.93 | 0.000583 | 725 | 162.85 | 66.19 | 1.81 |
| 16 | 3500 | 0.49 | 0.125 | 4 | 11.84 | 0.000403 | 876 | 205.20 | 50.26 | 1.56 |

| | | | | | | | | | | |
|----|------|------|-------|---|-------|----------|-----|--------|-------|------|
| 17 | 4000 | 0.49 | 0.110 | 4 | 8.94 | 0.000521 | 812 | 205.20 | 61.51 | 1.22 |
| 18 | 3500 | 0.27 | 0.110 | 5 | 10.58 | 0.000402 | 734 | 180.73 | 59.35 | 1.94 |
| 19 | 3000 | 0.27 | 0.177 | 3 | 10.45 | 0.000521 | 809 | 186.38 | 54.49 | 2.53 |
| 20 | 3500 | 0.27 | 0.125 | 3 | 11.14 | 0.000357 | 861 | 193.91 | 50.05 | 2.18 |
| 21 | 4000 | 0.27 | 0.177 | 4 | 10.51 | 0.000579 | 690 | 143.08 | 57.19 | 2.36 |
| 22 | 4000 | 0.27 | 0.125 | 3 | 11.34 | 0.000477 | 846 | 159.08 | 47.64 | 2.14 |
| 23 | 4000 | 0.49 | 0.125 | 3 | 11.42 | 0.000449 | 629 | 153.43 | 32.20 | 3.13 |
| 24 | 4000 | 0.38 | 0.177 | 5 | 10.89 | 0.00072 | 773 | 186.38 | 54.60 | 1.46 |
| 25 | 3000 | 0.27 | 0.125 | 4 | 10.88 | 0.000364 | 815 | 211.82 | 49.35 | 2.01 |
| 26 | 4000 | 0.38 | 0.110 | 5 | 10.92 | 0.000387 | 688 | 153.43 | 60.65 | 1.61 |
| 27 | 3500 | 0.49 | 0.177 | 4 | 9.82 | 0.000555 | 713 | 171.32 | 56.60 | 2.20 |

6.3.2 Network Architecture and Training

A total of 81 samples are used as inputs where the database vectors are randomly divided into 70%, 20%, 10% for training, validation and testing sets respectively, i.e., 57 sets are used for training, 16 sets for validation and 8 sets for testing in the neural network architectures. The network architecture initializes all the weights as zero. Once the learning process starts, the neural network is so designed that all the weights and thresholds between different layers adjust automatically. The mean square error between the actual network output and the target output is minimized. Network parameters are adjusted to achieve the required goal. The network algorithm is trained for different architectures and training schemes. The behavior of the neural network architecture depends on various parameters like input patterns to networks, target vectors, number of layers and number of neurons, activation function, training function, number of epochs, and so on. The present work is an attempt to understand the application of ANN using force and vibration signals to monitor the channel topography. The process can then later is used for the control and monitor the geometrical features.

The *trainlm* is found to be the most robust training algorithm in terms of accuracy and time taken. Architecture (1) involves no hidden layer, (2)-(5) involve one hidden layer each and the rest involve two hidden layers and the details are shown in Table 6.4. The corresponding performance diagrams of different network architectures

are shown in Figures 6.4. The performance of neural network architectures were analyzed and described in Table 6.5. It is observed that, the 9th architecture (6-12-10-4) gives the best results. The corresponding output of the network for training, validation and test sets though regression plot (6-12-10-4 architecture) is shown in Figure 6.5.

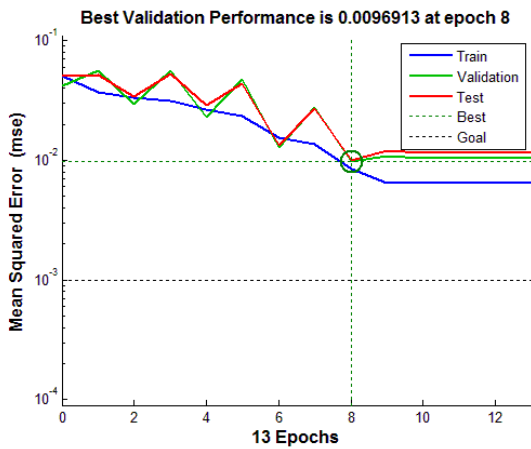
Table 6.4: List of neural network architectures

| S.No | Architecture | Training Function | Transfer Function | Validation (%) |
|------|------------------|--------------------------------------|-----------------------|----------------|
| 1 | 6-4 | <i>tansig, tansig</i> | <i>trainlm</i> | 80.912 |
| 2 | 6-2-4 | <i>tansig, tansig</i> | <i>trainlm</i> | 83.726 |
| 3 | 6-4-4 | <i>tansig, tansig</i> | <i>trainlm</i> | 80.492 |
| 4 | 6-8-4 | <i>tansig, tansig</i> | <i>trainlm</i> | 76.675 |
| 5 | 6-12-4 | <i>tansig, tansig</i> | <i>trainlm</i> | 85.424 |
| 6 | 6-8-8-4 | <i>tansig, tansig, tansig</i> | <i>trainlm</i> | 83.281 |
| 7 | 6-12-8-4 | <i>tansig, tansig, tansig</i> | <i>trainlm</i> | 69.116 |
| 8 | 6-20-8-4 | <i>tansig, tansig, tansig</i> | <i>trainlm</i> | 81.835 |
| 9 | 6-12-10-4 | <i>tansig, tansig, tansig</i> | <i>trainlm</i> | 90.915 |
| 10 | 6-20-12-4 | <i>tansig, tansig, tansig</i> | <i>trainlm</i> | 81.505 |

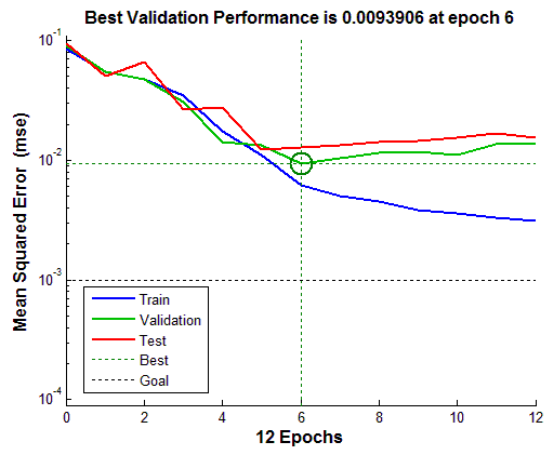
Table 6.5: Results for various ANN architectures

| Architecture No. | Network Architecture | Mean Square Error | | |
|------------------|----------------------|-------------------------------------|----------------|-----------------------------|
| | | Training set | Validation set | Testing set |
| 1 | 6-4 | $10^{-3}-10^{-2}$ | 0.00969 | $10^{-2}-10^{-1}$ |
| 2 | 6-2-4 | $10^{-3}-10^{-2}$ | 0.00939 | $10^{-2}-10^{-1}$ |
| 3 | 6-4-4 | $10^{-3}-10^{-2}$ | 0.01062 | $10^{-2}-10^{-1}$ |
| 4 | 6-8-4 | 10^{-2} | 0.006305 | $10^{-2}-10^{-1}$ |
| 5 | 6-12-4 | $10^{-3}-10^{-2}$ | 0.00990 | $10^{-2}-10^{-1}$ |
| 6 | 6-8-8-4 | $10^{-3}-10^{-2}$ | 0.008883 | $10^{-3}-10^{-2}$ |
| 7 | 6-12-8-4 | $10^{-3}-10^{-2}$ | 0.01311 | $10^{-2}-10^{-1}$ |
| 8 | 6-20-8-4 | $10^{-4}-10^{-3}$ | 0.00984 | $10^{-2}-10^{-1}$ |
| 9 | 6-12-10-4 | $10^{-4}-10^{-3}$ | 0.01098 | 10^{-2} |
| 10 | 6-20-12-4 | $10^{-3}-10^{-2}$ | 0.01062 | $10^{-2}-10^{-1}$ |

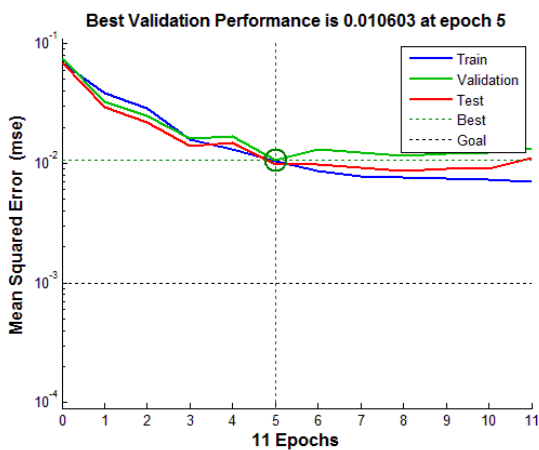
The experimental test vector values and the predicted values from the ANN model are presented in Table 6.6. Figure 6.6 shows various plots of the experimental and neural network results on width, depth, taper and surface roughness.



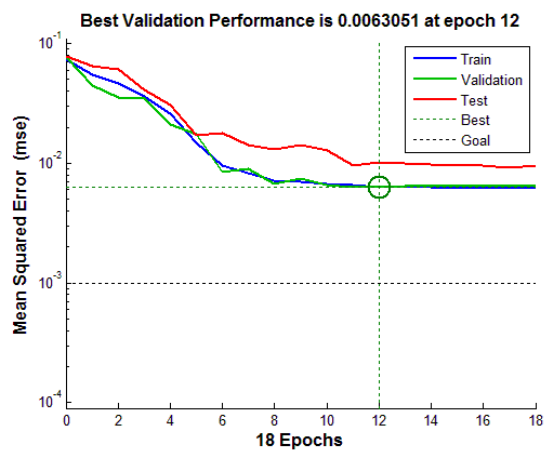
(1) Architecture 6-4



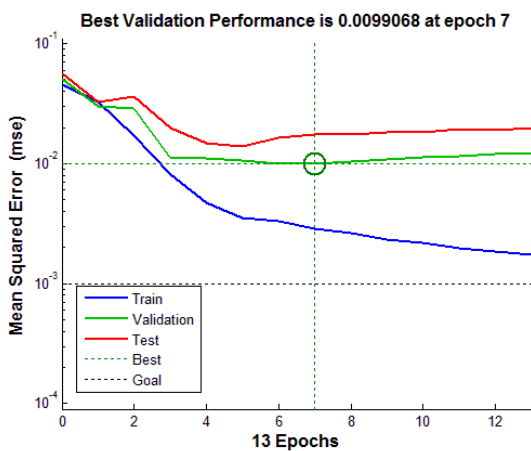
(2) Architecture 6-2-4



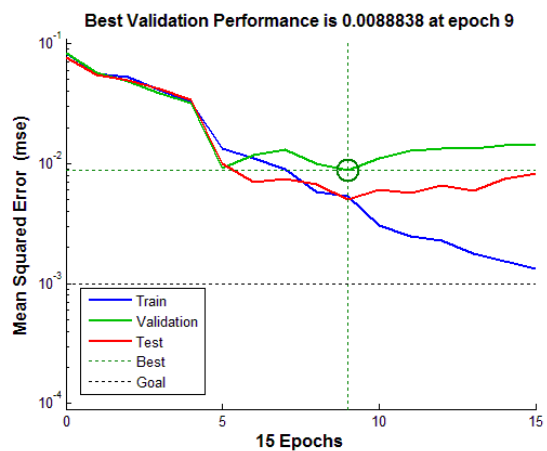
(3) Architecture 6-4-4



(4) Architecture 6-8-4

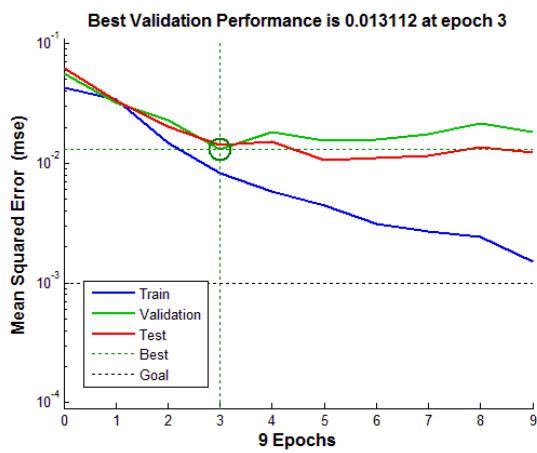


(5) Architecture 6-12-4

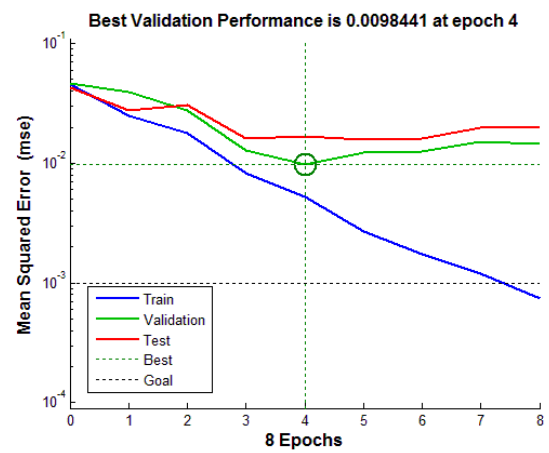


(6) Architecture 6-8-8-4

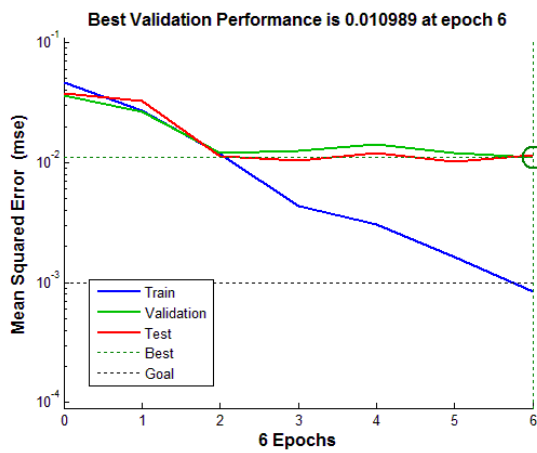
Fig.6.4: Convergence pattern for various Back Propagation Neural Networks



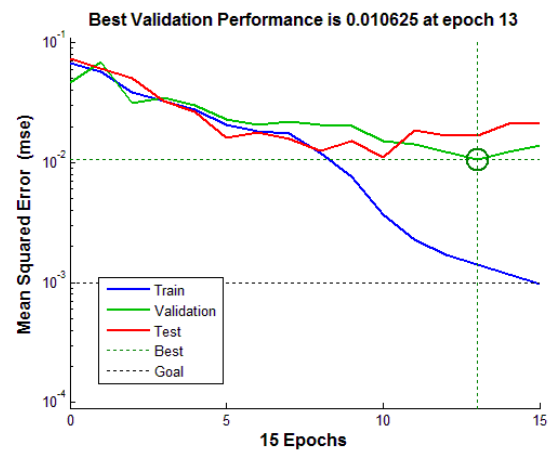
(7) Architecture 6-12-8-4



(8) Architecture 6-20-8-4



(9) Architecture 6-12-10-4



(10) Architecture 6-20-12-4

Fig. 6.4 (Contd.): Convergence pattern for various Back Propagation Neural Networks

Table 6.6: Experimental and ANN predicted values of the test set target parameters

| Test No. | <i>Experimental Values</i> | | | | <i>ANN predicted values</i> | | | |
|----------|---|---|--------------------|--------------------------------------|---|---|--------------------|--------------------------------------|
| | <i>Width (μm)</i> | <i>Depth (μm)</i> | <i>Taper (Deg)</i> | <i>$R_a(\mu\text{m})$</i> | <i>Width (μm)</i> | <i>Depth (μm)</i> | <i>Taper (Deg)</i> | <i>$R_a(\mu\text{m})$</i> |
| 1 | 860 | 157 | 69 | 1.28 | 845 | 145 | 71 | 1.16 |
| 2 | 774 | 173 | 66 | 2.24 | 792 | 169 | 66 | 2.00 |
| 3 | 783 | 203 | 66 | 2.08 | 775 | 206 | 63 | 2.03 |
| 4 | 840 | 217 | 62 | 1.75 | 830 | 221 | 62 | 1.78 |
| 5 | 813 | 188 | 65 | 1.97 | 790 | 179 | 67 | 1.88 |
| 6 | 785 | 179 | 65 | 1.97 | 834 | 195 | 65 | 2.07 |
| 7 | 783 | 174 | 66 | 2.32 | 805 | 184 | 62 | 2.25 |
| 8 | 608 | 233 | 59 | 2.35 | 652 | 212 | 58 | 2.62 |

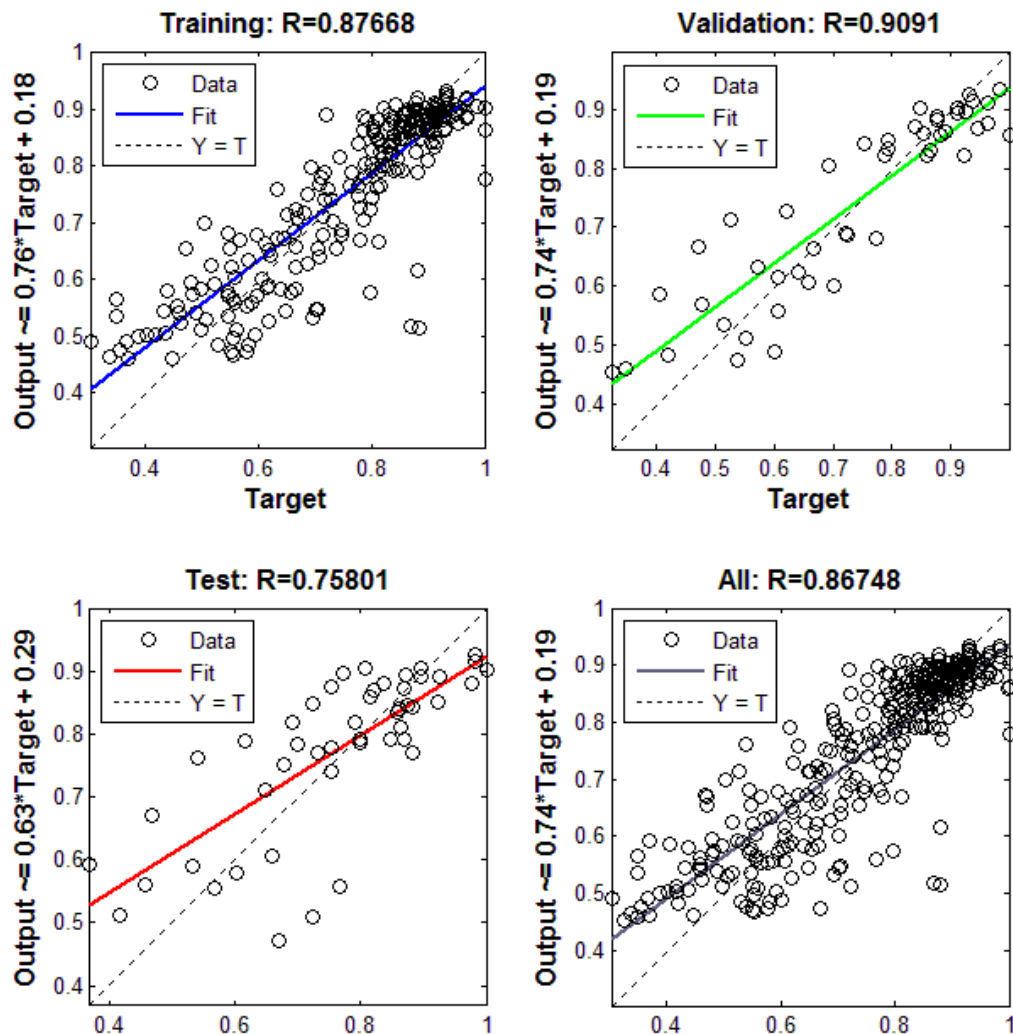


Fig.6.5: Regression Plot for Architecture 9 (6-12-10-4)

6.3.3 Results and discussion

In AWJM, the main focus of the process in using for micro-channel fabrication is to achieve close dimensional tolerances and accuracies. To supervise and control the dimensions of the channel it is necessary to know the input parameter values so as to achieve the best possible results. Another way of accessing the feature dimensions are to use the indirect method of measurements which are force, vibration, sound, etc. A brief study on the role of process parameters on the dimensional characteristics are studied in the previous chapters. In the present case, the sensor output in terms of the jet impact force and the jet vibration are used to control the process. The impact force influences the channel depth and the jet vibration correlates the width of the channel. The combination of both force and vibration results in taper and the surface roughness.

The motivation behind using the development of neural networks is to provide a new type of computer architecture in which the knowledge acquired and stored over time with the use of adaptive learning algorithms. In the present case, the use of feed forward neural networks is somewhat simple in structure and can be easily analyzed mathematically. The back-propagation network is first and most commonly used feed forward neural network because there exists a mathematical learning scheme to train the network and guarantee mapping between inputs and outputs.

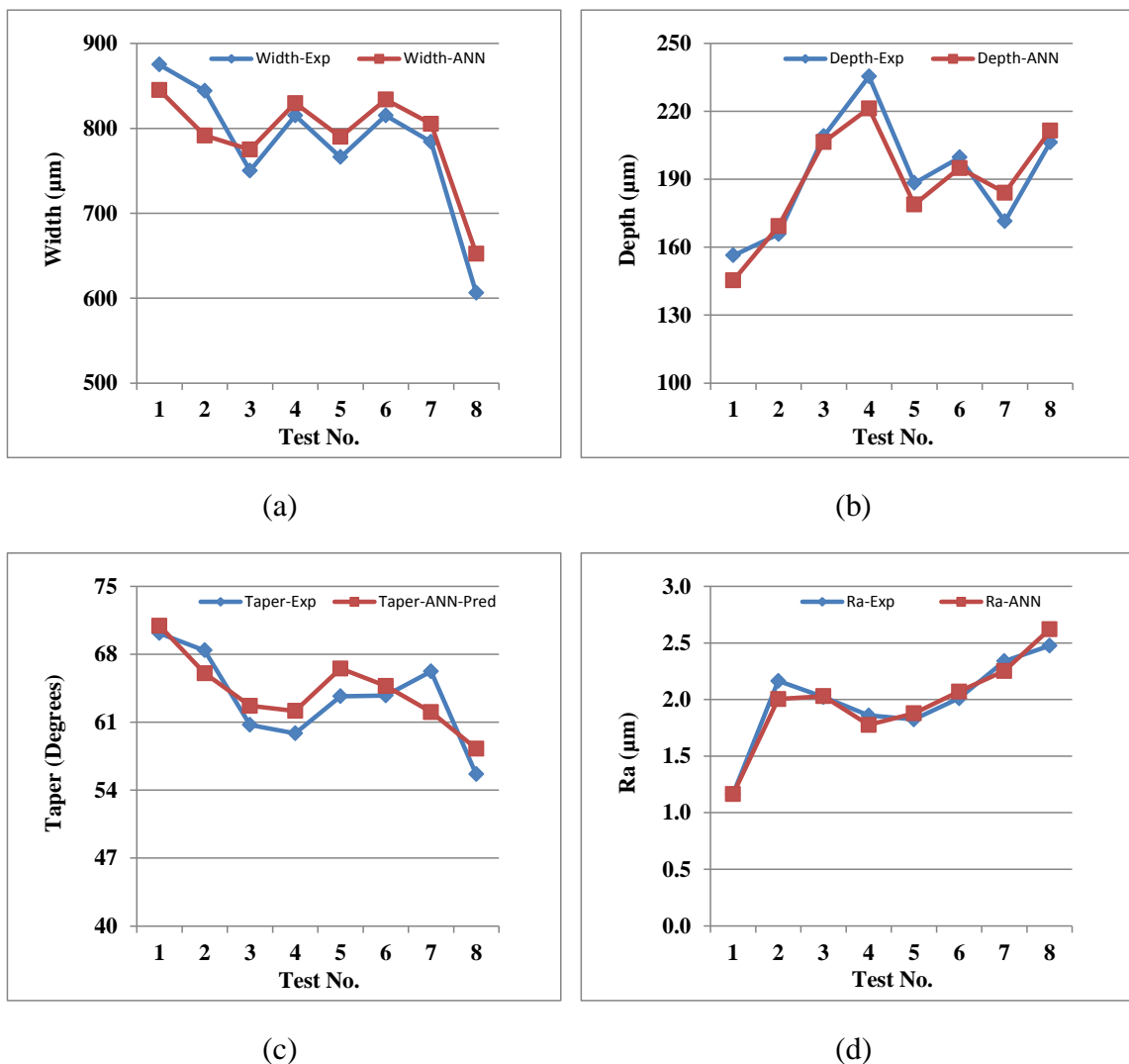


Fig. 6.6: Comparison of the experimental and ANN predicted values on (a) Width (b) Depth (c) Taper (d) Surface roughness

Using the above procedure, width, depth, taper and surface roughness has been computed for the machining conditions under which experiments are conducted. The experimental results are then compared with those obtained by neural network models discussed above. The surface roughness results predicted by ANN are in good

agreement with the experimental values as shown in Figure 6.12(d). The ANN results for taper when compared with the experimental results, the error prediction is higher, when calculated the percentage error is of the order of 5-6%. Even ANOVA results for the channel taper mentioned in the previous chapter are also not encouraging. In AWJM, taper is evaluated with a large set of input parameters. The results show that the channel taper is a difficult parameter to be predicted. An improved method to evaluate is to consider some more dominant parameters. The prediction for depth and width are the most appropriate parameters observed which are within the error range of 2-3 %. The method shows an effective way of monitoring the process in terms of the dimensional characteristics.

6.4 Summary

The AWJM technique is strongly a non-linear process influenced by a wide range of process parameters. These parameters are highly influenced by disturbances caused during the process of machining. It is always possible to control depth, width, taper and surface roughness with proper selection of process parameters and their control. The importance of the design of a control and feedback system depends on the process output which can be used as an automated compensation control system. In this chapter, the first phase is concentrated towards selection of optimum set of process parameters which would give the best possible set of responses for the micro-channel fabrication. The grey relational method is used to establish a relation between the response parameters with the input parametric set. The results obtained using this method shows that the set of process parameters are in conjunction with the ANOVA results.

The second part of the chapter shows the effectiveness of using back propagation neural networks for modeling of the AWJM for the micro-channel fabrication is demonstrated. Simulation results show a good agreement with the experimental results for a range of machining conditions. Based on these results, the possibility of using ANN model for predicting the dimensions of the channel has been confirmed. It is further observed the learning process could be enhanced by training the networks with large set of process parameters. This model can be used to study AWJ milling without performing any physical measurements by examining the effect of

process parameters with the aid of force and vibration signals. The neural network systems discussed is fairly general and can be extended to other applications of AWJM to improving the machining performance and efficiency. The proposed on-line control method of AWJM can be applied to a variety of processes.

Chapter 7

CONCLUSIONS AND SCOPE FOR FUTURE WORK

| | |
|---|-----|
| 7.1.Conclusions | 135 |
| 7.1.1. Pocket Milling | 135 |
| 7.1.2. Micro-channels | 136 |
| 7.1.3. Analysis of theoretical and empirical models | 137 |
| 7.1.4. Multi-response optimization | 138 |
| 7.1.5. Artificial neural networks | 138 |
| 7.2.Scope for future work | 138 |

7.1. Conclusions

The present research carried out is an attempt to study and understand the process of milling using Abrasive Water Jet. The process has major applications in engineering sectors like defense, space and automobile parts made of difficult to cut and exotic materials, where one of the application is partial removal of material from the components to reduce weight without losing its strength. The present day requirements in the above sectors is to fabricate parts with less weight, more strength, high fatigue life, more economical etc. Theoretical and experimental investigations have been made on the material removal rate, and force during the process of AWJ milling; besides to understand the feasibility of using AWJM for applications involving controlled material removal, unlike through cutting operations. Micro-channels are created using this technique to understand the process of milling in detail. Force and vibration signals are used for in-process monitoring applications to achieve the best performance in generating any feature. Based on the experimental and theoretical work reported in the thesis, the following conclusions can be drawn:

7.1.1. Pocket Milling

To understand the AWJ milling process, experiments are performed to create pockets with varying process parameters. The role of process parameters on the output

CONCLUSIONS AND SCOPE FOR FUTURE WORK

are studied in detail and some of the major observations during experimentation are as follows:

- In a pocket milling process the interaction time of the abrasive particle and the work surface is a crucial parameter. In the present work, the jet is allowed to move at very high traverse speeds. At high traverse speeds, better surface finish is obtained with reduced waviness on the surface. An optimum traverse speed has to be chosen keeping the material removal rate (MRR) and pocket dimensions as the target.
- It is observed that the material removal mechanism at low traverse speeds is of cutting wear mode and it is also dominant at abrasive flow rate of 0.38 kg/min and at standoff distance (SOD) of 4 mm.
- The increase in the abrasive flow rate increases the cutting ability, but increase in collisions in the particle mixing reduces the cutting performance which leads to a reduction in mrr and produces high surface roughness. At 0.38 kg/min of abrasive flow rate, higher MRR is obtained with good surface finish.
- An increase in the SOD leads to higher surface roughness due to the fluctuations in the jet when the jet is exposed to atmospheric pressure. At SOD of 4 mm, a better surface finish and higher MRR is obtained. This is due to the jet stabilization. At SOD 3 mm due to upward deflection of the jet, the surface quality deteriorates with reduced MRR.
- The use of # 160 abrasive particle gives a better finish due to the reduction in the abrasive size; but the MRR is decreased due to reduced kinetic energy of an individual particle for a given abrasive flow rate.
- The trends followed in the pocket depth are very much similar to AWJ cutting process. The pocket depth is reduced at high traverse speed, with minimum particle size and also at low abrasive flow rates.

7.1.2. Micro-Channels

The force signals captured with the dynamometer during pocket milling could not provide conclusive information to understand the milling process due to the digging phenomenon at the corners. This has led to the creation of micro-channels. During the micro-channel fabrication, impact force and jet vibrations are acquired for process monitoring. In AWJ milling, achieving dimensional tolerances is very important due to

the rebound of the abrasive particles after the impact. The following discussions are drawn from the micro-channel fabrication:

- The indentation depth depends on the abrasive size and the traverse speed, which is clearly visible in the experimental plots and ANOVA results also assess the same. The depth decreases with increase in the traverse speed and the phenomena of pocket milling is valid for micro-channel fabrication also.
- The change in width/depth ratio at 0.38 kg/min shows that the material removal mechanism shifts from cutting wear mode to deformation mode. The increase in the traverse speed and number of abrasives increases this ratio. The increase can be attributed due to increased number of cutting edges.
- The taper in the channel preparation is due to rebounding of the particle which depends on abrasive size and traverse speed. SOD has not shown much influence on the taper. The ANOVA results also reveal the same.
- Higher number of abrasives creates more fluctuation within the jet and generates peaks and valleys which increase the surface roughness. Surface roughness is an important response parameter in micro-machining which can be improved with fine abrasives.

7.1.3. Analysis of theoretical and empirical models

Empirical model developed for the MRR are valid for the combination of input parameters range and the target material. The model can be used to determine an optimum set of parameters for a required response parameter. The force model development is based on the momentum theory of the abrasive particle. From the models developed, the following inferences are drawn:

- The error percentage in MRR when compared between the generic and experimental results is of the order of 10-12% due to a limited number of input parameters.
- The analytical force model is validated for linear cut micro channels. The model is valid to an abrasive flow rate of 0.38 kg/min and the deviation beyond this rate can be attributed to collisions within the particles and absorption of most of the energy by the abrasives, which results in reduction in the machining efficiency.

- The purpose of investigation of the forces is to find out how much information can be extracted from the workpiece reaction force and relate to the channel geometry and its characterization.

7.1.4. Multi-response optimization

The multi-response optimization carried through grey relational analysis results in a parametric set which can be used achieve a channel of maximum depth and minimum taper, force and vibration with an improved surface finish having width equivalent to the jet diameter. Experiment no. 12 (traverse speed: 3000 mm/min; abrasive flow rate: 0.49 kg/min; abrasive size: # 160; and SOD: 4 mm) gives the best performance for the required set of responses.

7.1.5. Artificial neural networks

Development of a practical and robust process monitoring method to control and monitor the geometry of a micro-channel is an essential requirement in micro-manufacturing. In the preset thesis, ANN techniques are for monitoring and control of the channel characteristics using force and vibration signals. Among the various network architectures tested, architecture no. 6-12-10-4 gives the best performance which can be used to predict the geometry with an average error of 5-6%.

7.2. Scope for future work

Based on the exhaustive studies and investigations carried for AWJ milling, it was emphasized to enumerate the future scope of the work in AWJ milling as follows:

Optimization of process parameters: A large number of process parameters can be considered with different approaches and then can be integrated to suggest a suitable optimized set of process parameters.

Tool path optimization: Features can be generated with a series of tool paths, an approach for milling path optimization can be attempted which would take minimum machining time giving the maximum output.

Theoretical modeling of the AWJ milling process: A theoretical model can be developed including the rebound velocity of the abrasive particles.

Geometrical characteristics of the generated feature: Characterization of the feature geometry can be achieved and modeled with a given set of input parameters.

Force based modeling to understand the process: The force data can be used to model the mechanism of the milling process.

Monitoring using soft computing methods: Condition monitoring of the process with force and vibration signals for the process prediction can be developed using artificial intelligence techniques like fuzzy logics, genetic algorithms, etc.

Process Automation: Placement of intelligent sensors in the process can be used to explore to develop a fully automated AWJ milling process.

Hybrid machining process: Surface roughness which is a major drawback of AWJM process can be improved with a hybrid machining process possibility. A method to include a method like abrasive finishing process that can integrate with AWJ system can be explored.

CONCLUSIONS AND SCOPE FOR FUTURE WORK

REFERENCES

- Adnan Akkurt, Kulekci M K, Ulvi Seker, Fevzi Ercan, "Effect of feed rate on surface roughness in abrasive waterjet cutting applications," *Journal of Materials Processing Technology*, Vol. 47, 2004, pp.389-396
- Arola D, Ramulu M, "Mechanisms of material removal in abrasive water jet machining of common aerospace materials," *Proceedings of 7th American Water Jet Conference*, ASME, New York, 1993, pp. 43-64
- Arola D, Ramulu M, "A study of kerf characteristics in abrasive water jet machining of graphite/epoxy composites," *Journal of Engineering Materials and Technology*, Vol. 118, 1996, pp. 256-265
- Axinite D A, Gindy N, "Tool condition monitoring in broaching," *Wear*, Vol. 254, 2003, pp. 370-382
- Bitter J G A, "A study of wear phenomenon Part I," *Wear*, Vol. 6, 1963a, pp. 5-21
- Bitter J G A, "A study of wear phenomenon Part II," *Wear*, Vol. 6, 1963b, pp. 169-190
- Blickwedel H, Guo N S, Haferkamp H, Louis H, "Prediction of abrasive jet cutting performance and quality," *Proceedings of 10th International Symposium on Jet Cutting Technology*, Amsterdam, The Netherlands, 1990, pp. 163-189
- Brandt S, Louis H, Ohlsen J and Tebbing G, "Influence of nozzle geometry on abrasive water suspension jets," *Proceedings of 5th Pacific Rim International conference on Water Jet Technology*, New Delhi, India, 1998, pp. 330-344
- Brandt S, Louis H, "Controlling of high-pressure abrasive water suspension jets," *Proceedings of the 15th International conference on Jetting Technology*, Ronneby, Sweden, 2000, pp. 21-33
- Byrne G, Dornfeld D, Inasaki I, Ketteler G, König W, Teti T, "Tool Condition Monitoring (TCM): The Status of Research and Industrial Application," *Annals of the CIRP*, Vol. 44, 1995, pp. 541-567
- Capello E, Groppetti R, *Proceedings of the 7th American Water Jet Conference*, 1993, pp. 157-174
- Chakravarthy P S, Ramesh Babu N, "A semi empirical model for cutting granite with abrasive waterjets," *Proceedings of 17th AIMTDR*, 1997, pp. 259-262
- Chakravarthy P S, Ramesh Babu N, "A hybrid approach for selection of optimal process parameters in abrasive water jet cutting," *I.Mech.E, Journal of Engineering Manufacture*, Part B, Vol. 214, 2000, pp. 781-791

REFERENCES

- Chalmers E J, "Effect of parameter selection on abrasive waterjet performance," *Proceedings of the 6th American Waterjet Conference, Houston, USA, 1991*, pp. 345-354
- Chen F L, Siores E, Wong W C K, "Optimizing abrasive waterjet cutting of ceramic materials," *Journal of Material Processing Technology*, Vol. 74, 1998, pp. 251-254
- Chen F L, Siores E, "The effect of cutting jet variation on striation formation in abrasive water jet cutting," *International Journal of Machine Tool & Manufacture*, 2001, pp. 1479-1486
- Chen F L, Wang J, Lemma E, Siores E, "Striation formation mechanisms on the jet cutting surface," *Journal of Material Processing Technology*, 2003, pp. 213-218
- Chryssolouris G, Guillot H "A comparison of statistical and AI approaches to the selection of process parameters in intelligent machining," *Transactions of ASME Journal of Engineering for Industry*, Vol. 12, 1990, pp. 122-131
- Deam R T, Lemma E, Ahmed D H, "Modelling of abrasive water jet cutting process", *Wear*, Vol. 257, 2004, pp. 877-891
- Eltobgy M, E-G Ng, Elbestawi M A, "Modelling of Abrasive Waterjet Machining: A New Approach," *CIRP Annals, Manufacturing Technology*, Vol. 54, 2005, Issue 1, pp. 285-288
- Evans A G, Chesnutt J C, Nadler H, "Quasi-static solid particle in damage in brittle solids-II. Indentation friction," *Acta Metallurgica*, Vol. 24, 1976, pp. 867-870
- Evans A G, "Impact Damage Mechanism-Solid Projectile," *Treatise on Materials Science and Technology, Materials Erosion, Academic Press, New York*, Vol. 16, 1979, pp. 1-67
- Fan J M, Wang C Y, Wang J, "Modeling the erosion rate in micro abrasive air jet machining of glasses," *Wear*, 266 (9-10), 2009, pp. 968-974
- Finnie I, "The mechanism of erosion of ductile metals," *Proceedings of 3rd National Congress of Applied Mechanics, ASME, New York*, 1958, pp. 527-532
- Finnie I, "Erosion of surfaces by solid particles," *Wear*, Vol. 3, 1960, pp. 87-103
- Fowler G, Shipway P H, Pashby I R, "A technical note on grit embedment following abrasive water jet milling of titanium alloy," *Journal of Material Processing Technology*, 159, 2005a, pp. 356-368

- Fowler G, Shipway P H, Pashby, I R, "Abrasive Water-jet controlled depth milling of TiAl4V alloy-an investigation of role of jet-workpiece traverse speed and abrasive grit size on the characteristics of the milled surface," *Journal of Material Processing Technology*, Vol. 161, 2005b, pp. 407-414
- Fowler G, Shipway P H, Pashby I R, "The effect of particle hardness and shape when abrasive jet milling of titanium alloy Ti6Al4V," *Wear*, Vol. 266, 2009, Issues 7-8, pp. 613-620
- Groppetti R, Gutema T and Lucchio A D I "A contribution to the analysis of some kerf quality attributes for precision abrasive waterjet cutting," *Jetting Technology*, BHR Group, 1998, pp. 253-269
- Gudimetla, P, Wang J, Wong W, "Kerf formation analysis in the abrasive waterjet cutting of industrial ceramics," *Journal of Materials Processing Technology*, Vol. 128, 2001, pp. 123-129
- Guo N S, Louis H, Meier G, "Surface structure and kerf geometry in abrasive water jet cutting: formation and optimization," *Proceedings of 7th American Water Jet Conference, WJTA, St. Louis*, Vol. 1, 1993, pp. 1-25
- Harris W T, *Chemical Milling*, Oxford University Press, Oxford, 1976
- Hashish M, du Plessis M P, "Prediction equations relating high velocity jet cutting performance to stand off distance and multipasses," *Transactions of ASME, Journal of Engineering for Industry*, Vol. 101, 1979, pp. 311-318
- Hashish M, "A Modeling Study of Metal Cutting with Abrasive Waterjets," *Journal of Engineering Materials and Technology*, Vol. 106, 1984, pp. 88-100
- Hashish M, "Aspects of abrasive-waterjet (AWJ) performance optimization," *Proceedings of 8th International symposium on Jet cutting Technology, Durham*, 1986a, pp. 297-308
- Hashish M, "Turning with abrasive waterjets-a preliminary investigation," *PED Vol. 22*, 1986b, pp. 79-100
- Hashish M, "Milling with Abrasive-Waterjets-A Preliminary Investigation," *Proceedings of the 4th U.S. Water Jet Conference, Berkeley, California*, August 26-28, 1987, pp. 1-20
- Hashish M, "An Investigation of Milling with Abrasive Waterjets," *Transactions of ASME, Journal of Engineering for Industry*, Vol. 111, 1989a, pp. 158-166
- Hashish M, "Pressure effects in Abrasive Waterjet (AWJ) Machining," *Journal of Engineering Materials and Technology*, Vol. 111, 1989b, pp. 221-228

REFERENCES

- Hashish M, "Optimization factors in Abrasive Waterjet Machining," *Transactions of ASME, Journal of Engineering for Industry*, Vol. 113, 1991, pp. 29-37
- Hashish M, Monserud D O, Bondurant P D, Hake J C, Craigen S J, White G B, Coleman W J, "A new abrasive - waterjet nozzle for automated and intelligent machining," *Proceedings of 7th American Waterjet Conference, Seattle, USA*, 1993, pp. 829-842
- Hashish M, "Controlled depth milling of isogrid structures using AWJS," Reprinted from PED-Vol. 86-1, *Manufacturing Science and Engineering*, Book No. G0930A, 1994, pp. 413-419
- Hashish M, "Waterjet machine tool of the future," *Proceedings of 9th American Waterjet Conference, Dearborn*, 1997, pp. 769-778
- Hashish M, "Abrasive-waterjet (AWJ) studies," *Proceedings of 16th International conference on Water Jetting, BHR Group, France*, 2002, pp. 13- 47
- Hassan A I, Chen C, Kovacevic R, "On-line monitoring of depth of cut in AWJ cutting," *International Journal of Machine Tools and Manufacture*, Vol. 44, 2004, pp. 595- 605
- Hocheng H, Tsai H Y, Shiue J J, "Feasibility study of abrasive-waterjet milling of fiber-reinforced plastics," *ASME Journal of Manufacturing Science and Engineering*, Vol. 119, 1997, pp. 133-142
- Hollinger R H, Perry W D, Swanson R K, "Precision cutting with a low pressure, coherent abrasive suspension jet," *Proceedings of 5th American Water Jet Conference, WJTA, St. Louis*, 1989, pp. 245-252
- Hoogstrate A M, van Luttervelt C A, "Opportunities in abrasive water-jet machining," *Annals of the CIRP*, Vol. 46, 1997, pp. 697-714
- Huang J T, Liao Y S, "Optimization of machining parameters of wire-EDM based on grey relational and statistical analysis," *International Journal of Production Research*, Vol. 41, 2003, pp. 1707-1720
- Hunt D C, Kim T J, Reuber M, "Surface Finish Optimization for Abrasive Waterjet Cutting," *Proceedings of 9th International Symposium on Jet Cutting Technology, Sendai, Japan*, 1987, pp. 99 - 112.
- Hutchings I M, "Deformation of metal surfaces by the oblique impact of square plates," *International Journal of Mechanical Sciences*, Vol.19, 1977, pp. 45-52
- Hutchings I M, "Mechanical and metallurgical aspects of the erosion of metals," *International Conference on Corrosion-Erosion of Coal Conversion System Materials*, Conference, National Association of Corrosion Engineers (NACE), Houston, 1979a, pp. 393-428

- Hutchings I M, "Mechanisms of the erosion of metals by solid particles," *Erosion: Prevention and Useful Applications*, ASTM STP664, American Society Testing and Materials, 1979b, pp. 59-76
- Kenneth Levenberg, "A Method for the Solution of Certain Non-Linear Problems in Least Squares". *Quarterly of Applied Mathematics*, Vol. 2, 1944, pp. 164-168
- Knaupp M, "The application of sensors for process monitoring in high pressure waterjet Technology," *Proceedings of 7th American Waterjet Conference, Seattle, USA*, 1993, pp. 943- 949
- Ko"nig W, Ka"mpfe A, Mangler R, Schmelzer M, "Einflu" sse aufdie Effektivita" t des Wasserstrahlschneidens," DIMA Vol. 48 (7/8) 42, 1994
- Kong M C, Axinte D, Voice W, "Challenges in using waterjet machining of NiTi shaper memory alloys: An analysis of controlled-depth milling," *Journal of Materials Processing Technology*, Vol. 211, 2011, pp. 959-971
- Koster W P, Field M, "Effect of machining variables on the surface and structural integrity of Titanium," *Proceedings of North American Metal Working Research Conference, McMaster Univ. Hamilton*, 1973, pp. 67-87
- Kovacevic R, Liaw H H, Barrows J F, "Surface finish and its relationship to cutting parameters," SME TP, MR88-589, *Society of Manufacturing Engineers, Dearborn*, 1988, pp. 1-5
- Kovacevic R, Evizi M, "Nozzle wear detection in abrasive waterjet cutting systems," *Materials Evaluation*, Vol. 48, 1990, pp. 348-353
- Kovacevic R, "Surface texture in abrasive waterjet cutting," *Journal of Manufacturing Systems*, Vol. 10, Issue 1, 1991a, pp. 32-40
- Kovacevic R, "Development of opto-electronic sensor for monitoring the abrasive waterjet nozzle wear," *PED*, Vol. 44, 1991b, pp. 9-16
- Kovacevic R, "A new sensing system to monitor abrasive waterjet nozzle wear," *Journal of Materials Processing Technology*, Vol. 28, 1991c, pp. 117-125
- Kovacevic R, "Monitoring the depth of abrasive water jet penetration," *International Journal of Machine Tools & Manufacture*, Vol. 31, No.5, 1992, pp. 725-736
- Kovacevic R, Wang L and Zhang Y M, "Identification of abrasive waterjet nozzle wear based on parametric spectrum estimation of acoustic signal," *I.Mech.E, Part B, Journal of Engineering Manufacture*, Vol. 208, 1994a, pp. 173-181
- Kovacevic R, "Sensing the abrasive water jet nozzle wear," *International Journal of Water Jet Technology*, 1994b, pp. 1-10

REFERENCES

- Kovacevic R, Mohan R, Zhang Y M, "Cutting force dynamics as a tool for surface profile monitoring in abrasive waterjet," *ASME Journal of Engineering for Industry*, 117(3), 1995, pp. 340-350
- Kovacevic R, Hashish M, Mohan R, Ramulu M, Kim T J, Geskin E S, "State of the Art of Research and Development in Abrasive Waterjet Machining," *Transactions of ASME, Journal of Manufacturing Science and Engineering*, Vol. 119, 1997, pp. 776- 785
- Kulekci M K, "Processes and apparatus developments in industrial waterjet applications," *International Journal of Machine Tools and Manufacture*, Vol. 42, 2002, pp. 1297-1306
- Laurinat A, Louis M, Meier-W G, "A model for milling with abrasive water jet," *Proceedings of 7th American Water Jet Conference*, Vol.1, 1993, pp. 119-139
- Li H Z, Wang J, Fan J M, "Analysis and modeling of particle velocities in micro-abrasive air jet," *International Journal of Machine Tool & Manufacture*, Vol. 49, Issue 11, 2009, pp. 850-858
- Li Q L, Wang J, Huang C Z, "Erosion mechanisms of monocrystalline silicon under a micro particle laden air jet," *Journal of Applied Physics*, Vol. 104, 2008, pp. 34903-34910
- Louis H, Meier G, "Methods of process control of abrasive water jets," *Proceedings of 6th American Water Jet Conference, WJTA*, St. Louis, 1991, pp. 427-437
- Luttervelt C, Childs T H C, Jawahir I S, "Present situation and future trends in modelling of machining operations," *Annals of the CIRP*, Vol. 47, 1998, pp. 587-626
- Marchant B P, "Time-frequency Analysis for Biosystems Engineering," *Biosystems Engineering*, Vol. 85, 2003, pp. 261-281.
- Matsui S, Matsumura H, Ikemoto Y, Tsujita K, Shimizu M, "High Precision Cutting Method for Metallic Materials by Abrasive Waterjet," *Jet Cutting Technology, London*, 1991, pp. 263-278
- Mazurkiewicz M, Karlic, P, "Material response during hydro abrasive jet machining (HAJM)," *Proceedings of 4th US Water Jet Conference, ASME, New York*, 1987, pp. 159-167
- Mendi F, Kulekci M K, "İmalatta Su Jeti Uygulamalarının Değerlendirilmesi," *Pamukkale U'niversitesi Mu'hendislik Bilimleri Dergisi* 5 (2-3), 1999, pp. 1067-1075
- Meng H C, Ludema K C, "Wear models and prediction equations: their form and content," *Wear*, Vol. 181-183, 1995, pp. 443-457

- Mohan R, Momber A W, Kovacevic R, "On-line monitoring of the depth of AWJ penetration using acoustic emission technique", *Jet Cutting Technology*, Mechanical Engineering Publications, London, 1994, pp. 649-664
- Momber A W, "Energy transfer during the mixing of air and solid particles into a high-speed waterjet: an impact force study," *Experimental Thermal Fluid Science*, Vol. 25, 2001, pp. 31-41
- Momber A W, Eusch I, Kovacevic R, "Machining refractory ceramics with abrasive water jet", *Journal of Material Science*, Vol. 31, 1996, pp. 6485-6493
- Momber A W, Kovacevic R, "Principles of Abrasive Waterjet Machining," *Springer - Verlag London Ltd.*, London, 1998
- Momber A W, Kovacevic R, Kwak H, "Alternative method for the evaluation of the abrasive water-jet cutting of grey cast iron," *Journal of Material Processing Technology*, Vol. 65, Issue 1-3, 1997, pp. 65-72
- Nanduri M, Taggart D G, Kim T J, Ness E, Haney C N, and Bartkowiak C, "Wear patterns in abrasive waterjet nozzles," *Proceedings of 13th International Conference on Jetting Technology, Sardinia, Italy*, 1996, pp. 27-45
- Neusen K F, Rohatgi P K, Vaidyanathan C, "Abrasive waterjet cutting of metal matrix composites," *Proceedings of 4th US Water Jet Conference, ASME, New York*, 1987, pp. 175-182
- Niu M S, Kobayashi R, Yamaguchi T, "Kerf width in abrasive waterjet machining," *Proceedings of 4th Pacific Rim International Conference on Waterjet Technology*, 1995, pp. 59-70
- Ojmertz K M C, Amini N, "A discrete approach to the abrasive water jet milling process," *Jet Cutting Technology*, 1994, pp. 425-434
- Ojmertz K M C, "Abrasive waterjet machining," *Licentiate Thesis*, Chalmers University of Technology, Sweden, 1994
- Ojmertz K M C, "Analysis of surfaces produced by abrasive water jet milling technique," *Jet Cutting Technology*, Mechanical Engineering, Publishers, Bury St. Edmunds, 1996, pp. 753-768
- Pang K, Nguyen T, Fan J, Wang J, "Modelling of the micro-channeling process on glasses using an abrasive slurry jet," *International Journal of Machine Tools and Manufacture*, Vol. 53, 2012, pp. 118-126
- Papini M, Spelt J K, "Impact of rigid angular particles with fully plastic targets. Part I Analysis," *International Journal of Mechanical Sciences*, Vol. (5), 2000, pp. 991-1006

REFERENCES

- Paul S, Hoogstrate A M, van Luttervelt C A, Kals H J J, "Analytical and experimental modeling of the abrasive waterjet cutting of ductile materials," *Journal of Materials Processing Technology*, Vol. 73, 1998, pp. 189-199.
- Phadke M S, *Quality engineering using robust design*, Prentice Hall, 1989
- Preece C, "Treatise on materials science and technology-Erosion," *Academic Press, New York*, 1976
- Ramulu M, Arola D, "The influence of abrasive water jet cutting conditions on the surface quality of graphite/epoxy laminates," *International Journal of Machine Tools & Manufacture*, Vol. 34, Issue 3, 1994, pp. 295-313
- Ritter J E, "Erosion damage in structural ceramics," *Materials Science and Engineering* Vol. 71, 1985, pp. 194-201
- Ross P J, *Taguchi Techniques for Quality Engineering*, McGraw-Hill, New York, 1989
- Shaw M C, "*Principles of Abrasive Processing*," Clarendon Press, Oxford, 1996
- Sheldon G L, Finnie I, "The mechanism of material removal in the erosive cutting of brittle materials," *ASME Journal of Engineering Industry*, Vol. 88, 1966, pp. 393-400
- Shipway P H, Fowler G, Pashby I R, "Characteristics of the surface of titanium alloy following milling with abrasive water jets," *Wear*, Vol. 258, pp. 123-132
- Singh P J, Wei-Long Chen, Jose Munoz, "Comprehensive Evaluation of Abrasive Waterjet Cut Surface Quality," *Proceedings of 6th American Water Jet Conference, Texas, USA*, 1991, pp. 139-161
- Tönshoff H K, Friemuth T, Becker J C, "Process monitoring in Grinding," *Annals of the CIRP*, Vol. 51, 2002, pp. 551-571
- Wang J, Kuriyagawa T, Huang C Z, "An experimental study to enhance the cutting performance in abrasive waterjet machining," *Machining Science and Technology*, Vol. 7, 2003, pp. 191-207
- Wang J, Wong W C K, "A study of abrasive waterjet cutting of metallic coated sheet steel," *International Journal of Machine Tools & Manufacture*, Vol. 39, 1999, pp. 855-870
- Warisawa S, Kida A, Ito Y, "Visualization of the Water Jet Cutting by means of Ultrasonic Waves," *JSME International Journal Series C*, Vol. 44, 2001, pp. 816-824
- Water Jet Technology Association, *Recommended Practices for the use of Manually Operated High Pressure Water Jetting Equipment*, 1987

- Yanaida K, "Flow characteristics of water jets," *Proceedings of 2nd International Symposium on Jet Cutting Technology, BHRA, Cambridge, 1974*, pp. 19-32
- Yanaida K, Ohashi A, "Flow characteristics of water jets in air," *Proceedings of 4th International Symposium on Jet Cutting Technology, BHRA, England, 1978*, pp. 39-54
- Yie G G, "A pulsation-free fluid pressure intensifier," *Proceedings of 9th American Waterjet Conference, Dearborn, USA, 1997*, pp. 365-372
- Zeng J and Kim T J, "Erosion model for abrasive waterjet milling of polycrystalline ceramics," *Wear*, Vol. 199, 1996a, pp. 275-282
- Zeng J and Kim T J, "An erosion model of polycrystalline ceramics in abrasive waterjet cutting," *Wear* Vol. 193, 1996b, pp. 207-217
- Zeng J and Kim T J, "Development of an abrasive waterjet kerf cutting model for brittle materials," *Proceedings of 7th International Symposium on Jet cutting Technology*, 1992, pp. 483-501
- Zeng J, Munoz J, "Intelligent Automation of AWJ cutting for efficient production," *Proceedings of 12th International conf. Jet cutting Technology, Rouen, France, 1994*, pp. 401-408

REFERENCES

PUBLICATIONS

International Journals

T V K Gupta, J Ramkumar, Puneet Tandon, N S Vyas, "A study on the deviations of the jet with traverse speeds on different materials during pocket milling using Abrasive Water Jet Machining process," Applied Mechanics and Materials, Vol. 372 (2013), pp: 402-405

T V K Gupta, J Ramkumar, Puneet Tandon, N S Vyas, "Role of process parameters on pocket milling with Abrasive Water Jet Machining technique," International Journal of Mechanical Science & Engineering, VOL.7, No.10, 2013

International Conferences:

T V K Gupta, J Ramkumar, Nalinaksh S Vyas; "A study on the effect of process parameters in blind pocket milling using Abrasive Water Jet Machining", 6th International Conference on Precision, Meso, Micro and Nano Manufacturing (COPEN6), 11-12 Dec. 2009, PSG Coimbatore.

T V K Gupta, J Ramkumar, Nalinaksh S Vyas, Puneet Tandon, "Material removal rate prediction for blind pocket milling of SS304 using Abrasive Water Jet Machining Process," 2nd International Conference on Engineering and Applied Science (HKICEAS-2012), Dec. 14-16, 2012, Hong Kong, pp: 368-375.

T V K Gupta, J Ramkumar, Nalinaksh S Vyas, Puneet Tandon, "A Preliminary Investigation on the forces generated with process parameters during Abrasive Water Jet Milling on SS304" International Conference on Innovations in Design and Manufacturing (InnDeM 2012), PDPM IIITDM Jabalpur, Dec. 05-07, 2012.

T V K Gupta, J Ramkumar, Puneet Tandon, N S Vyas, "Influence of operating parameters on the dimensional accuracy of channels prepared on SS304 during Abrasive Water Jet Machining," Nov.15-21, 2013, ASME-IMECE 2013, San Diego, USA

T V K Gupta, J Ramkumar, Puneet Tandon, N S Vyas, "Application of Grey Relational Analysis for Geometrical Characteristics in Abrasive Water Jet Milled Channels," AIMTDR, IIT Guwahati, Dec.2014 (Accepted)

Journals under preparation

T V K Gupta, J Ramkumar, Puneet Tandon, N S Vyas, "State of the Art Research on Abrasive Water Jet Milling,"

T V K Gupta, N S Vyas, J Ramkumar, Puneet Tandon, "Predictive modeling of micro-channel topography using Artificial Neural Networks,"

T V K Gupta, J Ramkumar, Puneet Tandon, N S Vyas, "Geometry, topography, structure of AWJ milled micro-channels,"

T V K Gupta, J Ramkumar, Puneet Tandon, N S Vyas, "Experimental Investigations into force and vibration in AWJ Milling process,"

